

Predicting Processing and Filling Equipment with Complex Food Rheology



Students:

Ayupry Diptasari
Cynthia Andriani

Supervisor:

Björn Bergenståhl

Tetra Pak Supervisor:

Fredrik Innings
Dragana Arlov
Jannika Timander

Examiner:

Andreas Håkansson



Department of Food Technology, Engineering, and Nutrition
Lund University
2020

Abstract

As a food processing lines manufacturer with diverse product complexity, an understanding of fluid dynamics in a pipe system corresponding to the rheological properties and flow behavior is substantial. This will be beneficial to design suitable equipment and prevent processing-related issues, i.e. lowering filling performance, over-dimensioning pumps, excess energy consumption, etc. Therefore, the objectives of this study were (1) to obtain a better understanding of the time-dependent behavior consisted of thixotropy and rheopexy of liquid products with different complexities, (2) to predict the pressure drop in the straight pipe by using the rheological parameters, and (3) to investigate the correlation between the rheological parameters of liquid food products and their filling behavior responses systematically.

This study consisted of three main parts involving different complexity of liquid food products, i.e. orange juice concentrate, fermented milk or yoghurt, and tomato puree. First, rheology measurement by using a rotational rheometer to investigate time-dependent behavior through hysteresis loop, breakdown, and build-up test. The second part included pressure drop measurement by using a pressure drop rig, pressure drop prediction calculated from the rheology measurement, and comparison of the experimental and calculated pressure drop values. The last part was a filling experiment to correlate between rheology parameters of fermented milk products and filling behavior responses such as splashing, drippings, and filamentation.

The time-dependent behavior of the three liquid food products could be investigated through the hysteresis loop, breakdown, and build up test. *Naturell lätt* yoghurt had the highest thixotropy properties, followed by orange juice concentrate, and tomato puree with a slight rheopexy behavior at a certain shear rate range. The build-up test captured a clear structural recovery especially by the products with the time-dependent behavior.

Furthermore, the pressure drop experiment reported that the generated rheological parameters could predict the actual pressure drop to some extent. The determination of the model to predict pressure drop must be based on the product's rheological properties. It was due to the challenges from different product's properties and behavior. The orange juice concentrate had a better pressure drop prediction than *Naturell lätt* yoghurt and tomato puree due to its rheology simplicity. However, two other products had more complexity that complicated the rheological measurements in different ways as reflected in the pressure drop experiment. Yoghurt had an obvious thixotropy behavior, while tomato puree had both thixotropy and rheopexy behavior with an oscillatory effect during measurement.

Lastly, the filling prediction and correlation experiment have shown that systematic rheological parameters can be generated by using a different proportion of *Långfil* and *Naturell lätt* yoghurt and the Power Law prediction model. The result of correlation analysis has proven the possibility to correlate between rheology parameters, which are consistency index (K-value) and flow behavior index (n-value), and filling behavior responses (splash outside of the package and impact splash distance in the package) from the five systematic blends with $R^2 > 0.75$. However, the particle addition in the ambient drinking yoghurt did not cause any significant differences in the filling behavior responses. Above all, these three parts of the study would contribute to the pressure drop prediction from rheological characteristics and to the development of the filling behavior indicator (rheological parameters) for manufacturer application in the filling machine.

Keywords: *filling behavior responses, pressure drop, rheology parameters, rheopexy, thixotropy, time-dependent.*

Acknowledgements

*“The most complete give of God is a life based on knowledge”
-Ali Ibn Abu Talib-*



First, we would like to thank to the GOD for all the blessings that have been given to us. Therefore, finally we could finish this master thesis project. Secondly, we would like to thank the Department of Food Technology, Engineering, and Nutrition Lund University, Tetra Pak AB (Research and Technology), and all great supervisors: Fredrik Innings, Dragana Arlöv, Jannika Timander, and Björn Bergenståhl for the valuable advices and constructive feedback during finishing this project (January – June, 2020). Thirdly, we would like to thank to all the people that helped us during this project, Andreas Håkanson, Abdulrahman, Thomas, Göran, Christian, Henrik, Hans, Olexandr, Bernardo Paul, and Wanusavee (Nus).

Lastly, special thanks to our support systems (parents, husband, sisters, son, and beloved friends) that always support and continuously encourage us to finish strong what we have started here. We also realize that this report might be not perfect due to some limitations. Hopefully, this study would be beneficial for knowledge development, particularly in rheology. Enjoy reading! Finally, RHEOLOGY has taught us that *“there is no flow without pressure and stress”*.

Ayu & Cynthia
Lund, June 2020

Individual Contribution

This study has been done simultaneously together by both students (Ayupry and Cynthia) in terms of doing the laboratory work, collecting the data, and writing the report. This study was also supported by a weekly supervision meeting between Tetra Pak and LTH-Lund University that assisted the students for progress report, supervision, analysis, and discussion of the research project.

Table of Contents

Title	i
Abstract	ii
Acknowledgments	iii
Individual Contribution	iv
Table of Contents	v
List of Tables	vii
List of Figures	ix
List of Abbreviations and Symbols	xi
1. Introduction	1
1.1. Background and motivation	1
1.2. Objectives	3
1.3. Research questions	3
1.4. Limitations	3
2. Theoretical Framework	4
2.1. Rheology	4
2.1.1. Time-independent fluid behavior	4
2.1.1.1. Power Law model	4
2.1.1.2. Herschel-Bulkley model	5
2.1.2. Time-dependent fluid behavior: thixotropy and rheopexy	5
2.1.2.1. Hysteresis loop test	6
2.1.2.2. Breakdown test	6
2.1.2.3. Build-up test	7
2.2. Rheology measurement system (rotational rheometer)	7
2.3. Pressure drop	8
3. Materials and Methods	11
3.1. Materials	11
3.2. Methods	11
3.2.1. Sample preparation	11
3.2.2. Standard method for rotational rheometer measurement	12
3.2.3. Rheology measurements	13
3.2.4. Curve fitting method	14
3.2.5. Pressure drop measurement	14
3.2.6. Filling prediction and correlation	16
3.2.6.1. Experimental design	16
3.2.6.2. Filling behavior responses	17
3.2.6.3. Data analysis	18
4. Results Discussion	19

4.1. Rheology measurements	19
4.1.1. Stabilization time	19
4.1.2. Hysteresis loop	19
4.1.3. Breakdown	21
4.1.4. Build-up	22
4.2. Pressure drop rig	25
4.2.1. Pressure drop of orange juice concentrate	26
4.2.2. Pressure drop of <i>Naturell lätt yoghurt</i>	29
4.2.3. Pressure drop of tomato puree	31
4.3. One-shot filling rig test	33
4.3.1. Rheology parameters	33
4.3.2. Filling responses of systematic blends (<i>Naturell Lätt yoghurt</i> and <i>Långfil</i>)	36
4.3.3. Filling responses of ambient drinking yoghurt (ADY)	38
4.4. Uncertainty of the experiments	39
5. Conclusion and recommendation	41
5.1. Conclusion	41
5.2. Recommendation	42
6. List of references	44
7. Appendices	47
7.1. Rotational Kinexus rheometer procedure	47
7.2. Kinexus rheometer range and limitation	48
7.3. Determination of stabilization time	48
7.4. Pressure drop rig procedure	49
7.5. Pressure drop rig cleaning procedure	50
7.6. Bucket method for flowmeter calibration	50
7.7. Filling rig test procedure	51
7.8. Cup-bob geometry selection for tomato puree at different dilution % (w/w)	53
7.9. Build-up test with pre-shearing at 100 s^{-1}	54
7.10. Pressure drop data of orange juice concentrate	56
7.11. Pressure drop data of <i>Naturell lätt yoghurt</i>	57
7.12. Pressure drop data of tomato puree 100%	59
7.13. Pressure drop rig system calibration	61
7.14. Systematic blends hysteresis loop and curve fitting	61
7.15. Visualization of <i>Kaye</i> effect in theory	62
7.16. Filling responses in the one-shot filling rig	63
7.17. Statistical analysis of outside splash and impact splash distance by using SPSS 25	64
7.18. One-shot filling machine testing	66

List of Tables

List of Tables	Pages
Table 1. Sample for three stages of research study.	11
Table 2. General setting for the rheometer measurement.	13
Table 3. Measurement sequence for hysteresis loop test.	14
Table 4. Measurement design for breakdown test.	14
Table 5. Measurement design for build-up test.	14
Table 6. Design experiment of the pressure drop rig measurement.	16
Table 7. Description of experimental design used during one-shot filling rig testing at Tetra Pak AB.	17
Table 8. The type of filling behavior responses and inspection for each response.	17
Table 9. Stabilization time determination of the sample at three different shear rates.	19
Table 10. Percentage of viscosity (η) difference for breakdown test.	22
Table 11. Percentage of viscosity (η) difference for build-up test.	23
Table 12. Percentage (%) of relative deviation for pressure drop (dP) prediction of orange juice concentrate by using Power Law model.	28
Table 13. Percentage (%) of relative deviation for pressure drop (dP) prediction of orange juice concentrate by using Herschel-Bulkley model.	28
Table 14. Percentage (%) of relative deviation for pressure drop (dP) prediction of <i>Naturell Lätt</i> yoghurt by using Herschel-Bulkley model.	30
Table 15. Percentage (%) of relative deviation for pressure drop (dP) prediction of tomato puree 100% (28-30 °brix) by using Power Law model.	33
Table 16. Generated rheology parameters of five blends and ADY without particles as the curve fitting results with OLS and Power Law and Herschel-Bulkley model.	35
Table 17. Pressure drop (dP) prediction for orange juice concentrate by using Power Law model.	56
Table 18. Pressure drop (dP) prediction for orange juice concentrate by using Herschel-Bulkley model.	56
Table 19. Pressure drop (dP) prediction for <i>Naturell lätt</i> yoghurt by using Power Law model.	57
Table 20. Pressure drop (dP) prediction for <i>Naturell lätt</i> yoghurt by using Herschel-Bulkley model.	58
Table 21. Percentage (%) of relative deviation for pressure drop (dP) prediction of <i>Naturell lätt</i> yoghurt by using Herschel-Bulkley model.	58
Table 22. Pressure drop (dP) prediction for tomato puree 100% (28-30 °brix) by using Power Law model.	59
Table 23. Pressure drop (dP) prediction for tomato puree 100% (28-30 °brix) by using Herschel-Bulkley model.	60

Table 24. Percentage (%) of relative deviation for pressure drop (dP) prediction of tomato puree 100% (28-30 °brix) by using Power Law model.	60
Table 25. Pressure drop rig system calibration by using rapeseed oil.	61
Table 26. Filling behavior responses (per shot) of systematic blends and ambient drinking yogurt (ADY) from one-shot filling rig machine.	63
Table 27. Homogeneity of variance test for the systematic blends.	64
Table 28. ONE-WAY ANOVA test for the systematic blends.	64
Table 29. Post hoc test (Duncan) of outside splash response for systematic blends.	64
Table 30. Post hoc test (Dunnett T3) of impact splash distance response for systematic blends.	65
Table 31. Independent sample t-test for ambient drinking yoghurt (ADY) with/out particles.	65

List of Figures

List of Figures	Pages
Figure 1. Example of industrial food processing lines.	1
Figure 2. Tetra Pak® TT/3 AD (variant option: mid viscosity particle filling) is a filling and packaging machine for ambient drinking yoghurt.	2
Figure 3. Examples of different filling behavior responses documented during filling rig experiment. Ambient drinking yoghurt (ADY) with particle and <i>Naturell lätt</i> yoghurt.	2
Figure 4. Research design of the study consisted of three parts	3
Figure 5. Qualitative illustration of shear stress and viscosity flow curves of time-independent fluids.	4
Figure 6. Qualitative evaluation of thixotropy and rheopexy fluid by the hysteresis loop test.	6
Figure 7. Illustration of break down test sequence and result.	7
Figure 8. Viscosity curve of thixotropy and rheopexy material with modification. Breakdown occurs at a high shear rate, while build-up occurs at a very low shear.	7
Figure 9. Schematic representation of cup-and-bob rotational rheometer.	8
Figure 10. <i>Moody</i> diagram of Newtonian fluid for <i>Darcy</i> friction (f_D) factors.	9
Figure 11. Rotational rheometer and selected cup and bob geometry: serrated concentric cylinder bob, serrated cup, smooth concentric cylinder bob, and smooth cup.	12
Figure 12. Schematic design of the pressure drop rig.	15
Figure 13. Standalone filling rig machine and test package.	16
Figure 14. Visualization of filling behavior responses.	18
Figure 15. Logarithmic plot of shear viscosity (η) and shear rate ($\dot{\gamma}$) from the hysteresis loop test.	20
Figure 16. Logarithmic plot of shear stress (τ) and shear rate ($\dot{\gamma}$) from the hysteresis loop test.	21
Figure 17. Logarithmic plot of shear viscosity (η) and time from the breakdown test at three different shear rates ($\dot{\gamma}$).	22
Figure 18. Build-up test of <i>Naturell lätt</i> yoghurt with pre-shearing at 300 s^{-1} .	24
Figure 19. Build-up test of orange juice concentrate with pre-shearing at 300 s^{-1} .	24
Figure 20. Build-up test of tomato puree 25% (7-7.5 °brix) with pre-shearing at 300 s^{-1} .	24
Figure 21. Build-up-test of tomato puree 100% (28-30 °brix) with pre-shearing 300 s^{-1} .	25
Figure 22. Logarithmic plot of shear stress (τ) and shear rate ($\dot{\gamma}$) from the hysteresis loop test of three different products from the 1 st and 2 nd experiment.	25
Figure 23. Pressure drop measurement of orange juice concentrate from the pressure drop rig.	26
Figure 24. Logarithmic plot of hysteresis loop curve and OLS fitting curve of orange juice concentrate by using Power Law model.	26
Figure 25. Logarithmic plot of hysteresis loop curve and OLS fitting curve of orange juice concentrate for Herschel-Bulkley model.	27
Figure 26. Pressure drop measurement of <i>Naturell Lätt</i> yoghurt from pressure drop rig.	29

Figure 27. Logarithmic plot of hysteresis loop curve and OLS fitting curve of <i>Naturell Lätt</i> yoghurt.	30
Figure 28. Pressure drop measurement of tomato puree 100% (28-30 °brix) from the pressure drop rig.	31
Figure 29. Logarithmic plot of hysteresis loop curve and OLS fitting curve of tomato puree 100% (28-30 °brix) by using Power Law model.	32
Figure 30. Logarithmic plot of hysteresis loop curves (shear rate 1 – 1000 s ⁻¹) of five blends <i>Naturell lätt</i> yoghurt and <i>Långfil</i> and ADY without particles.	33
Figure 31. Logarithmic plot of hysteresis loop curves and OLS-Power Law curve fitting of five blends <i>Naturell lätt</i> yoghurt and <i>Långfil</i> and ADY without particles.	34
Figure 32. Generated K and n values from five blends (<i>Naturell lätt</i> yoghurt and <i>Långfil</i>) and ADY without particles from OLS curve fitting with Power Law model	35
Figure 33. Filamentation and dripping in the yoghurt filling.	36
Figure 34. Impact splash distance and splashing in the yoghurt filling.	36
Figure 35. Filling behavior responses of the systematic blends.	37
Figure 36. Visualization of <i>Kaye</i> effects in fermented milk product (<i>Naturell lätt</i> 75%).	38
Figure 37. Correlation analysis between variables with the filling behavior responses (outside splash and impact splash distance) from five systematic blends.	38
Figure 38. Filling behavior responses of the ADY with and without particle.	39
Figure 39. Kinexus rotational rheometer range and limitations.	48
Figure 40. Hysteresis loop of tomato puree at different dilution % (w/w) by using smooth cup-bob geometry.	53
Figure 41. Hysteresis loop of tomato puree at different dilution % (w/w) by using serrated cup-bob geometry.	53
Figure 42. Build-up test of <i>Naturell lätt</i> yoghurt with pre-shearing at 100 s ⁻¹ .	54
Figure 43. Build-up test of orange juice concentrate with pre-shearing at 100 s ⁻¹ .	54
Figure 44. Build-up test of tomato puree 25% (7-7.5 °brix) with pre-shearing at 100 s ⁻¹ .	54
Figure 45. Build-up-test of tomato puree 100% (28-30 °brix) with pre-shearing 100 s ⁻¹ .	55
Figure 46. Logarithmic plot of hysteresis loop curve and OLS fitting curve of <i>Naturell lätt</i> yoghurt for Herschel-Bulkley model.	57
Figure 47. Logarithmic plot of hysteresis loop curve and OLS fitting curve of tomato puree 100% (28-30 °brix) for Herschel-Bulkley model.	59
Figure 48. Logarithmic plot of hysteresis loop curves and Herschel-Bulkley curve fitting of five blends <i>Naturell lätt</i> yoghurt and <i>Långfil</i> and ADY without particles.	61
Figure 49. Visualization of <i>Kaye</i> effects for shear thinning fluid (shampoo).	62
Figure 50. Bar chart of filling behavior responses from one-shot filling rig machine.	63
Figure 51. Filling sequence (machine setting) of one-shot filling rig.	66

List of Abbreviations and Symbol

Abbreviation	Meaning	
ADY	Ambient Drinking Yoghurt	
AL	Aluminum	
ANOVA	Analysis of Variance	
CI	Confidence of interval	
CSR	Constant Shear Rate	
D20 or D ₂₀	Diameter outer of 20 mm	
D38 or D ₃₈	Diameter outer of 38 mm	
D _{in} (D _i) or Ø _{in}	Inner diameter	
D _{out} (D _o) or Ø _{out}	Outer diameter	
dP	Pressure drop	
dP _{exp}	Pressure drop value resulted from experiment	
dP _{calc}	Pressure drop value resulted from theoretical calculation	
FT	Flowrate Transmitter	
HB	Herschel-Bulkley	
ns	not significant	
OLS	Ordinary Least Square	
PT	Pressure Transmitter	
SSR	Sum of Squared Residuals	
tbsp	Tablespoon	
tsp	Teaspoon	
TT	Temperature Transmitter	
TT/3	Tetra Top 3	
SS	Stainless Steel	

Notation	Meaning	Units
η	Apparent viscosity	Pa.s
K	Fluid consistency in Power Law model	Pa.s ⁿ
n	Fluid behavior index in Power Law model	-
A	Fluid consistency in Herschel-Bulkley model	Pa.s ^b
b	Fluid behavior index in Herschel-Bulkley model	-
τ	Shear stress	Pa
$\dot{\gamma}$	Shear rate	s ⁻¹
τ_w	Wall shear stress	Pa
$\dot{\gamma}_w$	Wall shear rate	s ⁻¹
τ_0	Yield stress	Pa
d	Diameter of the pipe	m
r	Radius	m
Q	Flow rate	m ³ /s
L	Length	m
ΔP	Pressure drop	Pa
a	Dimensionless constant for <i>Chilton and Stainsby's</i> equations	-
b	Dimensionless constant for <i>Chilton and Stainsby's</i> equations	-
c	Dimensionless constant for <i>Chilton and Stainsby's</i> equations	-
X	Dimensionless constant for <i>Chilton and Stainsby's</i> equations	-

D_o	Outer diameter of the pipe	m
D_i	Inner diameter of the pipe	M
v	Velocity	m/s
t	Time	s
Δt or dt	Resting time in the build-up test	s
R^2	Regression coefficient	-
f_D	Darcy friction factors	-
Re	Reynold number	-
y_i	Measured data point	unit
y_j	Predicted data points	unit

1. Introduction

1.1. Background and motivation

As a worldwide company, Tetra Pak is selling more and more food processing lines and more diverse products are packed in Tetra Pak packages. However, some available liquid food products on the market are becoming more complicated with complex rheological properties that can lead to some issues in both the processing and filling lines. For food manufacturers, these typical liquid products are processed and conveyed through the piping systems through numerous heat exchangers and holding tubes (depicted in **Figure 1**). As a big picture, an understanding of fluid behavior such as pressure drop through the pipe plays an important role to determine the system design, efficiency, and longevity, also daily energy consumption (Solorio, 2018). Furthermore, it is also substantial to ensure the long-term reliability of the processing line and cost-saving potential.



Figure 1. Example of industrial food processing lines. From left: tube heat exchanger (AlfaLaval, 2020), modern design of food process line, and continuous cooker (GOLDPEG, 2020).

Furthermore, an understanding of liquid food rheological properties is fundamental to explain and predict how the food products behave in the manufacturers' machines with appropriate measurement, particularly in the pumping process (Martinez-Padilla, Arzate-Lopez, Delgado-Reyes, & Barbosa-Canovas, 1997). One substantial aspect related to fluid dynamics is fluid pressure which is the amount of energy of the fluid as the result of applied pressure on it (Solorio, 2018). This fluid pressure corresponds to the pressure drop.

One way to estimate pressure drop in pipes is by measuring the rheological parameters of the food products by using either a conventional viscometer or rotational rheometer (Martinez-Padilla, Arzate-Lopez, Delgado-Reyes, & Barbosa-Canovas, 1997; Bayod, 2008). However, the prediction of pressure drop in pipes and tubes based on rheological parameters from the rotational rheometer is sometimes found to be incorrect based on manufacturers' experience (Bayod, 2008). Therefore, accurate determination of pressure drop prediction as part of the machinery requirement will be beneficial to design appropriate processing lines for the liquid food products.

Another fluid-in-pipe application in the manufacturer is in the filling machine. Practically, this filling process could potentially result in some filling behavior responses as the consequence of the product's rheology properties. Thus, an understanding of food products rheological properties also can be used to predict several filling behavior responses in the filling machine. An example of the filling and packaging machine produced by Tetra Pak is a Tetra Pak® TT/3 AD (variant option: mid viscosity particle filling) (see **Figure 2** below) used mainly for ambient drinking yoghurt with fruits and cereal particles. Based on a previous study by Williamson & Ostreus (2019), there were several filling behavior responses detected when performing a correlation test in a stand-alone

filling rig, i.e. splashing, dripping, and filamentation (see example in **Figure 3** below). These filling behavior responses could be related to lower filling performance in commercial production. Furthermore, filling performance is an important part to secure operational efficiency and planning in a production plant.



Figure 2. Tetra Pak® TT/3 AD (variant option: mid viscosity particle filling) is a filling and packaging machine for ambient drinking yoghurt with fruits and cereal particles (Tetra Pak, 2020).

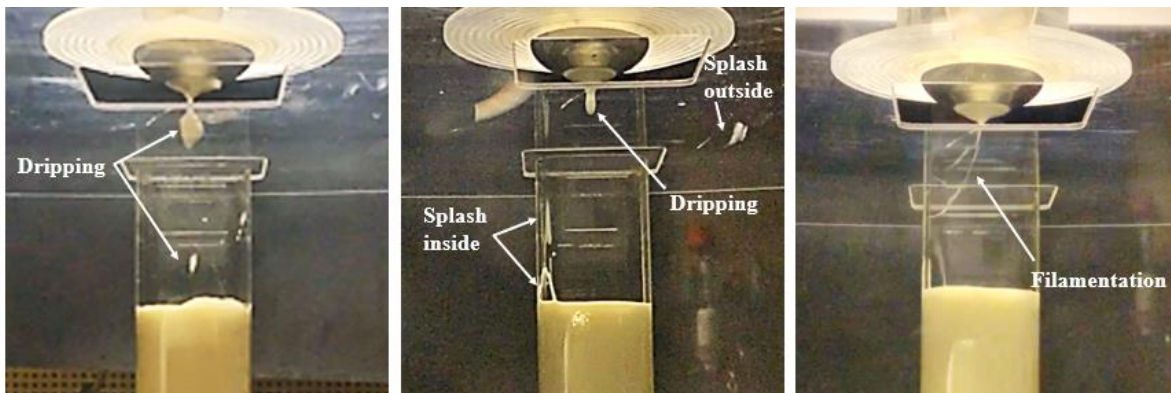


Figure 3. Examples of different filling behavior responses documented during filling rig experiment. Ambient drinking yoghurt (ADY) with particle (*left*) and *Naturell lätt* yoghurt (*right*).

Additionally, the previous study also reported a strong correlation between filling behavior responses (such as splashing and filamentation) and the flow behavior index (Williamson & Ostreus, 2019). Therefore, as a continuation of their study, varying rheological parameters generated from different proportions of two fermented milk products could be used to predict and understand filling responses in the filling machine. This investigation would be beneficial for the food industry to further optimize the filling performance in the filling machine.

Overall, this study was designated as a continuous project from two previous Master Thesis studies: (1) Characterizing the rheology of fermented dairy products during filling and (2) Approaches for improving the rheological characterization of fermented dairy products. The main ideas of this project were to gain an understanding of different liquid food products rheology (characteristics) including their flow behavior in the pipes and to correlate systematic rheological parameters with the filling behaviors (splashing, dripping, and filamentation). These three parts of the study would contribute to the pressure drop prediction from rheological characteristics and to the development of the filling responses indicator (rheological parameters) for industrial application in the filling machine.

1.2. Objectives

Main objectives of this study (visualized in **Figure 4** as the key research activities) were:

- **Obtain a better understanding of the time-dependent behavior of liquid food products with different complexities.**
- **Predict the pressure drop in a straight pipe by using the rheological parameters.**
This part has three sub-objectives, i.e. (1) to investigate and evaluate different rheological measurements and prediction models of liquid food products; (2) to conduct a real-time pressure drop measurement in the pressure drop rig; and (3) to correlate and compare theoretical and experimental pressure drop data.
- **Investigate the correlation between the rheological parameters of liquid food products and their filling behavior systematically.**
This part contains three specific objectives, i.e. (1) to obtain rheological parameters of blend products systematically; (2) to correlate systematic rheological parameters of blend products from point (1) and their filling behavior responses by conducting a one stand filling rig experiment; and (3) to investigate the filling behavior responses of ambient drinking yoghurt with and without particulates.

1.3. Research questions

The project was aimed to answer several research questions as listed below:

- How to describe the relevant rheology for different complex foods?
- How to predict a pressure drop of liquid foods experimentally in the pressure drop rig?
- Can the automatic filling behavior responses be predicted by using measurable systematic rheological parameters?

1.4. Limitations

Limitations of the study are described below:

- This work was based on four products and the mixture (blends) of two fermented milk products.
- Thixotropy behavior cannot be observed at a very low shear rate range $< 1 \text{ s}^{-1}$ and $< 5 \text{ s}^{-1}$ due to rheometer limitation to obtain the trustable value at a very short time (few seconds).

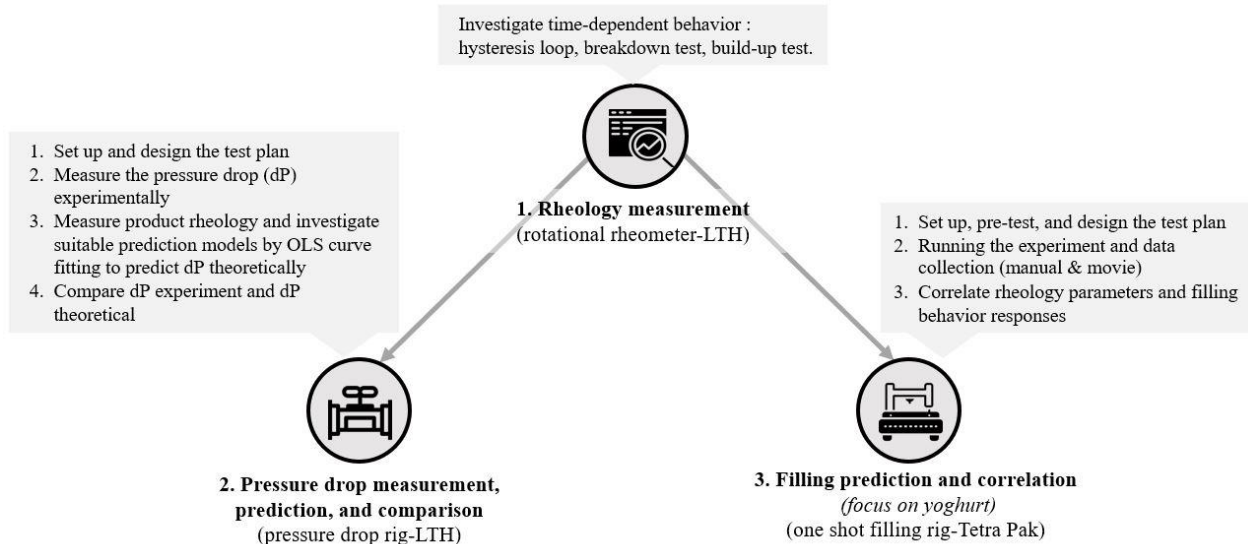


Figure 4. Research design of the study consisted of three parts.

2. Theoretical Framework

2.1. Rheology

Rheology is the study of material deformation and flow behavior. It is commonly associated with the application of the complex fluid materials as its response to stress or shear (Struble & Xihuang, 2001; Kumaran, 2010). Based on the time dependency factor, fluid behavior can be classified as below.

2.1.1. Time-independent fluid behavior

Time-independent fluids characterized by their apparent viscosity (η) are independent on the shear rate ($\dot{\gamma}$) (Collyer, 1973). Time-independent fluid can be divided into two groups of fluid, which are Newtonian and non-Newtonian fluids. The materials that are categorized as Newtonian fluid are water and liquids with low molecular weight. Meanwhile, non-Newtonian fluids have their apparent viscosity as a single function of shear rate or dependent on the shear rate. The material of non-Newtonian fluid has a high molecular weight, i.e. suspension of solid in liquid and high polymer (Collyer, 1973).

Generally, non-Newtonian fluids can be classified into two sub-groups, which are shear thinning and shear thickening (see **Figure 5**). Shear thinning fluids have a characteristic that their apparent viscosity gradually decreases along with the increasing of the shear rate. In contrast, shear thickening fluid shows the opposite characteristic (Collyer, 1973; Chabbra, 2010). Both shear thinning and shear thickening fluids might require yields stress to flow. Additionally, there is an exception for Bingham plastic. This typical fluid requires a certain amount of shear stress (yield stress) to flow or deform (Collyer, 1973). Bingham plastic is classified as non-Newtonian, but when the flow starts, it behaves like a Newtonian fluid with the shear rate is proportional to the shear stress (RheoSense, 2020).

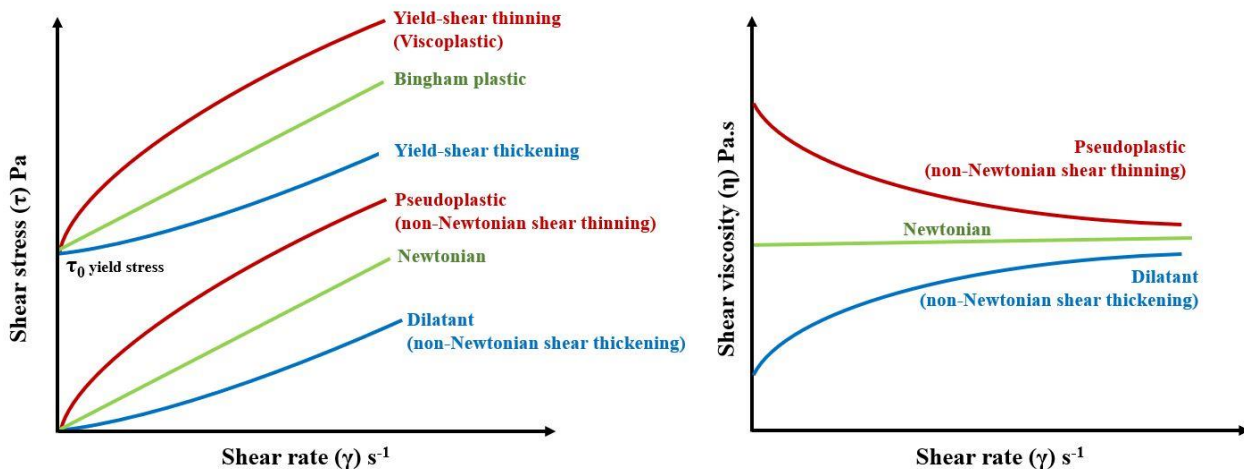


Figure 5. Qualitative illustration of shear stress and viscosity flow curves of time-independent fluids. Adapted from Polymerdatabase (2015) with modification.

Furthermore, mathematical models are commonly used as a tool to describe the rheological model of fluids. There are a variety of rheological models available for time-independent fluids, however, this study focused on these two prediction models:

2.1.1.1. Power Law model

The Power Law model is used to describe a non-Newtonian fluid, such as shear thinning and shear thickening fluids (AntonPaar, 2020). In the Power Law model, the equations can be written either

as shear stress or apparent viscosity equations. The Power Law shear stress equation is described below:

$$\tau = K \dot{\gamma}^{(n)} \quad \dots \text{Eq. 1}$$

Where often the relationship between shear stress (τ) (Pa) and shear rate ($\dot{\gamma}$) (s^{-1}) over log-log plotted can be approximated by a straight line over an interval of shear rate (Chhabra, 2010). The constants K-value ($Pa \cdot s^n$) and n-value describe the fluid consistency and flow behavior index, respectively. The flow behavior index (n) indicates the types of fluid, which are non-Newtonian shear thinning, Newtonian, and non-Newtonian shear thickening fluid with $n < 1$, $n = 1$, and $n > 1$, respectively.

The Power Law model can be expressed in terms of the apparent viscosity (η) equation and it should be used with the condition of shear rate ($\dot{\gamma}$) not equal to zero, as exemplified below:

$$\eta = K \dot{\gamma}^{(n-1)}; \dot{\gamma} \neq 0 \quad \dots \text{Eq. 2}$$

2.1.1.2. Herschel-Bulkley model

For non-Newtonian fluids, with yield stress (τ_0) can be described using HB model. The yield stress is the amount of stress for the fluid to start to flow. This type of fluid will behave like an elastic solid when the external shear stress applied is less than the static yield stress (τ_0). Conversely, when the external shear stress exceeds the value of τ_0 , the fluid may deform or flow, and exhibit either shear thinning or shear thickening behavior (Chhabra, 2010; Moelants, et al., 2014). A type of model that is frequently used to combine the presence of yield stress with different flow behaviors (shear thickening and shear thinning) is the Herschel-Bulkley model. In the Herschel-Bulkley model, the equations can be written either as shear stress or the viscosity equations. The Herschel-Bulkley shear stress equation is written below:

$$\tau = \tau_0 + A \dot{\gamma}^b \quad \dots \text{Eq. 3}$$

Then, the Herschel-Bulkley viscosity equation is exemplified below:

$$\eta = \frac{\tau_0}{\dot{\gamma}} + A \dot{\gamma}^{(b-1)}; \dot{\gamma} \neq 0 \quad \dots \text{Eq. 4}$$

Where the τ (Pa), τ_0 (Pa), η ($Pa \cdot s$), and $\dot{\gamma}$ (s^{-1}) are shear stress, yield stress, apparent viscosity, and shear rate respectively. The constants A ($Pa \cdot s^b$) and b (-) describe the fluid consistency and flow behavior index, respectively. There are three types of flow behavior index, which are $b < 1$, $b = 1$, and $b > 1$ for the case of yield-shear thinning, Bingham plastic, and yield-shear thickening fluids, respectively.

2.1.2. Time-dependent fluid behavior: thixotropy and rheopexy

Some food products exhibit flow behavior which cannot be accurately described by a time-independent rheological model (Chhabra, 2010). As their apparent viscosity (η) is not only a function of the applied shear stress (τ) and shear rate ($\dot{\gamma}$), but also, the time that the fluid has received certain shear. For example, how many stirring times are applied to the fluid in the sample preparation stage and the way the sample is loaded to the viscometer could affect the values of apparent viscosity, shear stress, and shear rate of the product (Chhabra, 2010). Time-dependent fluid behavior is divided into two types, which are thixotropy and rheopexy (see **Figure 6**). Thixotropy behavior means that the product experiencing a structural degradation when the shearing is applied and may regain its structure when at rest (Mezger, 2006). Meanwhile, rheopexy behavior means that the product increases its structural strength when shearing is performed and decreases its structural strength or decomposition when at rest (Mezger, 2006). Both thixotropy

and rheopexy behavior could be reversible or partially reversible (Benezech & Maingonnat, 1994). Qualitatively, there are some methods to evaluate the thixotropy and rheopexy behavior of fluids, and some of these methods are exemplified below:

2.1.2.1. Hysteresis loop test

The objective of the hysteresis loop test is to investigate the time-dependent behavior (thixotropy and rheopexy) of the food products by sweeping up and down the product at a wider range of shear rates. The fluid behavior is measured by applying a single experiment in which the value of the shear rate ($\dot{\gamma}$) continuously increases and decreases at the same rate range (Chabbra, 2010). The hysteresis loop curve can capture the structural decomposition phase. As depicted in **Figure 6**, the thixotropy behavior is indicated by the position of the upward sweep curve at the above of the downward sweep curve, whereas in a rheopexy material, the upward and downward position is inverted.

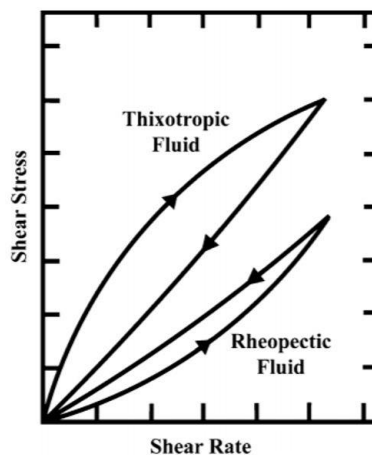


Figure 6. Qualitative evaluation of thixotropy and rheopexy fluid by the hysteresis loop test (Chabbra, 2010).

2.1.2.2. Breakdown test

Pre-shearing has a role to eliminate time effect behavior by applying shear for particular period (Muhammad, 2020). This pre-shearing principle is applied in the breakdown test that aims to investigate the product's breakdown phenomena when applying a constant shear rate for a certain duration as visualized in **Figure 7**. An optimum break down was reached when the viscosity reached a plateau condition, or the viscosity difference was close to 0%. In the break-down test, if the apparent viscosity (η) keeps decreasing during the duration of shearing, thus it shows thixotropy. The opposite result of this test shows a rheopexy behavior (Chabbra, 2010). In the case of a thixotropy fluid, the external shear fosters a breakdown of its structure. On the other hand, when an external shear is applied to a rheopexy fluid, this results in an ability to regain its structure (Chabbra, 2010). To evaluate whether the viscosity increases or decreases during the breakdown test, a viscosity difference ($\Delta\eta$) is calculated between the final viscosity of the product and the initial viscosity (after the target shear rate is obtained) (Mezger, 2006). Additionally, it is common for some fluids to exhibit both thixotropy and rheopexy under a certain combination of concentrations and shear rates (Chabbra, 2010). For instance, in a saturated polyester at 60°C, a time-independent behavior at the shear rate ($\dot{\gamma}$) around 918.5 s⁻¹ is exhibited, and the first rheopexy behavior is observed at the shear rate around 2755 s⁻¹ (Steg & Katz, 1965).

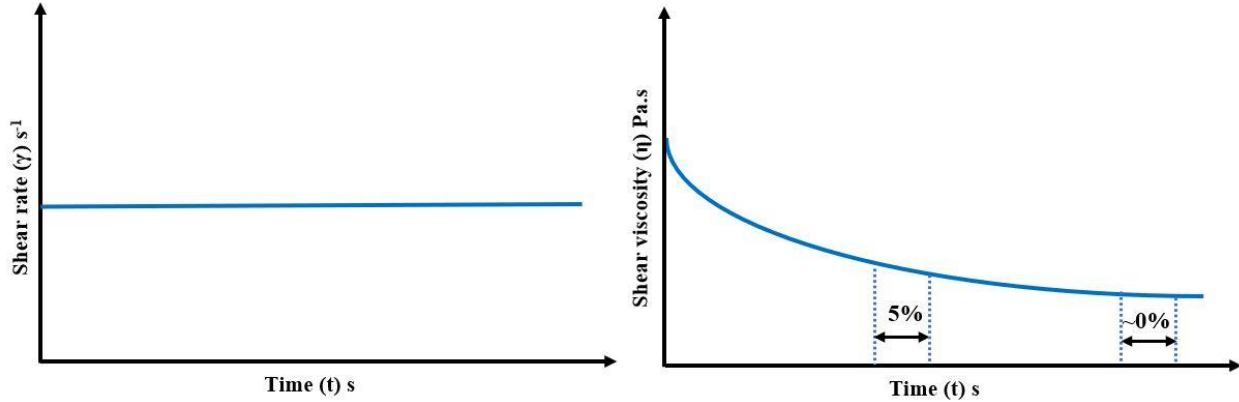


Figure 7. Illustration of break down test sequence (left) and result (right).

2.1.2.3. Build-up test

The build-up test aims to investigate the ability of the product to build-up or regain and recover its structure at very low shear rates after shearing and resting. In some thixotropy fluids, a broken-down or damaged structure may show the ability to regain their structure and come back to the initial viscosity (Struble & Xihuang, 2001). It might occur when the fluid can rest for a long period of time at a constant and low stress level (Chabbra, 2010). The ability of a thixotropy fluid to rebuild its structure can be observed by applying a constant higher shear rate for a certain period (pre-shearing), followed by resting of the material for a certain period of time without any shear as depicted in **Figure 8**. This would be followed by applying a very low constant shear rate for a longer period (Muhammad, 2020). In literature, this test has been investigated for certain thixotropy products, such as body lotion. It was reported when a lotion was sheared at 100 s^{-1} for 5 – 10 s, the apparent viscosity decreased from 80 Pa.s to 10 Pa.s. Then, upon removal of the shear, the product regained its structure almost to its initial viscosity within 50 – 60 s (Chabbra, 2010). Furthermore, this build-up test has been investigated in a food product by Muhammad (2020), which is *Naturell lätt* yoghurt. Based on his study, the longer resting time applied to the *Naturell lätt* yoghurt, the higher the build-up ability of the product.

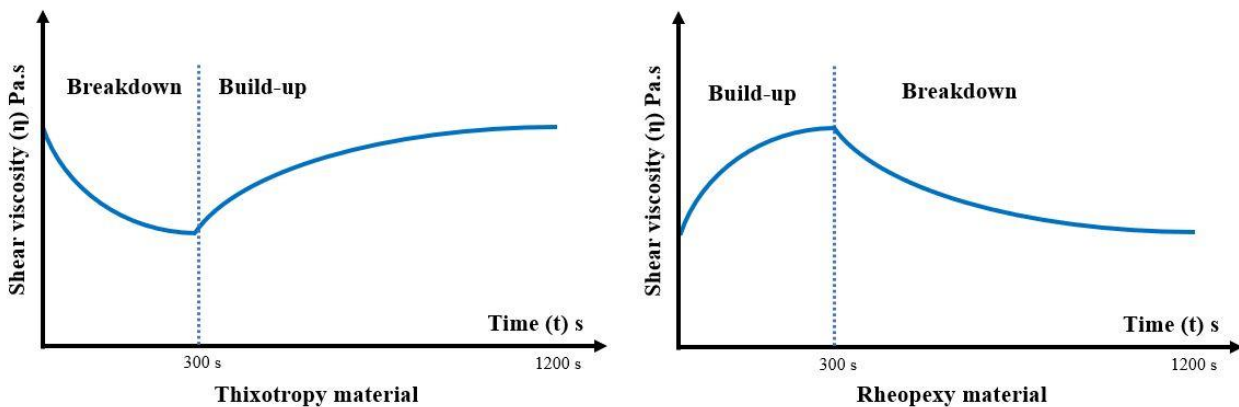


Figure 8. Viscosity curve of (left) thixotropy and (right) rheopecty material (Mezger, 2006) with modification. Breakdown occurs at a high shear rate, while build-up occurs at a very low shear rate.

2.2. Rheology measurement system (rotational rheometer)

A rotational rheometer is a dedicated instrument to enable the rheological measurement for both flow properties (i.e. shear viscosity) and dynamic material properties (i.e. viscoelastic modulus and

phase angle) (Malvern, 2020). This rheometer consists of two coaxial cylinders: rotational inner cylinder (bob) and stationary outer cylinder (cup) as depicted in **Figure 9**. The instrument will lower the bob inside a cup filled with a sample. Principally, this instrument works by measuring and converting the torque into shear stress; and the rotational speed into the shear rate by using a particular equation as a conversion factor (AntonPaar, 2020). The rotational test could be carried out by two operation modes: (1) preset the driving force via shear stress or (2) via shear rate (Muhammad, 2020).

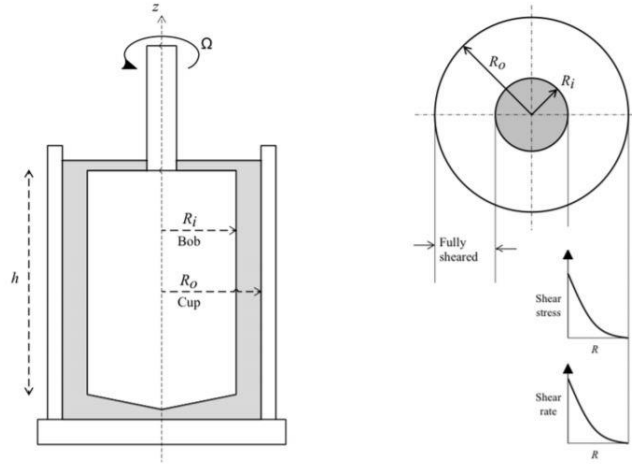


Figure 9. Schematic representation of cup-and-bob rotational rheometer (Radhakrishnan, Lier, & Clemens, 2018).

2.3. Pressure drop

The rig to predict the pressure drop was developed in the 19th century either to measure fluid viscosity in a laminar regime or to estimate pressure drop in the pipe. It is also commonly known as tube viscometer (Bayod, 2008). The advantage of using a pressure drop rig is the ability to measure food products with large particles ($>100 \mu\text{m}$), i.e. tomato puree and in the range of shear rates that applicable for food processing, i.e. $1 < \dot{\gamma} < 1000 \text{ s}^{-1}$. However, the drawbacks of using a pressure drop rig are space and product-consumption compared to the measurement by using a rotational rheometer (Bayod, 2008). In the pressure drop rig, the flow is driven by pressure thus creating a velocity gradient through the tube. The experimental pressure drop is determined over a straight section of the pipe by calculating the pressure difference (ΔP). Besides a pressure drop, a volumetric flow can also be measured in the pressure drop rig, and these two parameters can be used to determine the theoretical shear stress and shear rate, respectively (Bayod, 2008).

Furthermore, the theoretical pressure drops (ΔP) calculation requires the understanding of the type of fluid flow for example laminar, transient, and turbulent. In fluid mechanics, the *Moody* diagram could be used to predict the pressure drop or flow rate of Newtonian liquid flow in a pipe (Graham, Pullum, & J, 2016). This *Moody* chart presents a *Darcy* friction factor (f_D) as a function of the *Reynold* number and the relative internal roughness of the pipe (see **Figure 10**).

For non-laminar flow (*Reynold* number >2100), the *Moody* chart will be used to define the friction factor and to be included in the calculation. However, for laminar flow (*Reynold* number <2100) condition, the friction factor is defined from the theoretical *Darcy* factor (f_D) equation ($64/Re$) and not influenced by the surface roughness (Singh & Heldman, 2014). The pressure drop is calculated by inserting the f_D (where $f_D = 4f_f$) into the pressure drop equation as shown below:

$$\Delta p = f_D \frac{\rho v^2 L}{2d} \quad \dots \text{Eq. 5}$$

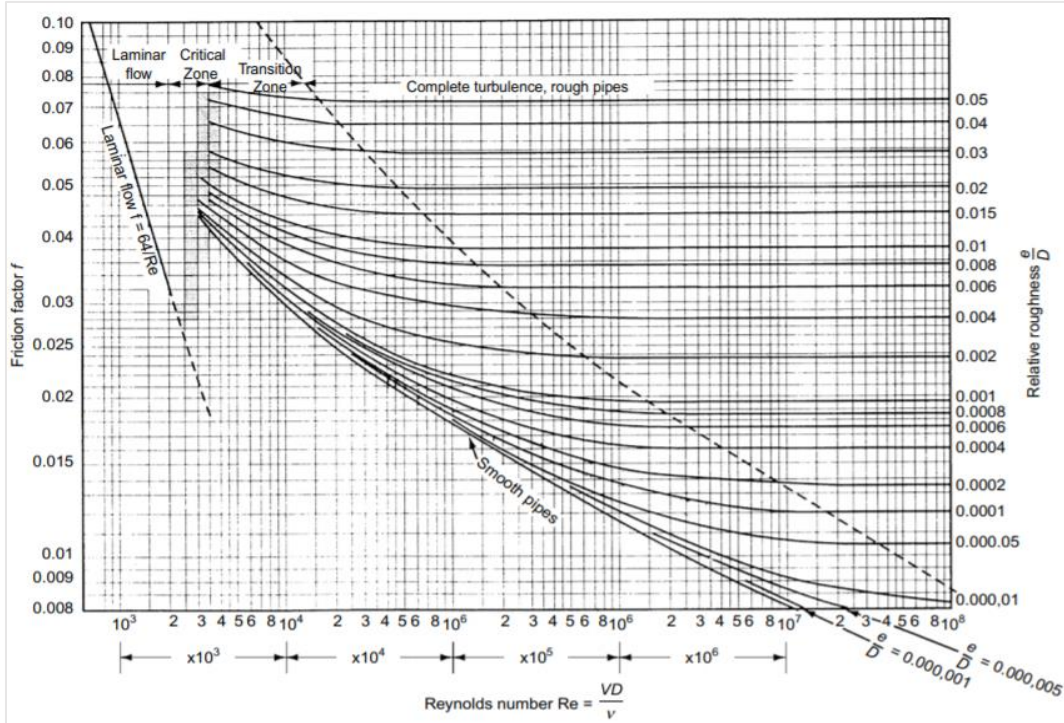


Figure 10. Moody diagram of Newtonian fluid for Darcy friction (f_D) factors (Shashi & Pramila, 2010).

In the case of non-Newtonian fluid with laminar flow, the theoretical value of pressure drop is determined by inserting the generated rheology parameters (n or b , K or A , and yield stress values) from the curve fitting into the *Rabinowitsch-Mooney* equations for Power Law model (Steffe, 1996) and *Chilton & Stainsby* equations for Herschel-Bulkley model (Chilton & Stainsby, 1998).

For generalized form (both Power Law and Herchel-Bulkley), the wall shear rate is defined as:

$$\gamma_w = \left(\frac{3n+1}{4n}\right) \left(\frac{32Q}{\pi d^3}\right) \quad \dots \text{Eq. 6}$$

Using the Power Law prediction model, the wall shear stress is generated from the volumetric flowrate equation below:

$$Q = \pi r^3 \left(\frac{n}{3n+1}\right) \left(\frac{\tau_w}{K}\right)^{1/n} \quad \dots \text{Eq. 7}$$

Using the Herschel-Bulkley prediction model, the wall shear stress is generated from the following equations below:

$$\frac{\Delta P}{L} = \frac{4K}{d} \left(\frac{8v}{d}\right)^n \left(\frac{3n+1}{4n}\right)^n \left(\frac{1}{1-X}\right) \left(\frac{1}{1-aX-bX^2-cX^3}\right)^n \quad \dots \text{Eq. 8}$$

where X , a , b , and c are given by,

$$X = \frac{\tau_0}{\tau_w} = \frac{4L\tau_0}{\Delta P d}; \quad a = \frac{1}{(2n+1)}; \quad b = \frac{2n}{(n+1)(2n+1)}; \quad \text{and} \quad c = \frac{2n^2}{(n+1)(2n+1)} \quad \dots \text{Eq. 9}$$

The *Chilton & Stainsby* equations above (**Eq. 8** and **9**) could be simplified becomes a volumetric flowrate equation (**Eq. 10**) as an analytical solution for wall shear stress.

$$Q = \pi r^3 \left(\frac{n}{3n+1}\right) \left(\frac{\tau_w}{K}\right)^{1/n} \left(1 - \frac{\tau_0}{\tau_w}\right)^{1/n} \left\{1 - \frac{\tau_0/\tau_w}{2n+1} \left[1 + \frac{2n}{n+1} \left(\frac{\tau_0}{\tau_w}\right) \left(1 + \frac{n\tau_0}{\tau_w}\right)\right]\right\} \quad \dots \text{Eq. 10}$$

Lastly, the pressure drop could be calculated by inserting calculated τ_w from previous equations into the wall shear stress equation below:

$$\tau_w = \frac{\Delta P d}{4L} \quad \dots \text{Eq. 11}$$

Where d (m), r (m), Q (m^3/s), v (m/s), and ΔP (Pa) are inner pipe diameter, inner pipe radius, flow rate, velocity, and the pressure drop in the pipe, respectively. L (m) is the distance (length) between pressure sensors 1 and 2 in the pipe. Meanwhile, γ_w (s^{-1}) and τ_w (Pa) are the wall shear rate and wall shear stress in the pipe, respectively.





3. Materials and Methods

This section will describe the materials and methods (including procedures) used to run the experiments in this study.

3.1 Materials

The liquid food products used for this study was presented in **Table 1** below. The products used for the 1st stage of the study were purchased from local retailers, while products used for the 2nd and 3rd stage were supplied from Tetra Pak.

Table 1. Sample for three stages of research study.

No.	Product	Description	Stage	Batch production
1		Naturell lätt yoghurt (1000 g) (0.5 % fat, brand <i>Skånemajerier</i>) Ingredients: pasteurized milk, milk protein, yoghurt culture, and vitamin D	1	Data from Muhammad (2019)
			2	Best before 02 Apr 20 (6) 06:38
			3	Best before 06 May 20 (6) 09:19
2		Tomato puree (200 g) (28-30° brix, brand ICA) Ingredients: tomato puree	1	Best before 30-11-2021 ATT1 J 325 <2>
3		Orange juice concentrate Apelsin (200 mL) (8.8 g sugar, brand I love Eco from ICA) Ingredients: orange juice from concentrate	1	Best before 17 Sep 20 16:12 (0016A)
4		Tomato puree (4.55 kg) (28-30° brix, brand <i>Arany Facan Suritett Paradicsom</i>).	2	Best before 12 Sep 22 (0219)
5		Orange juice concentrate Apelsin (1000 mL) (8.5% sugar, brand <i>Kiviks Musteri</i>)	2	Best before 20 Aug 20 17:14 0051
6		Långfil yoghurt (1000 g) (3.0% fat, brand Arla) Ingredients: high pasteurized milk, fil culture, and vitamin D	3	Best before 29 Apr 20 (SE 1009)
7		Ambient drinking yoghurt (ADY) (200 g) (contains fat and fruit particles, Tetra Pak) Ingredients: milk, sugar, yoghurt culture, and stabilizer.	3	Production date 28 Feb 19 batch 3

Note: stage 1 refers to the rheology measurement, stage 2 refers to the pressure drop measurement by using pressure drop rig, and stage 3 refers to the filling prediction and correlation by using one-shot filling rig.

3.2. Methods

3.2.1. Sample preparation

The procedure of sample preparation is exemplified below.

1. Freshly opened products within the shelf-life were used for each measurement.

2. The chilled products (*Naturell lätt* and *Långfil* yoghurt) were kept at ± 6 °C and the ambient products (tomato puree, orange juice concentrate, and ambient drinking yoghurt) were kept at ± 20 °C.
3. The products were homogenized by tilting up and down for 180°: 10 times for the *Naturell lätt* yoghurt, orange juice concentrate, and ambient drinking yoghurt, and 40 times for *Långfil* yoghurt. Meanwhile, the tomato puree did not require any inversions as the product is solid-thick and consistent.
4. The packaging of the products was opened by cutting from the top part by using scissors for the *Naturell lätt* yoghurt, orange juice concentrate, and ambient drinking yoghurt. Meanwhile, for the tomato puree in the tube package, the package was opened by cutting the bottom of the tube with scissors. The tomato puree in the can package was opened by cutting the lid with a can opener.
5. For the rheological analysis, the sample was poured into a plastic cup. Meanwhile, for the tube experiment, the sample was directly poured into the feeding (balance) tank.
6. The sample was stirred by using a spoon for two times (except for the tomato puree that required 20 times) in a clockwise direction.
7. For the rheological analysis, the sample was placed into the cup:
 - Approximately 17.16 ml or 4 tbsp for orange juice concentrate.
 - Approximately 17.16 g or 2-3 tbsp for *Naturell lätt*, *Långfil*, and ADY.
 - Approximately 4-5 tsp for tomato puree.
 The rheometer cup and bob were cleaned with distilled water and refilled with a new sample to start a new measurement.

3.2.2. Standard method for rotational rheometer measurement

Before measuring the samples, it was necessary to determine these following parameters:

1. Cup and bob geometry; a serrated cup (AL) and bob (SS) geometry were selected for *Naturell lätt* yoghurt, *Långfil*, ADY, and orange juice concentrate products. Meanwhile, a smooth cup (SS) and bob (SS) geometry were chosen for tomato puree products by considering the strange curve resulted from serrated geometry as presented in **Appendix 7.8**. The cup and bob geometry used in this study are presented in **Figure 11** below.

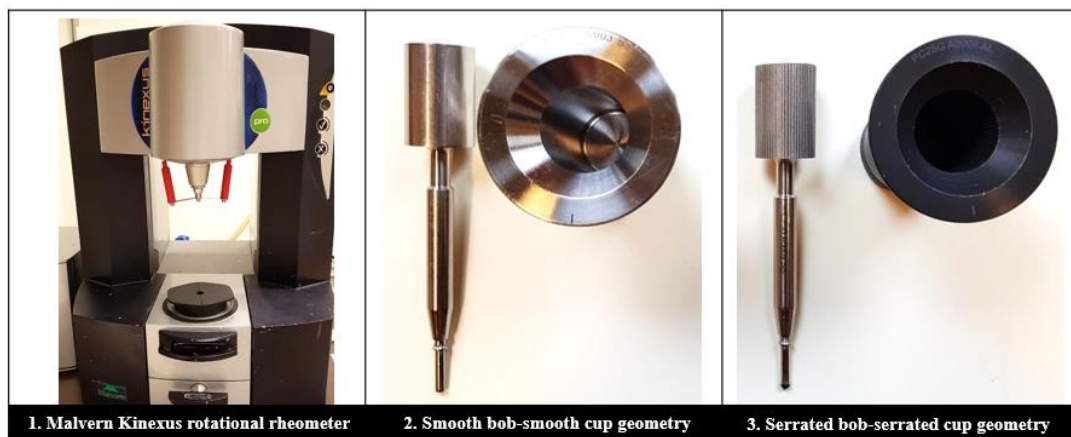


Figure 11. Rotational rheometer and selected cup and bob geometry: serrated concentric cylinder bob (C25G A0009SS: PC25 SPLINED), serrated cup (PC25G A0008AL), smooth concentric cylinder bob (C25 SC0053SS: PC25 DIN C0052 AL), and smooth cup (PC25 C0003SS).

2. Measurement temperature: is the temperature at which the measurement will be conducted. In the first stage of the study, the measurement temperature was set to be at 20 °C based on previous studies performed by Williamson and Ostreus (2019) and Muhammad (2020). Meanwhile, for the 2nd and 3rd stages, the measurement temperature was based on the actual temperature of the product in the pressure drop rig and filling rig experiment, which was 16 – 18 °C, and 22 °C, respectively.
3. Resting time; is the time required for adjusting the product temperature (temperature equilibration). It also aimed for product relaxation from any possible shearing after gap setting and loading step (Mezger, 2006). The resting time for all the measurements was set to be 60 s (Williamson & Ostreus, 2019; Muhammad, 2020). Shear rate range; is the value of shear ($\dot{\gamma}$) added into the program sequence of measurement. It refers to product characteristics and applications. The shear rate range 1 - 1000 s⁻¹ was selected according to a study by Muhammad (2020) to cover a wider range of shear rate applications in the hysteresis loop test.
4. Samples per decade; is defined as the number of sampling points captured by the rheometer during a decade. The 10-samples per decade was used according to (Muhammad, 2020).
5. Stabilization time; is the time required for the product to reach less than 5% of viscosity drop during a 10 s interval (Williamson & Ostreus, 2019). The stabilization time was determined by applying the constant shear rate (CSR) for each product. The importance of the stabilization time in practice is to improve the data accuracy during measurement since the sample tends to reach the plateau condition. Additionally, this parameter acts as a measurement duration to avoid transient effect at a low shear rate. Detail method about stabilization measurement and determination can be seen in **Appendix 7.3**.

Table 2. General setting for the rheometer measurement (detailed instruction in **Appendix 7.1**).

Measurement temperature	20 °C (or depends on the real application)
Resting time	60 s
Shear rate range	1 - 1000 s ⁻¹
Samples per decade	10
Stabilization time	(defined by CSR method)
Geometry	Serrated cup AL-bob SS (orange juice concentrate and <i>Naturell lätt</i> yoghurt) and smooth cup SS-bob SS (tomato puree)

3.2.3. Rheology measurements

The measurement sequences for hysteresis loop, breakdown, and build-up tests are presented in **Table 3**, **Table 4**, and **Table 5**, respectively. However, due to time constraints, only tomato puree 25%, and 100% were investigated for the build-up test, as the representative product of tomato puree at different dilutions. Evaluation of the build-up test was done by calculating a viscosity difference between the viscosity of the treated sample (at the t = 5 s) and the viscosity of the control sample (no pre-shear) (at the t = 5 s). Meanwhile, the breakdown test result was evaluated by calculating the viscosity difference between the final (at the t= 300 s) and the initial (at the t = 11 s) viscosity.

Table 3. Measurement sequence for hysteresis loop test.

Sample	Sequence	Stabilization time	Complete time	Sampling per decade	Cup-bob geometry
Orange juice concentrate	Sweep up (1-1000 s ⁻¹)	30 s	26 min	10 sampling points	Serrated
<i>Naturell lätt</i> yoghurt		50 s	52 min		Serrated
Tomato puree (w/w) (100%, 75%, 50%, 25%)	Sweep down (1000-1 s ⁻¹)	20 s	15 min		Smooth

Table 4. Measurement design for breakdown test.

Constant shear rate (s ⁻¹)	Time duration (s)	Sampling interval (per second)
30	300	1
100	300	1
300	300	1

Table 5. Measurement design for build-up test.

Treatment	Pre-shearing rate (s ⁻¹) for 300 s	Resting time (s) Δt	Build-up (s-1) for 900 s
Control (no pre-shear)	None		1
Treatment 1 pre-shearing	100	0	1
		30	
		90	
		300	
Treatment 2 pre-shearing	300	0	1
		30	
		90	
		300	

3.2.4. Curve fitting method

The non-linear regression analysis by using SOLVER was applied to investigate both the Power Law and Herschel-Bulkley prediction models. The Ordinary Least Square (OLS) linear regression was chosen as the curve fitting method due to its simplicity and reliability from a previous study by minimizing the sum of squared residual values (Muhammad, 2020). The formula used as the minimizing factor is exemplified below (measured data y_i and predicted data points y_j):

$$SSR = \min \sum [y_i - y_j]^2 \quad \dots \text{Eq. 12}$$

The sum of squared residuals (SSR) value generated from the OLS curve fitting describes the closeness of predicted data to the actual data. The lower the SSR value, the better the fit (Muhammad, 2020). The output from the flow curve (hysteresis loop) extrapolation is the rheology parameter i.e. consistency index, flow behavior index, and dynamic yield stress.

3.2.5. Pressure drop measurement

The design of the pressure drops rig in this study consisted of three different pipe diameters, which were $D_o = 0.020, 0.025,$ and 0.038 m. However, only two diameters ($D_o = 0.020$ and 0.038 m) were used in the experiment. A schematic design of the pressure drop rig is shown in **Figure 12** below.

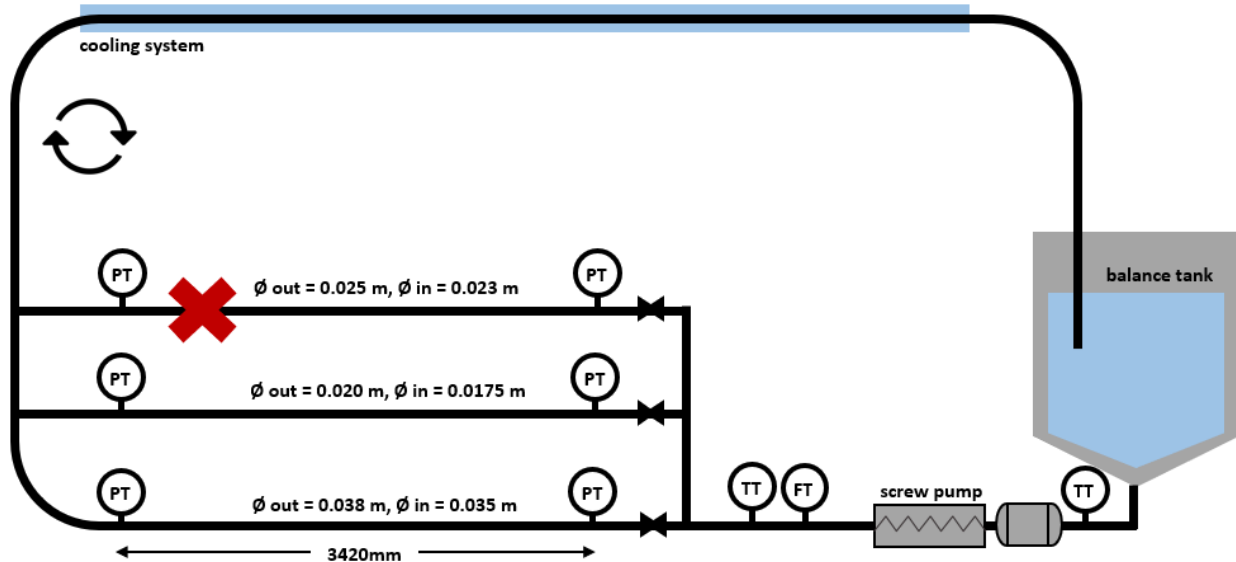


Figure 12. Schematic design of the pressure drop rig (only $D_{o=}$ 0.020 and 0.038 m used) (adapted from tube viscometer of Bayod, 2008 with modification).

Details and specification of the pressure drop rig

The product (sample) was poured into a balance or feeding tank (*Wedholms* type DH 653 AD, maximum capacity of 200 L). Then, the product was pumped from the balance tank by a screw pump (*Knoll Maschinenbau GmbH*, type MX 30-S-50/20, maximum 115 Hz). The pressure drop was measured over the pipe length of 3.42 m in each pipe by using two pressure transmitters (PT) (*Wika* P-11: 0-2.5 bars and 0-16 bars). The product temperature was measured by using a temperature transmitter (TT) from Tetra Pak, while the volumetric flow was determined by using a magnetic flow transmitter (*Process-Data Silkeborg ApS* Denmark, size C 25, maximum flow of 10 m³/h, maximum temperature and pressure of 100 °C and 10 bars).

The pressure drop rig system was calibrated with a rapeseed oil at 17 °C ($\eta = 0.08$ Pa.s, $n = 1$) to evaluate the accuracy of the system (see **Appendix 7.13**). After pouring the products into the balance tank, it was pumped through all of the pipes to fill in the system and recirculated at a low flow rate (± 300 l/h) for 5 min (for orange juice concentrate and *Naturell Lätt* yoghurt) and 10 min (for tomato puree 100% 28-30 °brix). The measurement was started by closing the valves from two other unused pipe diameters, then changed the frequencies to reach the target velocity (flow rate). The pressure drops, flow rate, and temperature were recorded by using **NiLabView 2018** software, with a sampling rate of 1/s during 300 s. The design experiment for each measurement is presented in **Table 6** below (see **Appendix 7.4** and **7.5** for detailed instructions), where the D_{20} was measured twice for thixotropy investigation. Also, the flowmeter performance for each product was calibrated by using bucket method as presented in **Appendix 7.6** (the correction constants for orange juice, *Naturell* yoghurt, and tomato puree were 0.91, 0.96, and 0.93, respectively).

During each measurement, the samples for the rheological parameter analysis in the Kinexus rotational rheometer were taken after first velocity (0.25 m/s) measurement in the first D_{20} and the last velocity (1.50 m/s) measurement in D_{38} pipe diameter. The method for the rheological

parameter analysis was referred to in **Chapter 3.2.3**. Due to time constraints, each measurement was performed only in one replication for both the pressure drop rig and the rotational rheometer.

Table 6. Design experiment of the pressure drop rig measurement.

Sequence of each measurement	Approximate velocities
1 st D _o 0.020 m (D _i 0.0175 m)	0.25 m/s, 0.5 m/s, 1 m/s, 2 m/s
D _o 0.038 m (D _i 0.0350 m)	0.25 m/s, 0.5 m/s, 1 m/s, 1.5 m/s
2 nd D _o 0.020 m (D _i 0.0175 m)	0.25 m/s, 0.5 m/s, 1 m/s, 2 m/s

3.2.6. Filling prediction and correlation

In this section, materials, equipment, experimental design, filling behavior responses, and statistical analysis tools for correlation analysis were presented. A detailed explanation of the test plan is presented in **Appendix 7.7**.

3.2.6.1. Experimental design

Material and equipment used for one-shot filling rig test were:

- Stand-alone filling rig: Tetra Top One-Shot (Tetra Pak AB, Lund, Sweden) (**Figure 13**).
- Installed camera in the filling rig and iPhone camera.
- 15 transparent dummy packages of Tetra Top® Mini 200 Taishan A38 packages.
- Image analysis software (Windows media player, Coach’s Eyes mobile apps).
- 5 blends of Långfil and *Naturell Lätt* yoghurt: 0%, 25%, 50%, 75%, and 100% (w/w)
- Same Ambient Drinking Yoghurt (ADY) product with and without particles (sieved).

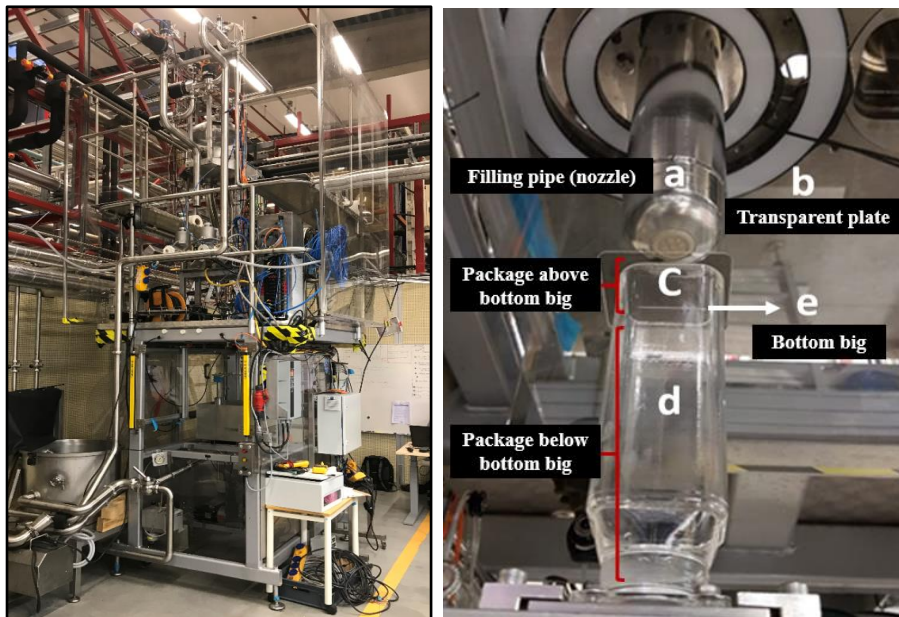


Figure 13. Stand-alone filling rig machine (*left*) and test package (*right*).

The experimental design of one-shot filling rig test was described in **Table 7** below.

Table 7. Description of experimental design used during one-shot filling rig testing at Tetra Pak AB.

Sample	Machine setting	Weight	Filling shots per product
5 blends (0%, 25%, 50%, 75% and 100% <i>Naturell</i>)	Setting 1	± 200 g	2 set x 15 = 30
2 ADY (with & without particles)	Setting 2	± 200 g	2 set x 15 = 30

Note: each set consisted of 15 filling shots.

During the one filling shot, the transparent package was raised towards the fill nozzle. At the same time, the fill nozzle was opened, and the product came out into the package. The endpoint of the fill cycle was indicated by closing off the fill nozzle. At the same time, the transparent package was lowered down to the default level. One filling cycle lasted for 1.6 s. Finally, the transparent package was taken manually by an operator, and the other new (empty) transparent package was placed into the filling rig to start the next filling shot. There were two different machine settings used: (1) setting 1 as the worst machine set up to generate the filling behavior responses, and (2) setting 2 as the standard-setting used at Tetra Pak AB in the commercial TT/3 filling machine. Both settings will lift the package in place before the product hits the bottom part of the package. The illustration diagram of machine setting 1 and 2 is presented in **Appendix 7.18**.

3.2.6.2. Filling behavior responses

The type of filling behavior responses and quantification method are exemplified in **Table 8** below.

Table 8. The type of filling behavior responses and inspection for each response.

No.	Type of Responses	Quantification		Detail
		Manual	Video	
1.	Splashing (droplet and streak) <ul style="list-style-type: none"> • Droplet & streak inside the package (below and above the bottom big) • Splashing outside the filling pipe. • Splashing on the transparent plate • Impact splash 	x	x	<ul style="list-style-type: none"> • Manual inspection per 5 shots in the filling pipe and transparent plate • Video (image) analysis per shot in the package below and above the bottom big and measure the splashing length by using caliper on the screen.
2.	Dripping		x	Video (image) analysis per shot.
3.	Filamentation		x	Video (image) analysis per shot. <i>For filamentation and dripping investigation, filming was set up to 2-3 s after each filling shot.</i>

(adapted from Williamson & Ostreus, 2019 with modification).

The visualization of each filling behavior response definition is depicted in **Figure 14**. Splashing is defined as the formation of a small jet of a product that detaches from the bulk of the product and moves outside of the desired fill volume (Williamson & Ostreus, 2019). This includes several types of splash response, which are: (1) droplet and streak inside the package (below and above the bottom big), (2) splashing outside the filling pipe; (3) splashing on the transparent plate; and (4) impact splash which means the first splash occurs from the bottom of the package, that is measured as the splash distance (cm) from the bottom big by using a caliper. Dripping is defined as a delayed formation of a droplet from the product remaining on the filling nozzle after the end of the filling

cycle. It can either dangle or fall into the package. Lastly, filamentation is the formation of a ‘string’ of the product reaching from the fill nozzle to the surface of the packaged product. It is caused by the stream of the fill jet narrowing, following by the closure of the filling nozzle. This filamentation still presents after the end of the filling cycle, indicated by the closing of filling nozzle (adapted from Williamson & Ostreus, 2019 with modification).

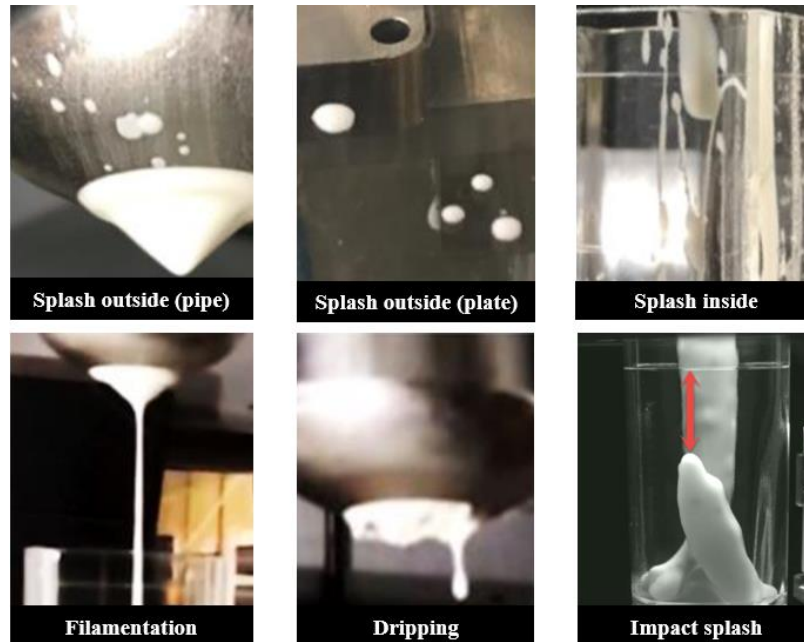


Figure 14. Visualization of filling behavior responses (Williamson & Ostreus, 2019; Tetra Pak “*TestResult*” template, 2020).

3.2.6.3. Data analysis

The quantified data per shot was analyzed by using Excel and IBM SPSS Statistics 25 (independent sample t-test for ADY and one-way Analysis of variance or ANOVA for systematic blends). Linear regression as correlation analysis by using TRENDLINE function from Excel was chosen to investigate the strength of the relationship between the independent variables (rheological parameters for the systematic blends) and responses (filling behaviors: outside splash of the package and impact splash distance in the package). The result would be presented in the form of a mathematical equation ($y=mx + c$) and regression coefficient ($0 < R^2 < 1$) (Kumari & Yadav, 2018), indicating goodness of fit for the linear regression model (Frost, 2020).

To minimize the limitations of the whole study, thus several control measures were applied:

- Always using newly opened product (sample) from the same best before date to minimize batch to batch variations for the same stage of this study.
- Conduct a preliminary study to investigate repeatability from the rheometer measurement.
- Apply Ordinary Least Square (OLS) curve fitting by considering its simplicity.
- Calibrate and verify the instrument used for measurement i.e. internal calibration by using rapeseed oil for pressure drop rig and verify the rotational rheometer by using sugar solution (Paul, 2020) in LTH, pressure sensor calibration, reference data from the literature (previous study), pre-test, and quality department analysis from Tetra Pak AB, Lund.

4. Results and discussion

4.1. Rheology measurements

All rheology measurements in this section were obtained from the sample with the same batch production.

4.1.1. Stabilization time

The determination of the stabilization time was based on the longest time at three different shear rates in each product. The constant shear rates (30 s^{-1} , 100 s^{-1} , and 300 s^{-1}) were selected to represent a wider range of shear rates in the further test, hysteresis loop ($1\text{-}1000 \text{ s}^{-1}$). Based on the data presented in **Table 9**, the stabilization time of tomato puree, orange juice concentrate, and *Naturell lätt* yoghurt, were 20 s, 30 s, and 50 s, respectively. These stabilization times would be used as one of the parameters to design measurement sequences for the hysteresis loop test as the time interval before picking the measured data point.

Table 9. Stabilization time determination of the sample at three different shear rates.

Sample	Shear rate (s^{-1})		
	30	100	300
Orange juice concentrate	20 s	30 s	30 s
<i>Naturell lätt</i> yoghurt	40 s	40 s	50 s
Tomato puree	20 s	20 s	20 s

Note: measurements were done in duplicate for tomato puree and orange juice concentrate, and triplicate for *Naturell lätt* yoghurt. Data of *Naturell lätt* yoghurt was obtained from *Muhammad (2020)*, while others from the 1st stage study.

The longer stabilization time needed for *Naturell lätt* yoghurt might be due to the complex structure or the network of the product (gel network from exopolysaccharides of yoghurt).

4.1.2. Hysteresis loop

The hysteresis loops of three different products consisting of the upward and downward sweep are presented in **Figure 15** and **16**. Four different phenomena can be observed from the hysteresis loop, which are: (1) the height of the curve indicating viscosity of the product; (2) the slope of the curve indicating the flow behavior index; (3) the position of sweep up and sweep down curve indicating time-dependent behavior (thixotropy and rheopexy); and (4) the curve shape (straight or bent).

First, as depicted in **Figure 15**, tomato puree 100% (28-30 °brix) had the highest viscosity or consistency or K-value (indicating by the higher curve height), followed by tomato puree 75% (21-22.5 °brix), tomato puree 50% (14-15 °brix), *Naturell lätt* yoghurt, tomato puree 25% (7-7.5 °brix) and orange juice concentrate. These results were aligned with the shear stress curve, as depicted in **Figure 16**. Second, as the slope refers to the flow behavior index (n-value), the thicker the product, the lower its slope is. Therefore, it could be seen qualitatively that orange juice concentrate had the highest slope, and tomato puree 100% (28-30 °brix) had the lowest slope or n-value. Meanwhile, the rest of the samples had quite similar slope.

Thirdly, both the thixotropy and rheopexy behavior can be qualitatively evaluated through the position of the upward and downward sweep curve. As can be observed in **Figure 16**, the logarithmic plot between shear stress and shear rate showed that all products had a shear thinning with thixotropy behavior (time-dependent) because of the upward curve position was above the downward curve. Besides, all products were not able to regain its initial structure after sweeping

up and down. As indicated with the initial shear stress was different from the final shear stress; thus, it can be concluded that a thixotropy behavior existed in these three products. However, it was also noticeable that the tomato puree (25%, 50%, 75%, and 100%) had a slight rheopexy behavior depending on the shear rate region. This rheopexy phenomenon also could be identified when the upward curve position was below the downward curve.

Lastly, the curves from all products showed a tendency of straight-line pattern with a slight bent for tomato puree products for either the viscosity-shear rate plot or the stress-shear rate plot (see **Figure 15** and **16**). This indicates that both the Power Law and Herschel-Bulkley approach might be suitable to explain the rheology properties and the phenomena of the studied products.

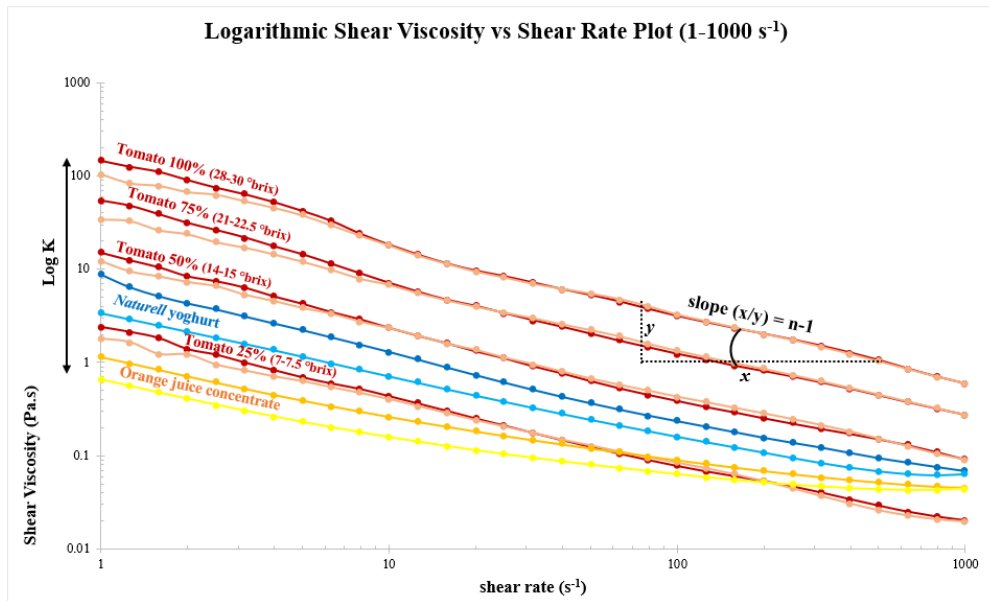


Figure 15. Logarithmic plot of shear viscosity (η) and shear rate ($\dot{\gamma}$) from the hysteresis loop test. Darker color represents UPWARD sweep, while a brighter color represents DOWNWARD sweep for each product. Measurements were done in one replicate for tomato puree (25%, 50%, and 75%) and duplicate for orange juice concentrate and tomato puree (100%), and triplicate for *Naturell lätt* yoghurt. *Naturell lätt* yoghurt data was from *Muhammad (2020)*.

Additionally, a qualitative comparison of the thixotropy effect in different products could be identified from the enclosed area between the upward and downward sweep as the degree of thixotropy or rheopexy (Benezech & Maingonnat, 1994). It could be concluded that the *Naturell lätt* yoghurt had the highest thixotropy behavior, followed by the orange juice concentrate. Meanwhile, tomato puree (25%, 50%, 75%, and 100%) did not show much thixotropy effect from this hysteresis loop test with slight rheopexy behavior. The big difference between the upward and the downward curve of the *Naturell lätt* yoghurt indicated that the product is shear sensitive. Stirring or shearing could damage yoghurt structure (coagulum). It can be summarized from the hysteresis loop test that the difference time-dependent behavior in each product might result from the complexity of product including its interaction (network) and structure.

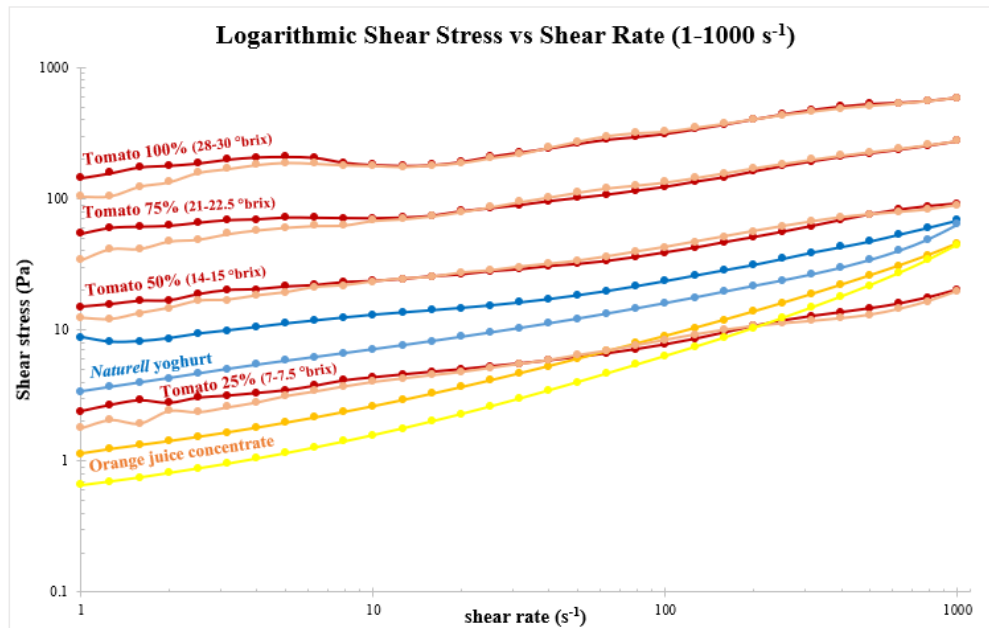


Figure 16. Logarithmic plot of shear stress (τ) and shear rate ($\dot{\gamma}$) from the hysteresis loop test. Darker color represents UPWARD sweep, while a brighter color represents DOWNWARD sweep for each product. Measurements were done in one replicate for tomato puree (25%, 50%, and 75%) and duplicate for orange juice concentrate and tomato puree (100%), and triplicate for *Naturell lätt yoghurt*. *Naturell lätt yoghurt* data was from Muhammad (2020).

4.1.3. Breakdown

Another test to investigate the time-dependent behavior was the breakdown test. In principle, the constant shear rate at a particular time was applied to observe the breakdown phenomena within the product as indicated by a decreasing or increasing viscosity versus time. The visual presentation of the breakdown effect was shown in **Figure 17** as the plot of shear viscosity and time. As could be seen visually, the viscosity of the orange juice concentrate and *Naturell lätt yoghurt* kept decreasing when a constant shear rate was applied to the products, which indicated a thixotropy behavior.

However, in the case of tomato puree at the shear rate of 300 s^{-1} , all the concentrations of tomato puree showed a slight rheopexy behavior where the viscosity kept increasing at a constant shear rate. However, at the shear rate 100 s^{-1} , only tomato puree 75% and 100% showed an increasing viscosity pattern. By applying three different shear rates (30 s^{-1} , 100 s^{-1} , and 300 s^{-1}) on the same product, the higher shear rate applied would result in a lower viscosity of the product. The response of the rheological parameter (shear stress or viscosity) measurement of non-Newtonian fluids depended on the shear rate application (region). It was also noticeable from the graph that *Naturell lätt yoghurt* experienced the most severe rheological (viscosity) breakdown compared to other products. It was caused by the steeper decline that occurred in the yoghurt product.

The more quantitative investigation could be done by calculating the viscosity difference (in %) between the final state (at $t=300 \text{ s}$) and initial (after 10 s of shear rate adjustment or $t=11 \text{ s}$). The result of this simple calculation was presented in **Table 10**. The positive value of % viscosity difference indicated a rheopexy behavior as the viscosity increased when a constant shear rate applied ($\eta_{\text{final}} > \eta_{\text{initial}}$). On the other hand, the negative value of % viscosity difference indicated a thixotropy behavior as the viscosity decreased when a constant shear rate applied ($\eta_{\text{final}} < \eta_{\text{initial}}$).

final $< \eta$ initial). Additionally, it was also observed that the higher the constant shear rate was applied, the higher the viscosity differences or more breakdown occurred (see **Table 10**).

From the % viscosity difference value, the *Naturell lätt* yoghurt had a dominant thixotropy behavior. Meanwhile, tomato puree had either a thixotropy or a rheopexy behavior, and it was depending on the shear rate region. This finding confirmed a hypothesis in the literature that for certain complex fluids, both a thixotropy and rheopexy behavior may appear under different shear rate region (Chabbra, 2010). In conclusion, the breakdown test could capture both thixotropy and rheopexy behavior either by visual identification of the graph or by calculating the % of viscosity difference.

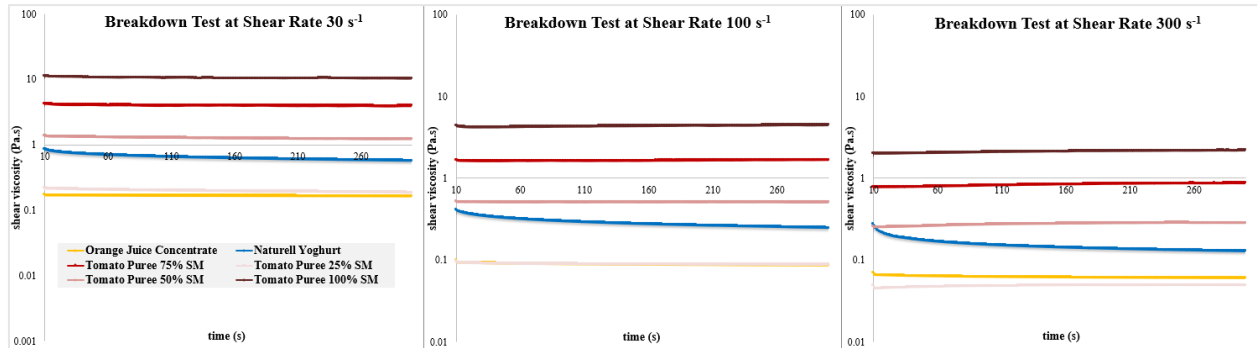


Figure 17. Logarithmic plot of shear viscosity (η) and time from the breakdown test at three different shear rates ($\dot{\gamma}$). The first 10 points of increasing viscosity were not considered, as an adjustment to achieve the target shear rate. Measurements were done in duplicate for tomato puree and orange juice concentrate, and triplicate for *Naturell lätt* yoghurt. *Naturell lätt* yoghurt data was from *Muhammad (2020)*.

Table 10. Percentage of viscosity (η) difference for breakdown test.

Sample	Viscosity difference (Pa.s)			% Viscosity difference (%)		
	30 s ⁻¹	100 s ⁻¹	300 s ⁻¹	30 s ⁻¹	100 s ⁻¹	300 s ⁻¹
Orange juice concentrate	$(-6.0 \pm 1) 10^{-3}$	$(-7.0 \pm 2) 10^{-3}$	$(-6.0 \pm 2) 10^{-3}$	-3.4 ± 0.4	-7.8 ± 2	-8.9 ± 4
<i>Naturell lätt</i> yoghurt	$(-2.7 \pm 0.1) 10^{-1}$	$(-1.6 \pm 0) 10^{-1}$	$(-1.3 \pm 0) 10^{-1}$	-32 ± 0.8	-39 ± 0.4	-50 ± 1
Tomato puree 25% (7-7.5 °brix)	$(-3.0 \pm 0.1) 10^{-2}$	$(-6.0 \pm 1) 10^{-3}$	$(4.0 \pm 0) 10^{-3}$	-14 ± 0.5	-6.1 ± 0.8	9.5 ± 0.8
Tomato puree 50% (14-15 °brix)	$(-1.4 \pm 0.2) 10^{-1}$	$(-7.0 \pm 3) 10^{-3}$	$(3.2 \pm 0.3) 10^{-2}$	-10 ± 1	-1.3 ± 0.3	12 ± 1
Tomato puree 75% (21-22.5 °brix)	$(-3.2 \pm 0.9) 10^{-1}$	$(2.7 \pm 0.4) 10^{-2}$	$(9.2 \pm 3) 10^{-2}$	-7.4 ± 2	1.6 ± 0.2	12 ± 4
Tomato puree 100% (28-30 °brix)	$(-9.4 \pm 2) 10^{-1}$	$(1.4 \pm 1) 10^{-1}$	$(1.9 \pm 0.4) 10^{-1}$	-8.4 ± 1	3.3 ± 3	9.5 ± 2

Note: values are expressed as Mean \pm SEM. Viscosity difference was calculated by subtracting the final viscosity value (at $t=300$ s) and the initial viscosity value (after 10 s of shear rate adjustment or $t= 11$ s). Negative value indicates a thixotropy behavior, positive value indicates a rheopexy behavior. Measurements were done in duplicate for tomato puree and orange juice concentrate, and triplicate for *Naturell lätt* yoghurt. *Naturell lätt* yoghurt data was from *Muhammad (2020)*.

4.1.4. Build-up

The sequence for the build-up measurement contained a pre-shear step at a constant shear rate for 300 s. Furthermore, different resting times (Δt) were applied, followed by applying a constant very low shear rate at 1 s^{-1} for 900 s to the sample. Additionally, the sample with no pre-shearing and resting time was treated with a very low shear rate at 1 s^{-1} as the standard comparison (control). The visualizations of viscosity monitoring during the build-up test of all products were presented in **Figure 18, 19, 20, 21,** and **Appendix 7.9** (for pre-shearing 100 s^{-1}). The pre-shearing stage had the same principle with the breakdown test where decreasing viscosity indicated thixotropy behavior

and increasing viscosity indicated rheopexy behavior. When different resting times were applied and followed by a sudden stepping down of shear rate to a 1 s^{-1} , it would result in the increase of viscosity or regaining of product structure. This phenomenon could be observed in the build-up phase graph when a constant low shear rate at 1 s^{-1} for 900 s was applied.

Table 11. Percentage of viscosity (η) difference for build-up test.

Treatment/samples	% viscosity difference (%)			
	Orange juice concentrate	Naturell lätt yoghurt	Tomato puree 100% (28-30° brix)	Tomato puree 25% (7-7.5° brix)
Pre-shear 100 s^{-1} dt=0 s	-33	-57	42	38
Pre-shear 100 s^{-1} dt=30 s	-11	-53	11	20
Pre-shear 100 s^{-1} dt=90 s	-11	-53	7	16
Pre-shear 100 s^{-1} dt=300 s	-10	-50	-9	10
Pre-shear 300 s^{-1} dt=0 s	-34	-58	16	65
Pre-shear 300 s^{-1} dt=30s	-22	-54	2	46
Pre-shear 300 s^{-1} dt=90s	-1	-51	-7	38
Pre-shear 300 s^{-1} dt=300s	-24	-48	-12	22

Note: measurements were done in one replicate for orange juice concentrate, tomato puree 25, and 100%, and triplicate for *Naturell lätt* yoghurt. The percentage of viscosity difference was calculated by subtracting the viscosity value of the treatment sample (at $t=5$ s) and the viscosity value of the control sample (without pre-shearing) (at $t=5$ s). The positive value of % viscosity difference indicates the viscosity of treated sample was higher than the viscosity of control sample (without pre-shearing).

In a previous study by Muhammad (2020), the hypothesis of “*the longer the time given for the sample to rest, the higher build-up was developed*” was proven only for the *Naturell lätt* yoghurt. The highest amount of build-up was achieved by the sample with the longest resting time (dt=300 s), and the least of build-up was developed by a sample without resting time (dt=0 s) for both pre-sheared yoghurt at 100 s^{-1} and 300 s^{-1} . Meanwhile, the opposite result was observed in the case of diluted tomato puree 25%. It was confirmed by the calculation result of product recovery after 5 s as presented in **Table 11**. This means that the structural build-up for yoghurt and diluted tomato puree 25% were dependent on the resting time. Also, the ability of *Naturell lätt* yoghurt to regain its structure was indicated by the increasing viscosity after a sudden drop of shear rate, indicated a thixotropy behavior (Muhammad, 2020). It is also noticeable that both diluted and undiluted tomato puree showed a tendency to regain its viscosity higher than the control sample without pre-shearing (indicating by the positive value of % viscosity difference). The ability to recover the product’s structure depends on the damage (structural change) that occurred during processing due to stirring, shearing, etc. However, in the case of orange juice concentrate and tomato puree 100% (28-30° brix) as presented in **Figure 19, 21, Appendix 7.9, and Table 11**, no pattern that could be concluded between the resting time of 30 s, 90 s, and 300 s and % viscosity differences. Thereby, this phenomenon indicated that the ability to regain the structure for those two products was less dependent on the time effect compared to *Naturell lätt* yoghurt and diluted tomato puree. It could also be seen in the build-up phase that the smooth geometry might not suitable for measuring the tomato puree 25% and 100% at a low shear rate for 900 s, as indicated by the wavy curve shape.

Overall, the thixotropy behavior mostly occurred in *Naturell lätt* yoghurt, followed by orange juice concentrate and tomato puree. Therefore, more breakdown and build-up occurred in *Naturell lätt* yoghurt sample, while not much breakdown and build-up phenomena could be observed in the product with fewer thixotropy properties. In addition, not all materials exhibit a reversible time-

dependent effect, some materials have partial or irreversible time-dependent behavior (Benezech & Maingonnat, 1994).

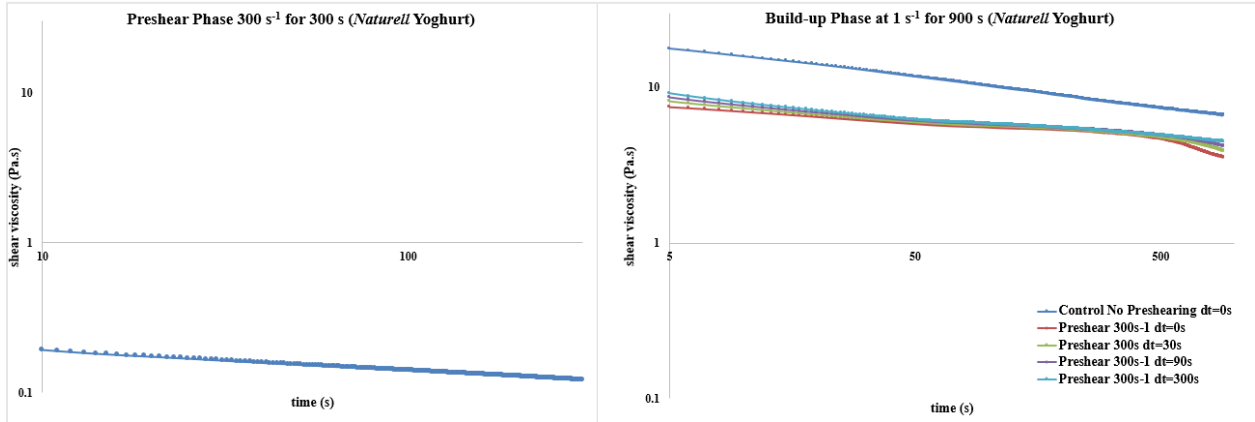


Figure 18. Build-up test of *Naturell lätt* yoghurt with pre-shearing at 300 s^{-1} (serrated geometry, triplicate). The first 10 points and the first 4 points of shear viscosity at pre-shearing and build-up phase were negligible due to shear rate adjustment. Data was obtained from *Muhammad (2020)*.

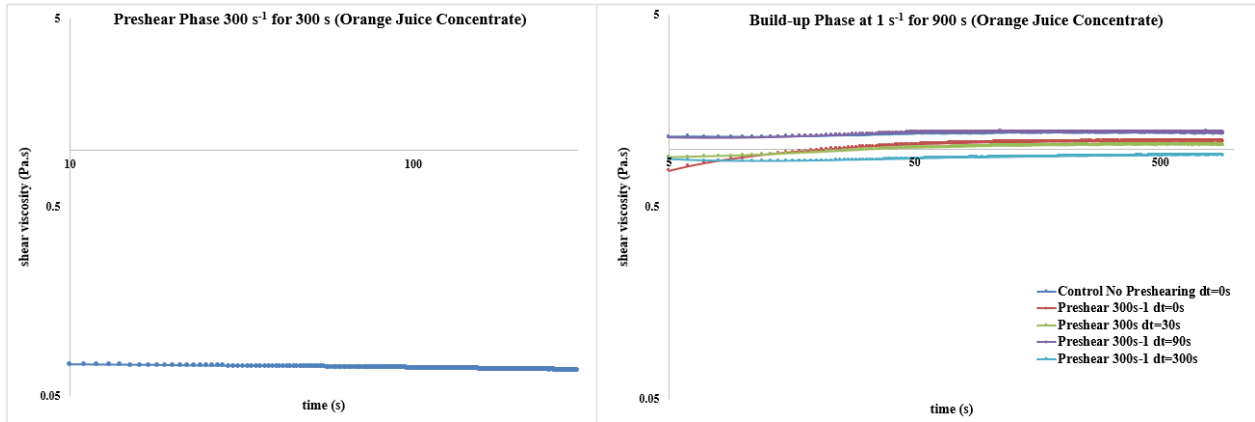


Figure 19. Build-up test of orange juice concentrate with pre-shearing at 300 s^{-1} (serrated geometry, one replication). The first 10 points and the first 4 points of shear viscosity at pre-shearing and build-up phase were negligible due to shear rate adjustment.

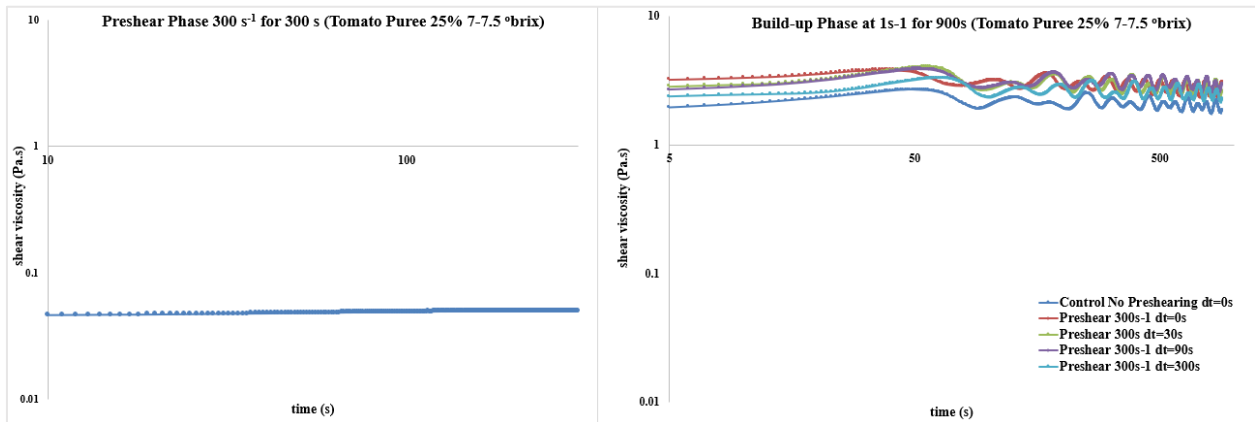


Figure 20. Build-up test of tomato puree 25% (7-7.5 °brix) with pre-shearing at 300 s^{-1} (smooth geometry, one replication). The first 10 points and the first 4 points of shear viscosity at pre-shearing and build-up phase were negligible due to shear rate adjustment.

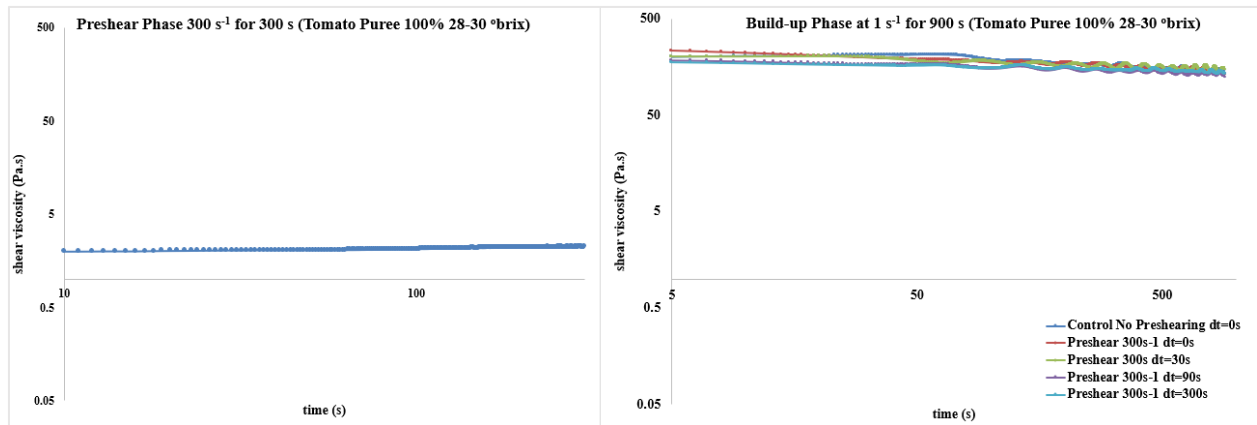


Figure 21. Build-up-test of tomato puree 100% (28-30 °brix) with pre-shearing at 300 s^{-1} (smooth geometry, one replicate). The first 10 points and the first 4 points of shear viscosity at pre-shearing and build-up phase were negligible due to shear rate adjustment.

4.2. Pressure drop rig

In the pressure drop rig experiment, a new batch of *Naturell lätt* yoghurt and new products of orange juice concentrate and tomato puree with different brands were used (see **Chapter 3.1** and **Table 1**). As can be seen from **Figure 22**, products used for the pressure drop experiment (2nd stage) had slightly different rheological properties compared to the products in the 1st stage rheological measurements. It might be caused by (1) different products' composition in each brand for orange juice and tomato puree, (2) batch variation for *Naturell lätt* yoghurt, and (3) pre-shearing application to the product before pressure drop measurement. Therefore, the hysteresis loop tests were re-conducted to obtain the rheological parameters in the pressure drop prediction experiment.

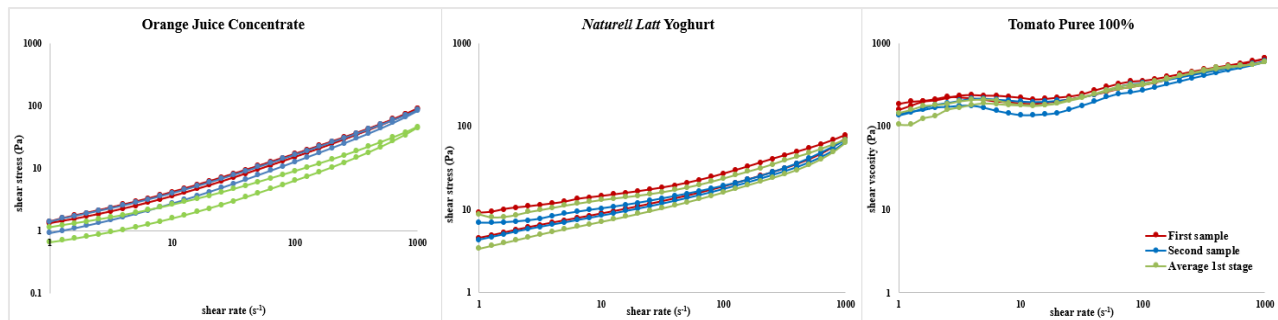


Figure 22. Logarithmic plot of shear stress (τ) and shear rate ($\dot{\gamma}$) from the hysteresis loop test of three different products from the 1st (rheology measurement) and 2nd (dP prediction rig) experiment.

4.2.1. Pressure drop of orange juice concentrate

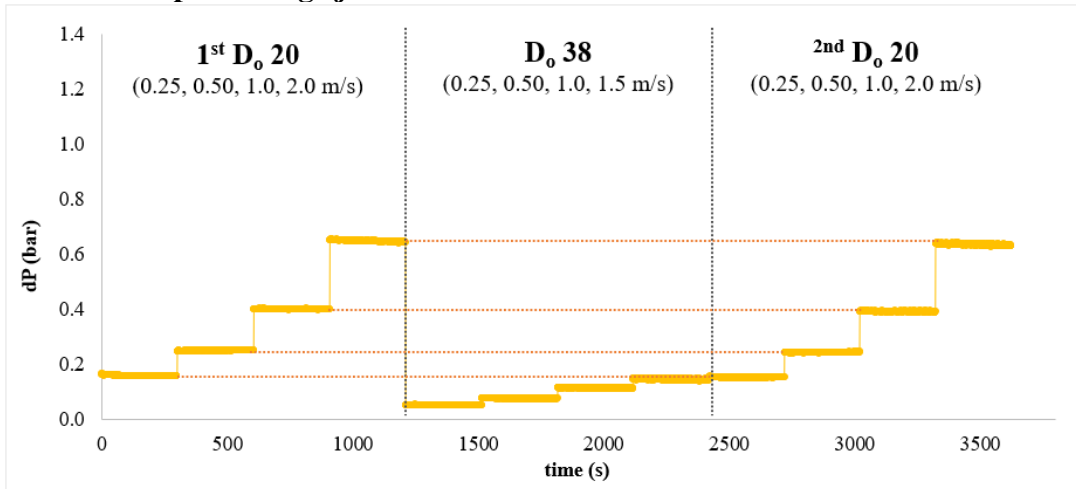


Figure 23. Pressure drop measurement of orange juice concentrate from the pressure drop rig.

The result of the pressure drop measurement for orange juice concentrate (experimental dP) is presented in **Figure 23**. From the experimental result graph, orange juice concentrate was a quite stable product where the pressure drops of the 1st D₂₀ and 2nd D₂₀ were quite similar (not much different). However, based on the quantitative data (**Appendix 7.10**), the dP from the 2nd D₂₀ measurement was slightly lower than the 1st D₂₀ measurement. It might be caused by the rheological characteristics of the less time-dependent product.

The hysteresis loop of two samplings from the rheometer measurement was divided into two shear rate regions 1 – 79.44 s⁻¹ and 100 – 1000 s⁻¹ (see **Figure 24** and **Figure 25** for Power Law and Herschel-Bulkley model curve fitting, respectively). The consideration is based on the relevancy of the actual shear rate in food processing applications (100 – 1000 s⁻¹) (Bayod, 2008). Then, the obtained hysteresis loop data both upward and downward curve (shear rate and shear stress plot) was analyzed by using non-linear regression, Ordinary Least Square (OLS) from SOLVER function in Excel. The output from this analysis was the rheological parameters such as K and n-value for the Power Law model, and A, b, and yield stress value for the Herschel-Bulkley prediction model.

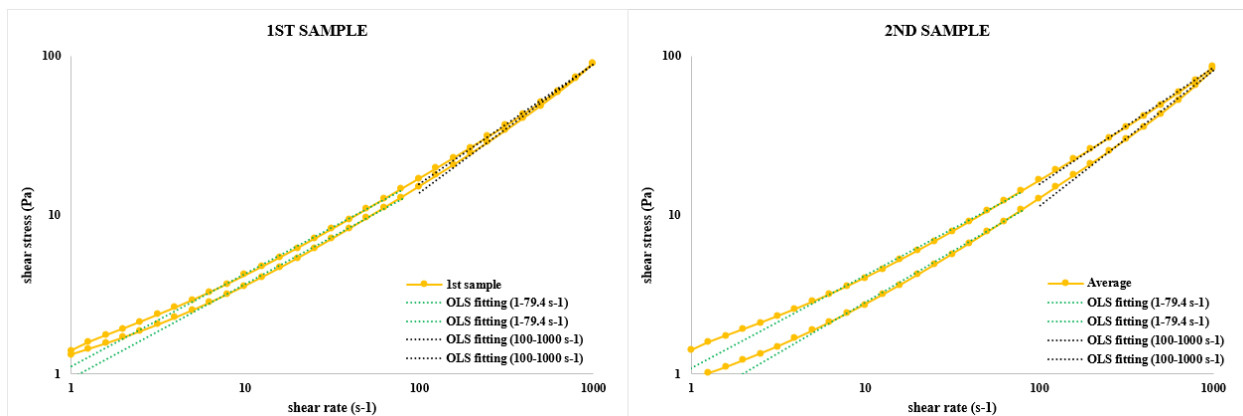


Figure 24. Logarithmic plot of hysteresis loop curve and OLS fitting curve of orange juice concentrate (*left*: 1st sample, *right*: 2nd sample) by using Power Law model. The measurement was done in duplicate.

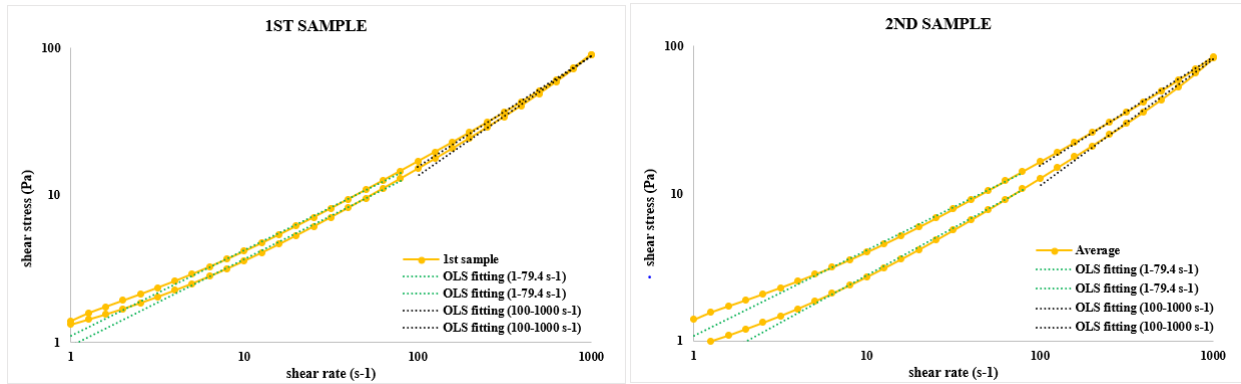


Figure 25. Logarithmic plot of hysteresis loop curve and OLS fitting curve of orange juice concentrate (*left*: 1st sample, *right*: 2nd sample) for Herschel-Bulkley model. The measurement was done in duplicate.

As can be seen from both figures above, the hysteresis loops had a straight-line shape tendency. However, the hysteresis loops of the 1st and 2nd samplings were different, where the loop from the 2nd sample had a larger enclosed area than the 1st sample. One of the presumptions was due to the 2nd sample waiting time of 1.5 hours before the rheometer measurement. From the generated rheological parameters in **Table 12** and **Table 13**, the downward sweep had thinner consistency (lower K or A-value, higher n or b-value) than the upward sweep. This also occurred when comparing two samplings, the 2nd sample had lower consistency than the 1st sample (sampling after 0.25 m/s velocity at D₂₀) due to more shearing experienced by the 2nd sample (sampling after 1.50 m/s velocity at D₃₈). This meant that the applied shearing would affect the product rheology although in the case of orange juice concentrate did not give much difference. From two prediction models, the Herschel-Bulkley gave a better fit than the Power Law model as indicated by the lower SSR value.

Furthermore, the theoretical pressure drop value was calculated by inserting those rheological parameters from the Power Law model into the *Rabinowitsch-Mooney* equations for non-Newtonian fluid with laminar flow. Meanwhile, rheological parameters from Herschel-Bulkley model were inserted into the equations by Chilton & Stainsby (1998) for non-Newtonian fluid with laminar flow (detailed information in **Chapter 2.3, Eq. 6-11**). The success of the pressure drop prediction was investigated by comparing the pressure drop value from the experimental measurement in the pressure drop rig with the theoretical value from the calculation. This comparison is presented as a relative deviation (%) (see **Eq. 13** below).

$$\% \text{ Relative deviation} = \frac{dP_{\text{experiment}} - dP_{\text{calculation}}}{dP_{\text{experiment}}} \cdot 100\% \quad \dots \text{Eq. 13}$$

The lower the relative deviation (%), the closer the prediction to the actual data from the experiment. Both experimental and theoretical pressure drop data for orange juice concentrate are attached in **Appendix 7.10**. Meanwhile, the rheology parameters and % relative deviation of pressure drops (dP) prediction based on Power-Law and HB are presented in **Table 12** and **Table 13**, respectively.

Table 12. Percentage (%) of relative deviation for pressure drop (dP) prediction of orange juice concentrate by using Power Law model.

D _o	Wall shear rate γ_w (s ⁻¹)	1 st sample UPWARD		1 st sample DOWNWARD		2 nd sample UPWARD		2 nd sample DOWNWARD	
		1-79.44 s ⁻¹	100-1000s ⁻¹	1-79.44 s ⁻¹	100-1000s ⁻¹	1-79.44 s ⁻¹	100-1000s ⁻¹	1-79.44 s ⁻¹	100-1000s ⁻¹
D20	139-157	-4%	1%	9%	10%	-1%	1%	20%	28%
	277-313	2%	-5%	13%	1%	4%	-4%	21%	18%
	555-627	8%	-10%	18%	-9%	11%	-8%	23%	8%
	1109-1254	15%	-14%	24%	-18%	18%	-10%	26%	-3%
D38	65-74	-4%	13%	9%	24%	-1%	11%	24%	41%
	131-148	-6%	0%	7%	10%	-3%	-1%	19%	28%
	262-296	-5%	-11%	7%	-5%	-2%	-10%	16%	14%
	392-443	-4%	-18%	7%	-14%	-1%	-16%	15%	4%
D20	139-157	-8%	-3%	5%	7%	-5%	-3%	17%	25%
	277-313	-1%	-8%	10%	-2%	2%	-7%	19%	16%
	555-627	6%	-13%	16%	-11%	9%	-10%	22%	5%
	1109-1255	14%	-17%	22%	-20%	16%	-13%	25%	-5%
Rheology parameter	<i>K-value</i>	1.12	0.48	0.94	0.33	1.09	0.53	0.65	0.22
	<i>n-value</i>	0.58	0.75	0.59	0.81	0.58	0.73	0.64	0.85
	<i>SSR</i>	0.76	16.15	0.93	16.05	0.95	5.97	0.54	16.08

Note: negative (-) % relative deviation = overestimation or dP exp < dP calc, positive (+) % relative deviation = underestimation or dP exp > dP calc. The wall shear rate (γ_w) was calculated from the *Rabinowitsch-Mooney* equations.

Table 13. Percentage (%) of relative deviation for pressure drop (dP) prediction of orange juice concentrate by using Herschel-Bulkley model.

D _o	Wall shear rate γ_w (s ⁻¹)	1 st sample UPWARD		1 st sample DOWNWARD		2 nd sample UPWARD		2 nd sample DOWNWARD	
		1-79.44 s ⁻¹	100-1000s ⁻¹	1-79.44 s ⁻¹	100-1000s ⁻¹	1-79.44	100-1000	1-79.44 s ⁻¹	100-1000s ⁻¹
D20	132-147	49%	46%	54%	51%	50%	49%	62%	58%
	262-295	41%	41%	46%	46%	42%	42%	54%	53%
	525-596	36%	34%	40%	37%	37%	36%	47%	45%
	1055-1189	27%	18%	30%	19%	27%	22%	37%	26%
D38	62-70	39%	26%	47%	34%	41%	33%	57%	43%
	125-140	23%	18%	32%	27%	25%	23%	43%	37%
	250-282	1%	1%	10%	9%	3%	3%	22%	21%
	372-420	-21%	-22%	-12%	-14%	-19%	-20%	2%	1%
D20	132-147	10%	5%	20%	14%	14%	10%	32%	27%
	266-295	-5%	-5%	3%	3%	-3%	-3%	18%	15%
	529-598	-11%	-15%	-4%	-8%	-10%	-12%	8%	4%
	1056-1189	-9%	-23%	-5%	-21%	-10%	-17%	5%	-11%
Rheology parameter	<i>A-value</i>	0.71	0.14	0.54	0.10	0.64	0.24	0.39	0.06
	<i>b-value</i>	0.68	0.92	0.71	0.97	0.69	0.84	0.75	1.03
	<i>Ys</i>	0.77	7.79	0.81	7.00	0.85	5.30	0.56	6.31
	<i>SSR</i>	0.01	2.37	0.00	2.19	0.02	0.81	0.00	2.48

Note: negative (-) % relative deviation = overestimation or dP exp < dP calc, positive (+) % relative deviation = underestimation or dP exp > dP calc. The wall shear rate (γ_w) was calculated from the *Rabinowitsch-Mooney* equations.

From the pressure drop prediction comparison, it showed that the Power Law model was more suitable for a less complex product like orange juice concentrate, which could be seen by a lower % relative deviation. The reason for this is that the Power Law is more relevant for the fluid with a linear pattern of rheology correlation between shear stress and shear rate as depicted in its hysteresis loop curve without initial yields stress value. Furthermore, the selection of the shear rate range to generate the rheology parameters and to predict pressure drop value should be based on the actual application in the pressure drop rig. Therefore, the shear rate range of 100 -1000 s⁻¹ was

selected as it was more relevant with the actual shear rate in the pressure drop rig experiment. Based on **Table 12** (for Power Law), in the case of orange juice concentrate, the rheology parameters generated from the upward sweep curve gave better dP prediction values than the downward sweep as indicated with the lower % relative deviation of upward sweep compared to downward sweep curves. Additionally, due to the 2nd sample of orange juice concentrate had been waiting for ± 1.5 hours before the rheology measurement, it was not completely representing the actual sample condition in the pipe flow. For that reason, the 1st sample would be more accurate to represent the actual rheological properties of orange juice concentrate.

4.2.2. Pressure drop of *Naturell lätt* yoghurt

The pressure drop measurement (experimental dP) for *Naturell Lätt* yoghurt is depicted in **Figure 26**. The thixotropy property of yoghurt could be seen clearly from **Figure 26** when the pressure drops (dP) kept decreasing during 300 s of measurement time, especially at a higher velocity (in smaller pipe diameter D_{20}). This thixotropy effect decreased on the 2nd D_{20} experiment due to more shearing had been applied to the sample. It was indicated by comparing pressure drop from the 1st D_{20} and the 2nd D_{20} , where the dP from the 2nd D_{20} was lower and the decreasing dP was less steep than the 1st D_{20} . This qualitative observation was aligned with the quantitative pressure drop data (see **Appendix 7.11**).

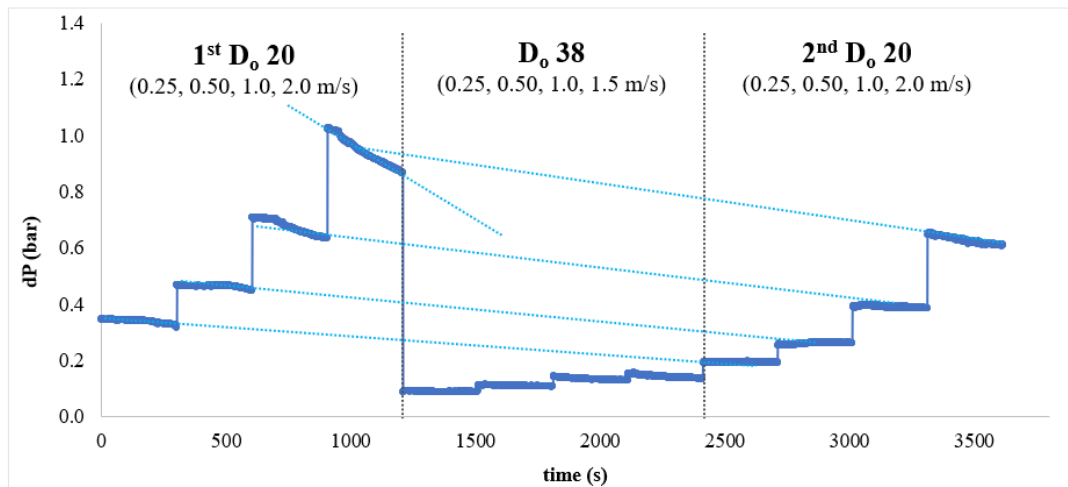


Figure 26. Pressure drop measurement of *Naturell Lätt* yoghurt from the pressure drop rig.

As presented in **Figure 27** below, the hysteresis loop shape of *Naturell Lätt* yoghurt was not exactly like a straight line. In the case of *Naturell Lätt* yoghurt, the curve fitting of the hysteresis loop with OLS – Power Law and Herschel-Bulkley model was also divided into the same range as orange juice concentrate as it was based on the actual shear rate application in the pressure drop rig, as presented in **Figure 27** below and **Appendix 7.11**, respectively. Based on the curve fittings (both Power Law and Herschel-Bulkley), the enclosed area of the hysteresis loop curve from the 2nd sample was smaller than the 1st sample. It indicated that the more shear applied to the sample would reduce the thixotropy effect in *Naturell lätt* yoghurt. This was reflected by the lower consistency index from the 2nd sample, compared to the 1st sample (experienced less shearing) (see **Table 14** and **Appendix 7.11**).

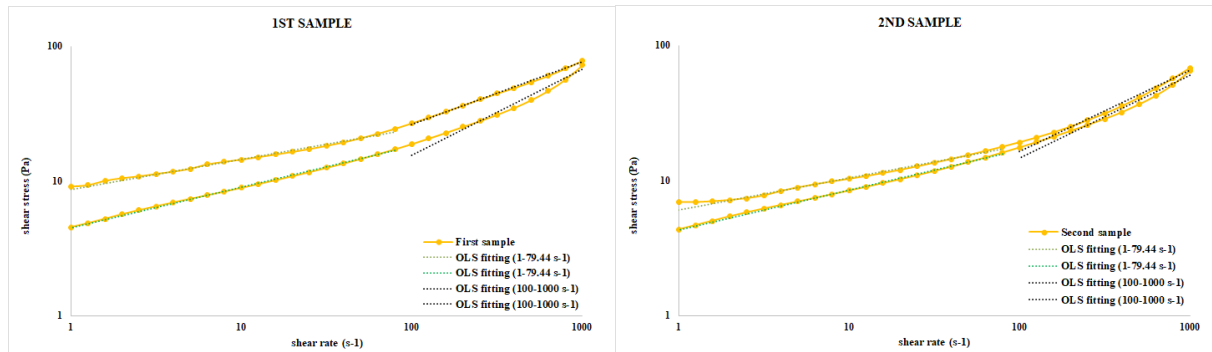


Figure 27. Logarithmic plot of hysteresis loop curve and OLS fitting curve of *Naturell Lätt* yoghurt (left: 1st sample, right: 2nd sample) by using Power Law model. The measurement was done in one replicate.

Based on the curve fitting, it is noticeable that the Herschel-Bulkley model resulted in a better fit to the experimental data compared to the Power Law, as the SSR values generated from the HB model were smaller than for the Power Law. This result was aligned with the % relative deviation of pressure drop prediction in the pipe, the Herschel-Bulkley model could predict the yoghurt pressure drop better than the Power Law model, as indicated with lower % relative deviation values resulted from HB (see **Table 14** and **Appendix 7.11**). Then, it seems that the yoghurt required a certain amount of stress to maintain the flow (dynamic yield stress) as the real measurement application in the pipe has been shown. Therefore, the pressure drop prediction for *Naturell Lätt* yoghurt referred to the Herschel-Bulkley prediction model.

Table 14. Percentage (%) of relative deviation for pressure drop (dP) prediction of *Naturell Lätt* yoghurt by using Herschel-Bulkley model.

D ₀	Wall shear rate γ_w (s ⁻¹)	1 st sample UPWARD		1 st sample DOWNWARD		2 nd sample UPWARD		2 nd sample DOWNWARD	
		1-79.44 s ⁻¹	100-1000s ⁻¹	1-79.44 s ⁻¹	100-1000s ⁻¹	1-79.44 s ⁻¹	100-1000s ⁻¹	1-79.44 s ⁻¹	100-1000s ⁻¹
D20	120-181	27%	22%	47%	39%	45%	41%	51%	45%
	231-345	35%	25%	52%	46%	50%	45%	55%	52%
	456-688	45%	31%	59%	49%	57%	47%	61%	57%
	912-1364	51%	31%	62%	41%	61%	40%	65%	52%
D38	56-85	-13%	-16%	21%	-2%	16%	7%	26%	8%
	112-169	-11%	-19%	20%	7%	16%	11%	25%	16%
	224-336	-11%	-28%	17%	7%	14%	6%	23%	18%
	337-505	-19%	-43%	11%	-3%	8%	-7%	17%	10%
D20	120-181	-28%	-38%	8%	-8%	3%	-3%	14%	4%
	231-345	-15%	-33%	14%	3%	11%	2%	20%	15%
	456-688	5%	-20%	28%	12%	25%	8%	33%	24%
	907-1364	26%	-4%	43%	12%	41%	9%	47%	28%
Rheology parameter	A-value	3.61	1.20	3.23	0.01	2.38	0.06	2.99	0.01
	b-value	0.37	0.58	0.36	1.24	0.40	0.99	0.36	1.20
	Y _s	5.73	9.69	1.48	17.02	4.22	13.81	1.53	15.64
	SSR	1.54	2.21	0.21	9.59	0.41	0.21	0.22	7.24

Note: negative (-) % relative deviation = overestimation or dP exp < dP calc, positive (+) % relative deviation = underestimation or dP exp > dP calc. The wall shear rate (γ_w) was calculated from the *Rabinowitsch-Mooney* equations.

The percentage relative deviation of pressure drops, as presented in **Table 14**, showed that the selection of shear rate range matters for pressure drop prediction. It was indicated by a better pressure drop prediction at a suitable shear rate region of 100-1000 s⁻¹ (compare with the wall shear rate value). However, the pressure drop prediction of *Naturell lätt* yoghurt was not as good as the

orange juice concentrate due to the higher relative deviation values (more than 20%) (see **Table 14** and **Appendix 7.11**). The presumption might be caused by a thixotropy property as a part of the yoghurt's characteristics is sensitive to shearing. At a low shear rate, the extra polysaccharide is presented in a filamentous network attached to the starter and casein matrix, while at a high shear rate, this network is broken down, and this influenced the viscosity (Benezech & Maingonnat, 1994). The previous study from Jdayil, Nasser, and Ghannam (2013), also reported the possibility to estimate the stirred yoghurt behavior in the pipe flow from the rheological measurements. However, besides the thixotropy behavior of the product, yoghurt has an elastic property due to its casein and fat content that will affect the prediction accuracy of dimensionless structure number (Se) in the pipe flow (Jdayil, Nasser, & Ghannam, 2013). This thixotropy reducing effect in the 2nd D_{20} experiment caused a decreasing % relative deviation as could be observed from the 1st and 2nd of D_{20} pipe diameter. Additionally, the product had experienced the accumulated shearing history in the pipe during the measurement that might result in the change of its structure and behavior to become less time-dependent.

Although for this typical thixotropy product like *Naturell lätt* yoghurt could result in better dP prediction by shearing application, the Herschel-Bulkley was not completely suitable to predict the pressure drop. Both the Power Law and the Herschel-Bulkley models did not consider the time-dependency effect of thixotropy products in their equations. Therefore, it is recommended to use another rheological modeling of complex fluids for a better pressure drop prediction of the thixotropy materials (unsteady behavior product), i.e. Maxwell, Gumulya *et al.*, De Kee *et al.* model (Quemada, 1999; Gumulya, Horsley, & Pareek, 2014; Benezech & Maingonnat, 1994). These models combine both time-dependent and viscoelasticity effects by introducing more rheological parameters, i.e. relaxation time, shear modulus, and limiting viscosity.

4.2.3. Pressure drop of tomato puree

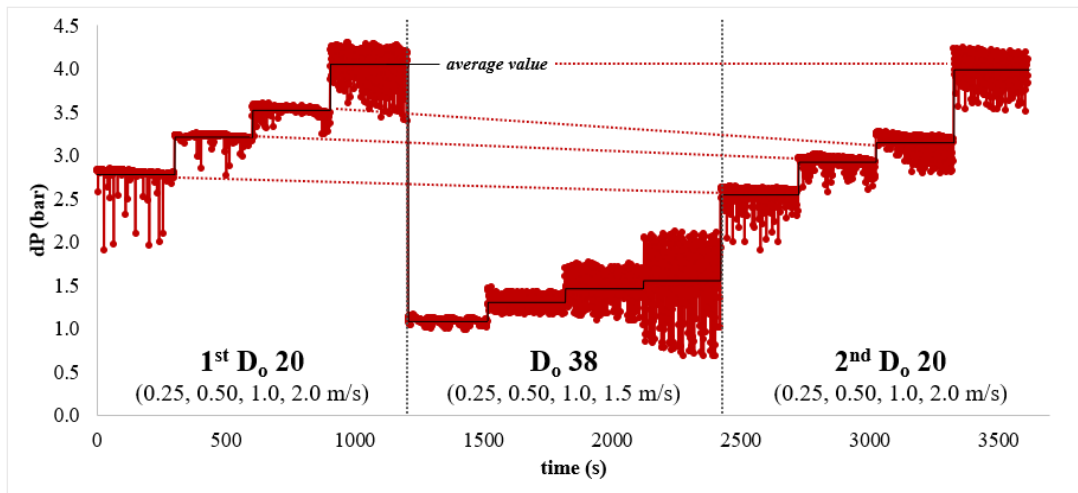


Figure 28. Pressure drop measurement of tomato puree 100% (28-30 °brix) from the pressure drop rig.

The experimental result of pressure drop measurement for tomato puree 100% is depicted in **Figure 28** above. As can be seen from **Figure 28**, the measured pressure drop value was fluctuating especially at a higher velocity and larger pipe diameter. Since the pump was run at a very high frequency (flowrate), one of the presumptions might be due to the presence of some air bubbles inside the pump that could affect the actual flowrate (~5% difference), thus reducing the measured dP value. The lower experimental dP value was caused by the utilization of an average dP value

during the 300 s measurement, instead of using the maximum dP value. The second possibility to explain the oscillation phenomenon was the consequences of product properties. Tomato puree exhibits complex rheological behavior and properties, due to the high concentration of large particles ($> 10 \mu\text{m}$) that constitute its main structural component (Bayod, Willers, & Tornberg, 2007). As the same trend with orange juice concentrate and *Naturell lätt* yoghurt, the measured dP from the 2nd D₂₀ was lower than the dP measured at the 1st D₂₀. It was caused by the more shearing experienced by the product at the 2nd D₂₀ measurement.

In the case of tomato puree, the hysteresis loop curve was not as linear (straight) as either orange juice concentrate or *Naturell lätt* yoghurt, particularly in the shear rate between 1 to 100 s⁻¹. Therefore, choosing the right shear rate of 100 - 1000 s⁻¹ was substantial not only because of the actual shear rate application in the pressure drop rig but also based on the shape of the curves. Besides, the hysteresis loop curve of tomato puree clearly showed a more dominant rheopexy behavior with slightly thixotropy behavior as depicted in **Figure 29**, with the position of the downward sweep curve above of the upward sweep curve (both for 1st and 2nd samples). According to Mezger (2006), the rheopexy material has an inhomogeneous flow tendency, thus it could be a possible explanation for the curve shape of tomato puree. As the same pattern with two previous products, the 2nd sample had lower shear stress and shear viscosity than the 1st sample due to previously applied shearing. Thus, it generated a lower consistency (lower K-value) and more flowable properties (higher n-value) for the 2nd sample from the Power Law prediction model. For the Herschel-Bulkley model, the 2nd sample also had a lower consistency (A-value) and lower dynamic yield stress value.

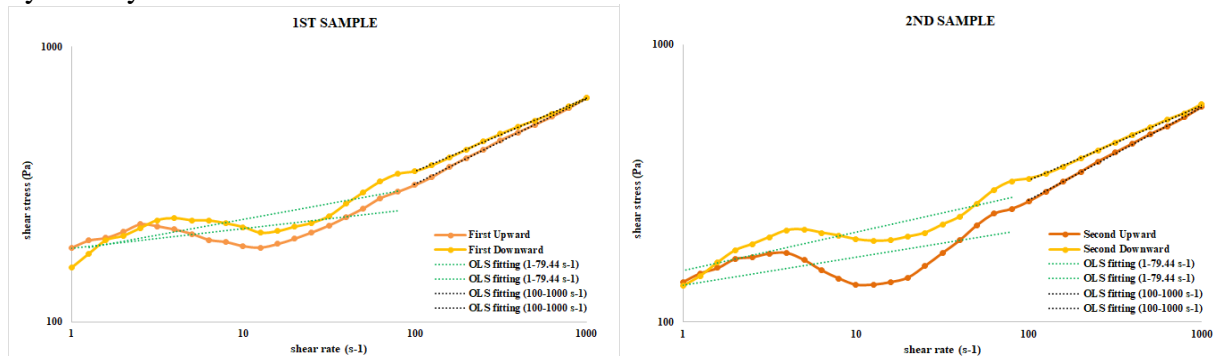


Figure 29. Logarithmic plot of hysteresis loop curve and OLS fitting curve of tomato puree 100% (28-30 °brix) (*left*: 1st sample, *right*: 2nd sample) by using Power Law model. The measurement was done in one replicate.

The percentage (%) relative deviation of the predicted pressure drop of tomato puree 100% (28-30 °brix) for the Power Law and the Herschel-Bulkley models are presented in **Table 15** and **Appendix 7.12**, respectively. The high relative deviation at the higher velocity resulted from the oscillation that occurred during the pressure drop rig measurement. This oscillation resulted in unstable experimental data. Thus, the experimental dP value was obtained from the average of those fluctuated data. This might not represent the actual and precise measurement value of dP from the rig (overestimated dP value). Furthermore, rheological parameters generated from the 2nd sample of upward sweep curve gave a better dP prediction, as indicated with a lower % of relative deviation than the 1st sample of upward sweep curve. It was also noticeable that a higher shear rate applied to the tomato puree resulted in a worse dP prediction value due to changes in its structure. This could be the result of the more frequent oscillation occurred during measurement and the changes in product's structure (i.e. merging of the large particles during shearing). Furthermore, as presented in **Appendix 7.12**, the OLS curve fitting for Herschel-Bulkley model has some

limitations that could not generate all the dynamic yield stress value in the case of tomato puree 100% (for certain shear rate range, i.e. 100 – 1000 s⁻¹ for the 1st and 2nd samples of upward sweep curve). Thus, the pressure drops prediction calculated from non-generated yield stress in the HB model would give the same value as the Power Law model. For Power Law model, it is noticeable that at the application-relevant shear rate range of 100-1000 s⁻¹, the more shear applied to the product would result in the worse pressure drop prediction. Additionally, the utilization of rheological parameters generated from the upward sweep curve could give better estimation dP value. Those were caused as the consequence of shearing which could affect the product’s structure and rheology property.

Table 15. Percentage (%) of relative deviation for pressure drop (dP) prediction of tomato puree 100% (28-30 °brax) by using Power Law model.

D ₀	Wall shear rate $\dot{\gamma}_w$ (s ⁻¹)	1 st sample UPWARD		1 st sample DOWNWARD		2 nd sample UPWARD		2 nd sample DOWNWARD	
		1-79.44 s ⁻¹	100-1000s ⁻¹	1-79.44 s ⁻¹	100-1000s ⁻¹	1-79.44	100-1000	1-79.44 s ⁻¹	100-1000s ⁻¹
		D20	189-542	19%	-9%	2%	-23%	30%	6%
	368-1055	27%	-16%	8%	-27%	35%	-1%	8%	-15%
	716-2053	30%	-30%	10%	-39%	37%	-15%	8%	-25%
	1384-3968	36%	-38%	16%	-44%	42%	-24%	13%	-30%
D38	86-247	2%	-9%	-16%	-27%	17%	7%	-11%	-15%
	169-485	14%	-12%	-3%	-27%	26%	4%	-1%	-15%
	328-941	20%	-23%	1%	-36%	30%	-7%	1%	-22%
	475-1362	23%	-29%	3%	-41%	32%	-14%	2%	-27%
D20	176-504	12%	-16%	-6%	-32%	24%	0%	-4%	-19%
	343-983	20%	-24%	0%	-37%	29%	-9%	0%	-24%
	680-1949	22%	-43%	0%	-53%	30%	-27%	-2%	-38%
	1382-3962	35%	-40%	15%	-47%	41%	-26%	11%	-32%
Rheology parameter	K-value	185.07	75.28	181.70	103.02	136.05	59.14	152.84	92.99
	n-value	0.07	0.31	0.11	0.27	0.10	0.33	0.14	0.27
	SSR	10366.2	107.16	11082.4	93.38	14088.2	93.90	9246.12	127.06

Note: negative (-) % relative deviation = overestimation or dP exp < dP calc, positive (+) % relative deviation = underestimation or dP exp > dP calc. The wall shear rate ($\dot{\gamma}_w$) was calculated from the *Rabinowitsch-Mooney* equations.

4.3. One-shot filling rig test

4.3.1. Rheology parameters

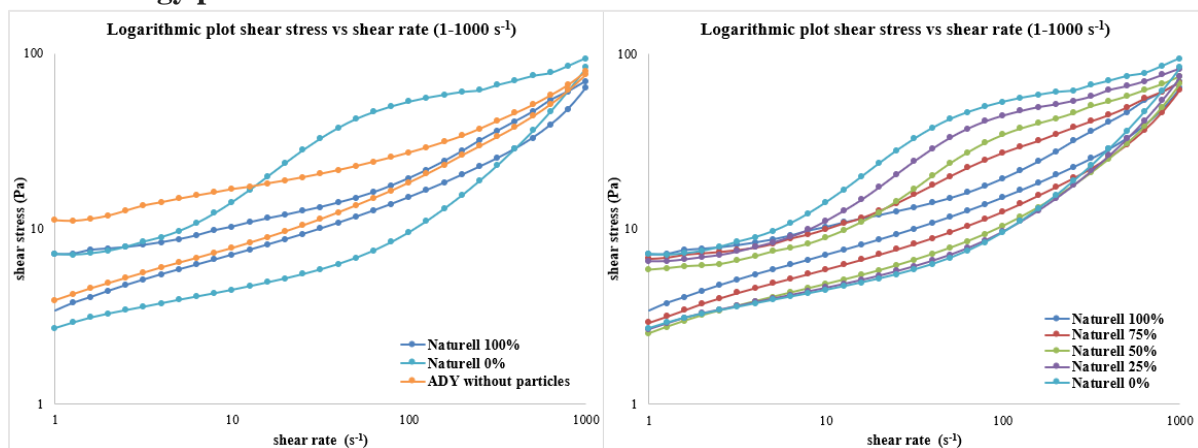


Figure 30. Logarithmic plot of hysteresis loop curves (shear rate 1 – 1000 s⁻¹) of five blends *Naturell lätt* yoghurt and *Långfil* (right) and ADY without particles (left). Measurements were conducted one replicate for each sample.

Hysteresis loop curves and OLS curve fitting generated from the shear rate range of 1 - 1000 s⁻¹ of five blends *Naturell lätt* yoghurt and *Långfil* and ADY without particles are depicted in **Figure 30** (for Power Law model) and **Appendix 7.14** (for Herschel-Bulkley model). It is noticeable that the higher proportion of *Långfil* (or smaller proportion of *Naturell lätt* yoghurt) in the blends resulted in a larger enclosed area of the hysteresis loop curve. Besides, the hysteresis loop shape of all the samples was not fully straight. Therefore, the shear rate range selection for curve fitting was based on the shape linearity of the curve and its actual application in the filling rig test, which was between 100 and 1000 s⁻¹ (around 400 s⁻¹ in the filling machine estimated from Tetra Pak's simulation). Previous studies also confirmed that the hysteresis loop area of yoghurt was proportional to the shear rate when above 100 s⁻¹ (Benezech & Maingonnat, 1994).

Based on **Figure 31**, it clearly showed that the OLS curve fitting of the Power Law model from the upward sweep curve resulted in a better fit compared to the downward sweep curve. This result also aligned with the higher SSR values of the downward sweep curves with the OLS curve fitting – the Power Law model than the upward sweep curves (see **Table 16**). Further details about the rheologic parameters generated from the curve fitting of OLS - Power Law and Herschel-Bulkley prediction model can be found in **Table 16**.

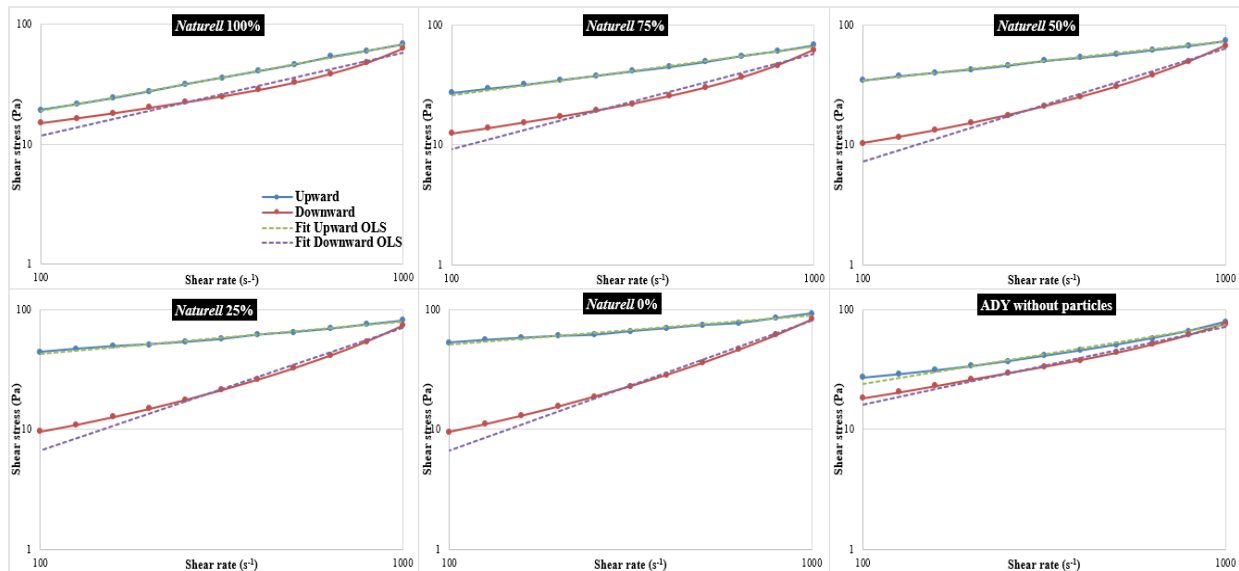


Figure 31. Logarithmic plot of hysteresis loop curves and OLS-Power Law curve fitting of five blends *Naturell lätt* yoghurt and *Långfil* and ADY without particles. Measurements were conducted one replicate for each sample.

As presented in **Table 16** below, a systematic rheological parameter was generated only from the OLS curve fitting with the Power Law prediction model. As also clearly depicted in **Figure 32** below, the higher proportion of *Långfil* resulted in an increase of the K-value and a decrease in the n-value. Meanwhile, the opposite systematic rheology pattern had been shown in the downward sweep curve. It might indicate the characteristic of *Långfil* of being more sensitive to shear. Also, it might be due to the long shear applied to the sample in the hysteresis loop test, thus affecting the product's structure (TAInstrument, 2020). Therefore, for the curve fitting, it would be more relevant and accurate to use the rheology parameters generated from the upward sweep curve. It was also based on another consideration of its actual application in the filling rig test where the product would not be sheared for a long period of time (approximately 52 min per measurement).

Table 16. Generated rheology parameters of five blends and ADY without particles as the curve fitting results with OLS and Power Law and Herschel-Bulkley model (shear rate 100 – 1000 s⁻¹).

Sample	POWER LAW (OLS)			HERSCHEL-BULKLEY (OLS)		
	Parameter	UPWARD	DOWNWARD	Parameter	UPWARD	DOWNWARD
100% Naturell (BUCKET)	K	1.42	0.49	A	1.27	0.00
	n	0.56	0.69	b	0.58	1.37
	SSR	1.17	81.53	Ys	0.96	14.25
				SSR	1.12	8.37
75% Naturell (BUCKET)	K	4.04	0.24	A	0.98	0.00
	n	0.41	0.79	b	0.58	1.43
	SSR	6.03	74.80	Ys	13.10	11.79
				SSR	0.77	6.11
50% Naturell (TANK)	K	7.54	0.10	A	3.27	0.00
	n	0.33	0.94	b	0.43	1.41
	SSR	3.19	56.91	Ys	11.66	8.96
				SSR	1.70	3.91
25% Naturell (TANK)	K	12.47	0.06	A	1.09	0.00
	n	0.27	1.02	b	0.56	1.40
	SSR	14.13	47.34	Ys	30.55	7.72
				SSR	2.21	3.02
0% Naturell (TANK)	K	16.52	0.05	A	0.32	0.01
	n	0.24	1.08	b	0.73	1.38
	SSR	40.58	41.81	Ys	44.91	7.02
				SSR	6.26	2.56
Ambient Drinking Yoghurt (BUCKET)	K	2.50	0.80	A	0.10	0.06
	n	0.49	0.65	b	0.92	1.00
	SSR	45.62	40.44	Ys	20.59	13.18
				SSR	2.35	6.16

Note: measurements were conducted one replicate for each sample. The consideration to obtain samples from tank or bucket was to minimize the rheological effect during mixing and transferring before filling experiment.

Although the OLS curve fitting with the HB model resulted in a better fit to the experimental or actual data (lower SSR values), it was not possible to generate a systematic rheological parameter. Therefore, only rheology parameters from the OLS curve fitting with the Power Law model from the upward sweep that would be used in the further correlation analysis by using a TRENDLINE linear regression in Excel.

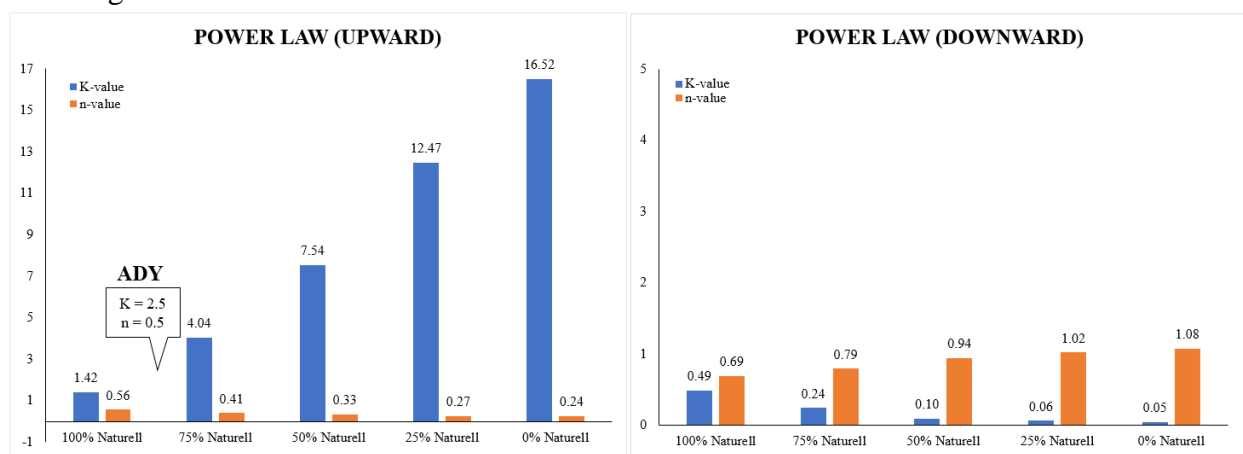


Figure 32. Generated K and n values from five blends (*Naturell lätt yoghurt* and *Långfil*) and ADY without particles from OLS curve fitting with Power Law model (*left*: upward sweep, *right*: downward sweep).

4.3.2. Filling responses of systematic blends (*Naturell Lätt* yoghurt and *Långfil*)

One-shot filling rig tests of five systematic blends from *Naturell lätt* yoghurt and *Långfil* have generated several types of filling responses as presented in **Appendix 7.16**. Several filling behavior responses that were investigated from this study include splash outside of the package, splash inside the package, impact splash distance in the package, and the occurrence of filamentation and dripping in the package (see **Figure 33 and 34** below). The current study aimed to focus only on two responses, which were splash outside of the package and impact splash distance in the package. The reason is that these have shown indicative relation to the potential splash that could occur in continuous production in the filling machine. The consideration of only choosing these two behavior responses was also based on the previous experience of Tetra Pak's internal test. The result indicated that a shorter distance of impact splash and a higher amount of splash outside of the package could be linked to more splash in the continuous filling application.

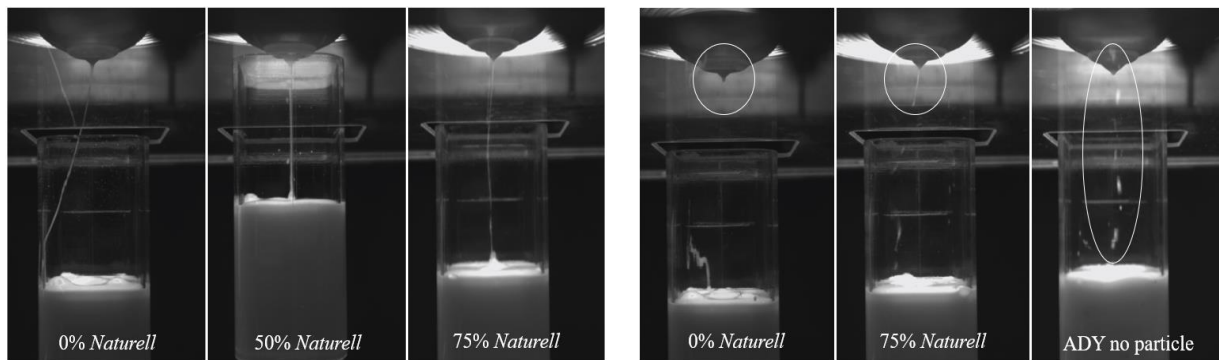


Figure 33. Filamentation (*left*) and dripping (*right*) in the yoghurt filling.

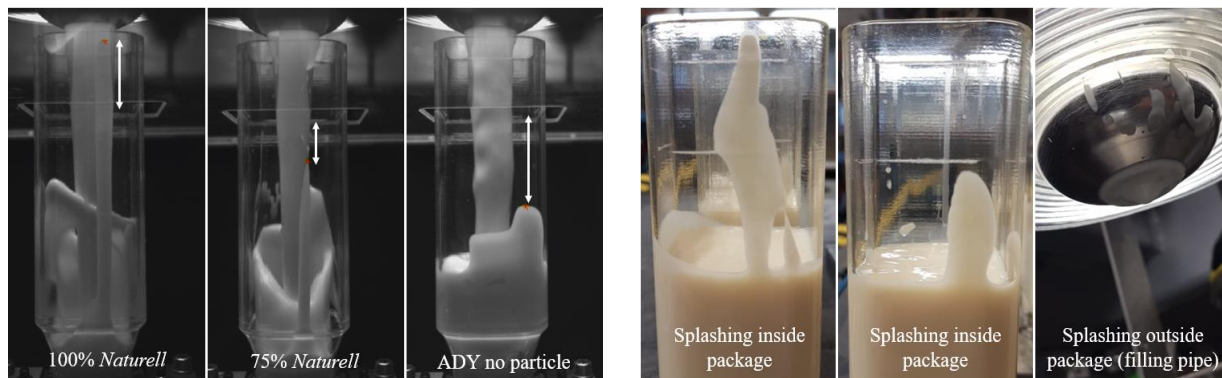


Figure 34. Impact splash distance (*left*) and splashing (*right*) in the yoghurt filling.

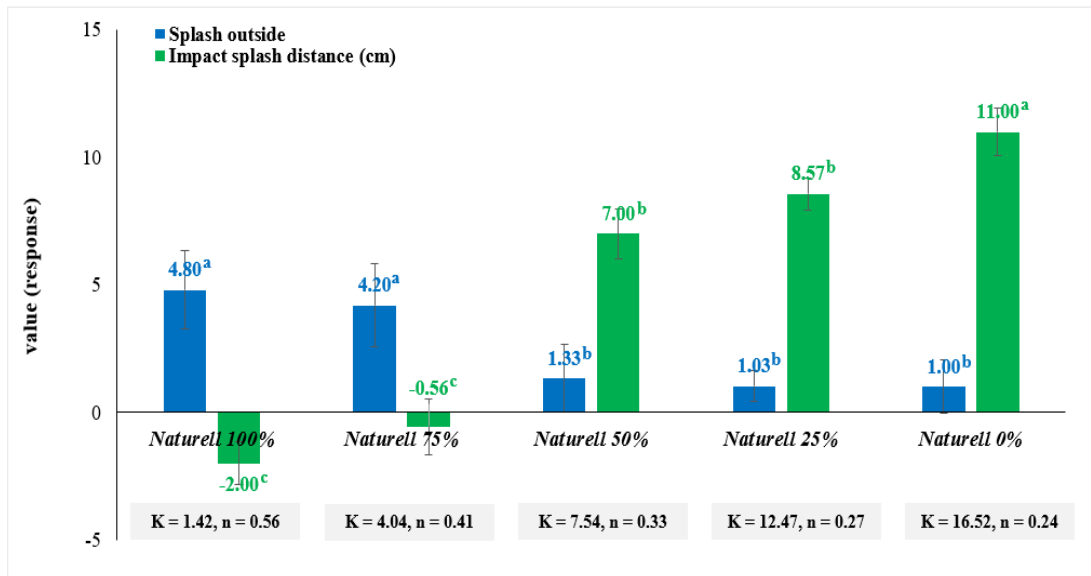


Figure 35. Filling behavior responses of the systematic blends. Data points of splash outside n=6, while impact splash distance in cm n=30. The result is reported as mean value based on the number and distance per shot. Different superscript with the same color indicated significantly different values ($p < 0.05$ using Duncan for outside splash and Dunnett T3 multiple range test for impact splash distance). Analysis was done by using IBM SPSS Statistics 25.

The result of splash outside of the package and impact splash distance in the package from the five systematic blends is quantitatively depicted in **Figure 35**. For the case of fermented milk blends, the proportion (% w/w) of each product affected both the product consistency and flow behavior index. The higher K- and lower n-value in the systematic blends resulted in a longer impact splash distance (in cm) from the bottom big, which corresponds to the smaller impact splash occurred inside the package. A similar pattern occurs on the splash outside response which showed that the increasing K- and decreasing n-value resulted in the lower numbers of a splash on the pipe and plate surface. Also, it was clearly seen that when the K-value was less than 7.54 and the n-value was higher than 0.33, it consequently generates a shorter impact splash distance (in cm) from the bottom big and higher number of a splash outside of the package. It is also noticeable in **Figure 35** above that there was a high variation in the result of a splash outside and impact splash distance from 30 individual filling shots. It is indicated by the wider range of confidence of interval (CI), particularly in the sample *Naturell lätt* 75%.

The observed phenomenon of impact splash in the package that was found in the current study might be associated with the *Kaye* effect. *Kaye* effect is described as a phenomenon when a stream jet of shear thinning fluid shoots sideways or rebound from the liquid surface, hits the pool surface, then starts coiling, and forms a small heap along the surface as captured in **Appendix 7.15** (Lee, Li, Marston, Bonito, & Thoroddsen, 2013). As depicted in **Figure 36**, the fermented milk product (yoghurt) also experienced almost the same phenomenon indicated by the bouncing effect of the product when hit the bottom part of the transparent package. A previous study reported that these bouncing and reflection effects were associated with the continuous flow phenomenon as occurring in the filling rig for a short time (Versluis, Blom, D, Weele, & Lohse, 2006). In addition, Lee *et al.* (2013)'s study about *Kaye* effect on shampoo reported that the presence of the air layer as the underlying cause of the *Kaye* phenomenon. The air layer gave a lubricating effect between the jet

and pool surfaces, where the jet slides on this lubricating air layer. Then, this air layer also could break up into threads and bubbles.

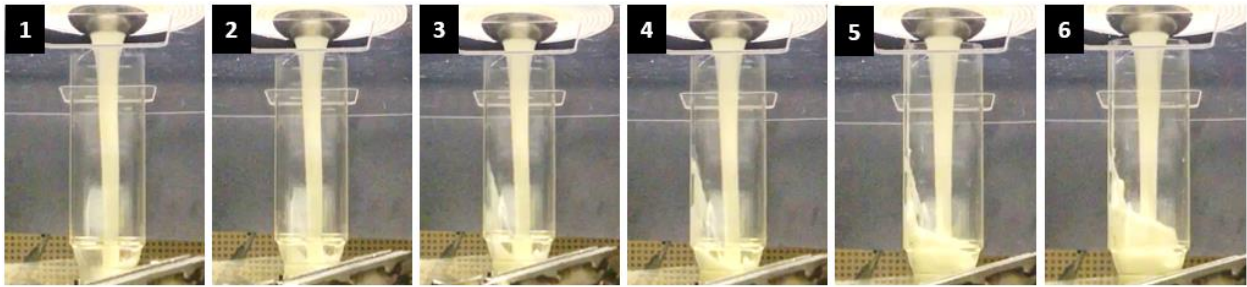


Figure 36. Visualization of *Kaye* effects in fermented milk product (*Naturell lätt 75%*). [1] product hit the bottom part of package, [2] formation of a viscous heap through piling, buckling, and coiling, [3] [4] rising of the jet, [5] [6] the raising jet splashes along the wall surface as the end of *Kaye* effect.

Furthermore, a linear regression analysis (TRENDLINE) was conducted to evaluate the correlation between variables (K- and n-value) and filling behavior responses (impact splash distance in the package and splash outside of the package), as depicted in **Figure 37** below. From the generated linear equations and R^2 values, it can be seen that the n-value has a similarly strong correlation with two observed responses: a positive correlation with the splash outside response ($R^2 = 0.867$) and a negative correlation with the impact splash response ($R^2 = 0.8838$). On the other hand, the K-value has a stronger positive correlation with the impact splash distance ($R^2 = 0.9062$) compared to the splash outside response with a negative correlation ($R^2 = 0.7838$). This correlation analysis also aligned with the previous statement about the increase of K-value resulted in the longer impact splash distance and a smaller number of splashes outside as seen in bar chart visualization. Meanwhile, the opposite result was observed in the case of n-value and those two filling behavior responses.

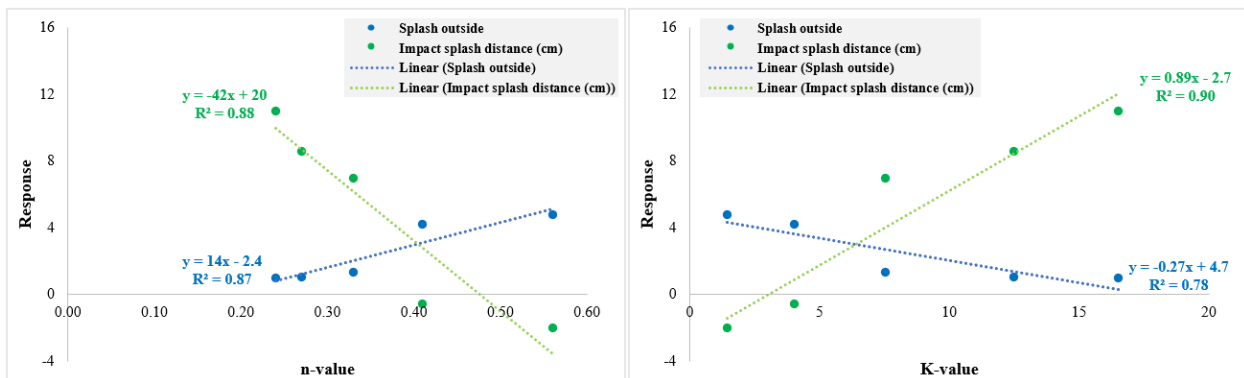


Figure 37. Correlation analysis between variables (K- and n- values) with the filling behavior responses (outside splash of the product and impact splash distance in the package) from five systematic blends.

4.3.3. Filling responses of ambient drinking yoghurt (ADY)

In the case of ADY with and without particle, there was no significant difference between the two samples for the impact splash distance in the package and splash outside of the package responses, as depicted in **Figure 38**. It is noticeable that there was a high variability of filling behavior responses particularly for ADY without particle, as indicated by the wider range of CI. Although

the rheological parameters of ADY were in the range between *Naturell lätt* 100% and 75%, ($K = 2.50$ and $n = 0.49$), it is not possible to predict the filling behavior response from the systematic blends as explained in **Chapter 4.3.2**. Theoretically from the systematic blends filling behaviors, the typical rheology characteristics of ADY will result in longer splash distance and a higher number of splashes outside. However, the opposite results were generated from the actual experiment of ADY with and without particle (see **Figure 38** below).

The difference between machine setting and product type (composition) used in the filling rig test of the five blends (setting 1) and ADY (setting 2) could be two of the factors that cause the product to behave differently.

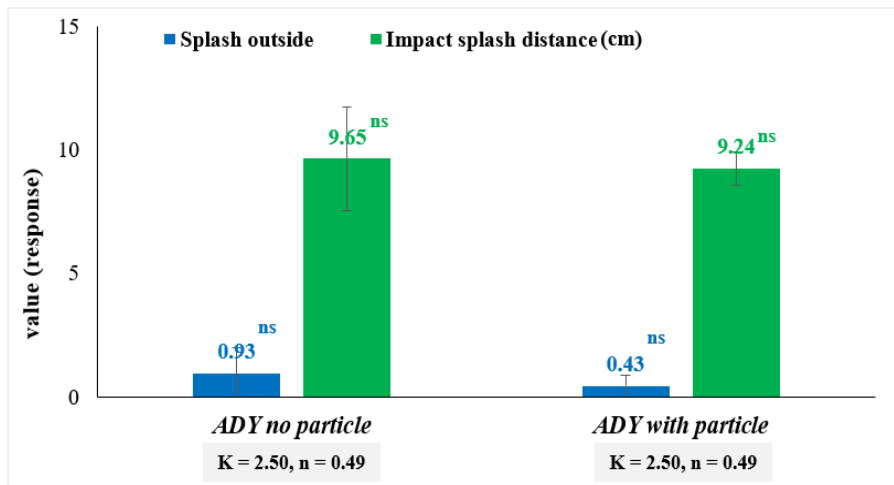


Figure 38. Filling behavior responses of the ADY with and without particle. Data is presented as mean value per shot from 6 data points (outside splash) and 30 data points (impact splash distance in cm). The superscript ns means not significant difference ($p > 0.05$) by using Independent Sample T-test from IBM SPSS Statistics 25.

4.4. Uncertainty of the experiments

Several factors contribute to the deviation of experimental or prediction data from the true value as described as uncertainty consisted of random and systematic uncertainties (Bell, 2001). This covers the concept of error, accuracy, quality, validity, reliability, and confidence (Dungan, Gao, & Pang, 2002). The experiment uncertainties on each stage of the study would be further described below.

In the first stage of the study, the accuracy of the instrument (Kinexus rotational rheometer) also might contribute to generate systematic errors in the experiment. Therefore, it is important to calibrate the instrument annually from the Kinexus company by using calibration oil to define the instrument accuracy and to conduct an internal verification activity with a Newtonian liquid (i.e. sugar solution with a relative deviation of $< 1\%$) (Paul, 2020). It is also mentioned that a correction factor is required as a part of uncertainties source in a coaxial-cylinder system or rotational rheometer (Benezech & Maingonnat, 1994).

In the second stage of the study, several factors could affect and contribute to the uncertainty in pressure drop prediction by using a pressure drop rig were: (1) the product properties including its behavior and structural changes during processing, (2) the measurement of predicted rheological parameters, including shear rate range selection and pre-shearing, and (3) the errors that resulted from the machine calibration i.e. flowmeter, pressure sensor, and pressure drop rig. Product's

structural change during processing might result from the particle orientation toward the flow direction, particle deformation, particle's network breakdown, particle clustering, and others (Moelants, et al., 2014). Then, the different measurement principles between the pressure drop rig and the rotational rheometer also must be highlighted. The pressure drop rig captures the pressure drop close to the real flow condition, while the rheometer captures the rheological parameters based on a small quantity of fluid entrapped between two geometric surfaces of motor and stator (Schaschke, 2016). Additionally, the accuracy of the instruments (i.e. pressure drop rig) also might contribute to the uncertainty of pressure drop prediction. As stated in **Chapter 3.2.5**, the pressure drop rig has been calibrated by using rapeseed oil and resulted in a maximum relative deviation of 16% (see **Appendix 7.13**). Furthermore, the product's temperature during the pressure drop experiment might also contribute to the accuracy (2-3% of relative deviation) of pressure drop prediction. Therefore, it is important to maintain a product's temperature by cooling the product with circulating cold water and monitoring the product's temperature online in the system by installing a temperature sensor. Lastly, the gap time between sampling from pressure drop rig and analysis by using a rotational rheometer must be as minimum as possible. The longer gap time might contribute to the least accuracy of the rheological parameter and increasing relative deviation of pressure drop prediction in pressure drop rig.

In the third stage of the study, during the one-shot filling rig test, one of the limitations was the design of the equipment that might contribute to the variability of filling responses. The filling rig test was conducted as an individual filling shot with semi-manual automation of the transparent package placement in the machine at every end of filling shot. However, in the actual application in the manufacturer, the filling process was conducted continuously for 20 hours. Additionally, the camera for video recording was installed only at one side of the machine, thus the filling was shot only from one side and could not capture the filling phenomena from the other side. Modification of the filling rig design could reduce the uncertainties from this experiment by running the filling process continuously. This could minimize the variability of filling behavior responses as per individual shot. Meanwhile, uncertainties from the latter issue could be minimized by counting some of the filling behavior responses (i.e. droplets and streaks) directly after each filling set instead of watching video footage.

5. Conclusion and recommendation

5.1. Conclusion

From the first stage of the study, it could be summarized that the time-dependent behavior of liquid food products can be investigated through the hysteresis loop, breakdown test, and build up test. It is clearly shown that *Naturell lätt* yoghurt had the highest thixotropy property, followed by orange juice concentrate and tomato puree. Also, in the case of tomato puree, it was shown to have a slight rheopexy behavior at a certain shear rate range. The latter result was confirming a previous study that reported a material that could exhibit both a thixotropy and rheopexy behavior based on a certain shear rate region. Lastly, build-up test could perform a clear structural recovery for the sample with the time-dependent behavior. It was observed that a higher amount of build-up or recovery would be reached by the samples either with the longest resting time ($dt=300$ s) or the shortest resting time ($dt=0$ s) depending on the product characteristics.

The second stage of this study summed up a conclusion that generated rheological parameters could predict the actual pressure drop (dP) measurement to some extent. Each product has a challenge due to its properties and behavior. This affected the pressure drop (dP) prediction from the theoretical calculation from the rheometer measurement compared to the pressure drop rig experiment as the actual application. The dP prediction required rheological parameters as the input generated from the hysteresis loop of upward sweep curve where the product had not been sheared too much and at a relevant shear rate region of $100 - 1000 \text{ s}^{-1}$. Then, a comparison between theoretical and experimental dP values was described by the % relative deviation value. The orange juice concentrate had a better pressure drop prediction than *Naturell lätt* yoghurt and undiluted tomato puree due to its rheology simplicity. However, two other products had more complexity that complicated the rheological measurements in different ways as reflected in the pressure drop rig experiment. Yoghurt had a thixotropy behavior noticed from the decreasing dP at a constant flowrate like the breakdown test principle. A product with thixotropy behavior could achieve a better dP prediction by applying more shearing to the product. The tomato puree's complexity was from the dominant rheopexy behavior with an oscillatory effect during pressure drop measurement in the pipe. Those factors could give some challenges to the dP prediction that would increase the % relative deviation. In addition, this study has proven that the selection of prediction models must be based on the product's rheological properties where orange juice concentrate was more suitable with the Power Law model and *Naturell lätt* yoghurt fitted better with the Herschel-Bulkley model. Meanwhile, both the Power Law and the HB model were not completely able to predict the pressure drop of undiluted tomato puree.

The third stage of the study has proven that systematic rheological parameters could be generated by using a different proportion of *Långfil* and *Naturell lätt* yoghurt. However, only the Power Law model was able to generate a systematic rheological parameter (K and n -value), while the Herschel-Bulkley model failed to generate the systematic rheological parameters. Therefore, rheological parameters from upward sweep and curve-fitting by using OLS and Power-Law model were used in the correlation analysis by using TRENDLINE linear regression. This study focused more on splash outside of the package and impact splash distance in the package response because of its relevancy with the current company development project of the real filling process application. The result of correlation analysis has proven the possibility to correlate between rheology parameters

(K and n-value) and filling behavior responses (splash outside of the package and impact splash distance in the package) from the five systematic blends with $R^2 > 0.75$. However, the addition of particle in the ADY did not cause any significant differences in the filling behavior responses compared to ADY without particle. It is also concluded that from the systematic blends pattern, we could not predict the filling behavior responses of ADY from its rheological parameters and probably due to several factors that one of them is different filling machine settings.

5.2. Recommendation

To get a clearer build-up phenomenon, it is suggested to apply a higher shear rate at the pre-shearing stage, aiming to enhance the product's breakdown. However, it is also important to consider that the product would not experience permanent damage due to higher shear application. The second possibility is to perform sufficiently low shear ($< 1 \text{ s}^{-1}$) for longer periods. Both are expected to capture either the thixotropy and rheopexy phenomena, and whether it is reversible, partial, or irreversible time-dependent effects.

To obtain a better prediction of the pressure drop, for more complex products, it is recommended to find a more suitable model besides Power Law and Herschel-Bulkley that considers the more complex product's behavior such as the time-dependency effect, but also thixotropy-viscoplastic (TVP) models by incorporating other rheology parameters for example storage (G') or loss modulus (G'').

To obtain application-specific methodology based on shear application. It will generate more relevant rheological parameters from the hysteresis loop curve of rheometer measurements, from the selection of relevant shear rate region, then pick the upward curve with less shearing impact to the product structure. As the measurement method (sequence) used in this study could affect the results. Due to a hysteresis loop test, with a sweep up ($1 - 1000 \text{ s}^{-1}$) and down ($1000-1 \text{ s}^{-1}$) in combination with a longer stabilization time would give a shearing effect to the product i.e. structure modification or changes. Therefore, it would be more accurate to use the rheological parameters generated from the upward sweep curve (see **Chapter 4.3.1**) or to apply the shear rate range based on the actual application in the pipes and filling machine. In addition, it is also suggested to minimize the 'waiting time' between sampling from the pipe flow and measurement by using a rheometer.

To reduce the systematic error and obtain reliable results from the rheological measurement instrument (rheometer), it is recommended to conduct an annual calibration for the rotational rheometer.

To reduce the variability of filling behavior responses between individual filling shots in the filling rig experiment, each filling shot can be done continuously as mimicking the real application. This can be done either by modifying the current filling rig instrument design with some adjustments i.e. image scanning installation and the continuous filling setting or by using another filling rig with more filling shots capacity (up to 30 shots).

Trying to vary only one rheological parameter might be an interesting idea as the continuation of this study. Therefore, one possible alternative is using products with more stable rheology characteristics or properties. It is based on the understanding that fermented product is a 'living

product'. Lastly, to predict automatic filling behavior responses of a certain product by using measurable systematic rheological parameters, the same machine setting must be applied in the design of the experiment. It is also important to consider whether the tested product has comparable and similar characteristics with the systematic blend product or not.

6. List of references

- AlfaLaval. (2020, May 25). *Tube-in-tube heat exchangers*. Retrieved from <https://www.alfalaval.com/>: <https://www.alfalaval.com/products/heat-transfer/tubular-heat-exchangers/tube-in-tube-heat-exchangers/>
- AntonPaar. (2020, May 8). *Anton Paar GmbH*. Retrieved from Anton Paar GmbH: <https://wiki.anton-paar.com/en/flow-curve-and-yield-point-determination-with-rotational-viscometry/>
- Bayod, E. (2008). *Microstructure and Rheological Properties of Concentrated Tomato Suspensions during Processing (Doctoral Thesis)*. Lund: Lund University.
- Bayod, E., Willers, E. P., & Tornberg, E. (2007). Rheological and structural characterization of tomato paste and its influence on the quality of ketchup. *LWT - Food Science and Technology*.
- Bell, S. (2001). *A Beginner's Guide to Uncertainty of Measurement*. Middlesex, UK: National Physical Laboratory.
- Benezech, T., & Maingonnat, J. F. (1994). Characterization of the rheological properties of yoghurt - a review. *Journal of Food Engineering*, 21(4), 447-472. doi:[https://doi.org/10.1016/0260-8774\(94\)90066-3](https://doi.org/10.1016/0260-8774(94)90066-3)
- Chabbra, R. P. (2010). Chapter 1: Non-Newtonian Fluids - An Introduction. In A. P. Deshpande, J. M. Krishnan, & P. B. Kumar, *Rheology of Complex Fluids* (p. 13). New York, Dordrecht, Heidelberg, London.: Springer.
- Chilton, R., & Stainsby, R. (1998). Pressure loss equations for laminar and turbulent non-Newtonian pipe flow. *Journal of Hydraulic Engineering*, 124(5), 522-529.
- Collyer, A. A. (1973). Time Independent Fluids. *Physics Education*, 8, 333. Retrieved May 19, 2020, from <https://iopscience-iop-org.ludwig.lub.lu.se/article/10.1088/0031-9120/8/5/009/pdf>
- Dungan, J. L., Gao, D., & Pang, A. T. (2002, April 13). *Definition of Uncertainty-White paper draft*. Retrieved from <ftp.cse.ucsc.edu>: <ftp.cse.ucsc.edu>
- Frost, J. (2020, May 14). *How to interpret R-square in regression analysis*. Retrieved from Statistics By Jim: <https://statisticsbyjim.com/regression/interpret-r-squared-regression/>
- GOLDPEG. (2020, May 25). *GOLD PEG Systems for Evolutions*. Retrieved from <https://www.goldpeg.com/>: <https://www.goldpeg.com/food-processing-equipment/>
- Graham, L. J., Pullum, L., & J, W. (2016). Flow on non-Newtonian fluids in pipes with large roughness. *The Canadian Journal of Chemical Engineering*, 24, 1102-1107. doi:<https://doi.org/10.1002/cjce.22494>
- Gumulya, M., Horsley, R., & Pareek, V. (2014). Numerical simulation of the settling behaviour of particles in thixotropic fluids. *Physics of Fluids*, 26, 1-16. doi:doi: 10.1063/1.4866320

- Jdayil, B. A., Nasser, M. S., & Ghannam, M. (2013). Structure breakdown of stirred yoghurt in a circular pipe as affected by casein and fat content. *Food Science and Technology*, 19(2), 277-286.
- Kumaran, V. (2010). Fundamentals of Rheology. In A. P. Deshpande, J. M. Krishnan, & P. B. Kumar, *Rheology of Complex Fluids* (pp. 35-65). New York: Springer.
- Kumari, K., & Yadav, S. (2018). Linear regression analysis study. *Journal of the Practice of Cardiovascular Sciences*, 4(1), 33-36. doi:DOI: 10.4103/jpcs.jpcs_8_18
- Lee, S., Li, E. Q., Marston, J. O., Bonito, A., & Thoroddsen, S. T. (2013). Leaping shampoo lides on a lubricatin air layer. *Physical Review E*87, 87(6), 1-4. doi:https://doi.org/10.1103/PhysRevE.87.061001
- Malvern. (2020, May 8). *Rheological properties*. Retrieved from www.malvern.com: https://www.malvernanalytical.com/en/assets/MRK2263-03-EN-01_Kinexus_DSR_Brochure_LRA4_tcm50-54840.pdf
- Martinez-Padilla, L., Arzate-Lopez, A., Delgado-Reyes, V. A., & Barbosa-Canovas, G. V. (1997). Measurement and prediction of pressure drop inside a pipe: The case of a model food suspension with a newtonian phase. *Journal of food process engineering*, 20, 477-497.
- Mezger, T. G. (2006). *The Rheology Handbook 2nd Edition: For Users for Rotational and Oscillatory Rheometer*. Hannover: Vincentz Network GmbH.
- Moelants, K. R., Cardinaels, R., Buggenhout, S. V., Loey, A. M., Moldenaers, P., & Hendrickx, M. E. (2014, April 16). A Review on the Relationships between Processing, Food Structure, and Rheological Properties of Plant-Tissue-Based Food Suspension. *Comprehensive Reviews in Food Science and Food Safety Vol.13*, pp. 241-260.
- Muhammad, A. (2020). *Approaches for improving the rheological characterization of fermented dairy products*. Lund University, Food Technology, Engineering and Nutrition. Lund: Lund University.
- Paul, B. (2020, May 27). Verification of rotational rheometer by using a sugar solution. (C. Andriani, Interviewer)
- Polymerdatabase. (2015). *Polymer Properties Database: Flow properties of polymers - time independent fluids*. Retrieved from Polymer database: <https://polymerdatabase.com/polymer%20physics/Viscosity2.html>
- Quemada, D. (1999). Rheological modelling of complex fluids: IV: Thixotropic and “thixoelastic” behaviour. Start-up and stress relaxation, creep tests and hysteresis cycles. *The European Physical Journal Applied Physics*, 5(2), 191-207. doi: <https://doi.org/10.1051/epjap:1999128>
- Radhakrishnan, A., Lier, J., & Clemens, F. (2018). Rheology of un-sieved concentrated domestic slurry. *Water*, 2-4.

- RheoSense. (2020, May 28). *Viscosity of Newtonian and non-Newtonian Fluids*. Retrieved from <https://www.rheosense.com/>: <https://www.rheosense.com/applications/viscosity/newtonian-non-newtonian>
- Schaschke, C. J. (2016). *Solved Practical Problems in Fluid Mechanics*. New York: CRC Press Taylor & Francis Group.
- Shashi, E. M., & Pramila, S. M. (2010). *Working Guide to Pumps and Pumping Stations*. Oxford: Gulf Professional Publishing (Elsevier).
- Singh, R. P., & Heldman, D. (2014). *Introduction to Food Engineering 5th Edition*. Academic Press.
- Solorio, J. (2018, August 21). *How to design an industrial piping system for ideal flow rate and velocity*. Retrieved from <https://www.corzan.com/>: <https://www.corzan.com/blog/how-to-design-an-industrial-piping-system-for-ideal-flow-rate-and-velocity>
- Steffe, J. F. (1996). *Rheological Methods in Food Processing Engineering. Second Edition*. USA: Freeman Press.
- Steg, I., & Katz, D. (1965). Rheopexy in some polar fluids and in their concentrated solutions in slightly polar solvents. *Journal Applied Polymer Science*, 9, 3177-3193.
doi:<https://doi.org/10.1002/app.1965.070090922>
- Struble, L., & Xihuang, J. (2001). Rheology. In V. R. Beaudoin, *Handbook of Analytical Techniques in Concrete Science and Technology* (pp. 333-367). William Andrew Inc.
- TAInstrument. (2020, May 12). *Undestandin Rheology of Structured Fluids*. Retrieved from <http://www.tainstruments.com/>: http://www.tainstruments.com/pdf/literature/AAN016_V1_U_StructFluids.pdf
- Tetra Pak. (2020). *Tetra Pak® TT/3 AD*. Retrieved May 23, 2020, from Tetra Pak website: <https://www.tetrapak.com/packaging/tetra-top-3-ad>
- Versluis, M., Blom, C., D, M. D., Weele, K. V., & Lohse, D. (2006). Leaping shampoo and the stable Kaye effect. *Journal of Statistical Mechanics Theory and Experiment*, 2006, 1-25.
- Williamson, H., & Ostreus, R. (2019). *Characterising the Rheology of Fermented Dairy Products During Filling*. Lund: Department of Food Technology, Lund University.

7. Appendices

7.1. Rotational Kinexus rheometer procedure

1. Open the compressed air supply valve until the pressure is set at 3-4 bar. Do not turn on the rheometer machine before setting the pressure because it could be damaged.
2. Turn on the computer and open rSpace for the Kinexus icon to start the software.
3. Switch on the power of the Kinexus rheometer by pressing the button at the backside of the machine.
4. Insert the chosen geometry for bob and cup based on the characteristic of the products and lock it by moving the black handle to the right. Note: the serrated cup aimed to minimize the wall-slip effect from the sample.
5. In the rSpace software, press zero-gap initialization and follow the instructions from the program.
6. Prepare the sample as follows to **Chapter 3.1.1. Sample Preparation.**
7. Select the sequence to run the analysis by clicking: File → Open → Sequence → choose or set the sequence → OK
8. Load the sample by pouring the sample into the chosen insert cup geometry until the cup is full, press the “Load Sample” button, and follow the instructions presented on the screen
9. Sequence setting:
Fill in the set-up information
 - a. Shear rate or shear stress range (1/s)
 - b. Number of samples per decade (always select the logarithmic mode)
 - c. Sampling interval - time (s)
 - d. Stabilization time (s)
 - e. Measurement temperature (°C)After setting the sequence, save, and name the sequence.
10. Start the sequence and wait up to 60 s for the product’s temperature stabilization and rest, and then press the “Skip” button.
11. When the sequence is completely done, the raw data (result) will be presented in the tab “Table”. Save the results: select all → sent to the main menu → select all → export data → to save in csv. file type. Important: do not forget to checklist the “final result” by right-click the data, then click properties.
12. Press the “Unload Sample” button and follow the instructions presented on the screen.
13. Remove the cup and bob geometry. Clean and wash with water, then dry by using a paper towel.
14. Reinsert the protective bob and cup cover. Turn off the Kinexus machine, close the gas valve, close the software, and turn off the computer.

7.2. Kinexus rheometer range and limitation

	pro+
Rheometer platform	Meeting rheological needs in research and development
Standard operating modes	.
Torque range – Viscometry (rate and stress control)	10nNm – 200mNm
Torque range – Oscillation (strain and stress control)	2nNm – 200mNm
Torque resolution	0.1nNm
Position resolution	<10nrad
Angular velocity range	10nrads ⁻¹ to 500rads ⁻¹
Step change in strain	<10ms
Frequency range	6.28μrads ⁻¹ to 942rads ⁻¹ (1μHz to 150Hz)
Motor inertia	13μN.m.s ²
Normal Force range	0.001N - 20N (50N optional)
Normal Force resolution	0.5mN
Normal Force response time	<10ms
Vertical lift speed	0.1μms ⁻¹ to 35mms ⁻¹
Vertical lift range (measureable)	230mm
Gap resolution (over full vertical lift range)	0.1μm

Figure 39. Kinexus rotational rheometer range and limitations (adapted from Williamson & Ostreus, 2019).

7.3. Determination of stabilization time

The stabilization time differs in each product and must be done at the beginning before conducting the sequence test by applying a constant shear rate (CSR) sequence, as described below.

1. A Constant shear rate (CSR) test was applied at three different shear rate values: 30 s⁻¹, 100 s⁻¹, and 300 s⁻¹. The sequence for tomato puree was designated without the sample loading step, by adding a set gap (20 N, 9.15 mm gap target) and followed by CSR at a certain shear rate.
2. The product viscosity was measured within 10 s interval and 60 s of resting time at the beginning (Muhammad, 2020).
3. The total number of sampling points was 30 with an estimated measurement of 5 min.
4. Stabilization time was defined as the time when the difference in viscosity of the products dropped less than 5% during a 10 s interval by analyzing the data using Ms. Excel.
5. From three different constant shear rate values, the chosen stabilization time was the one with the longest time (Muhammad, 2020).

7.4. Pressure drop rig procedure

1. Set up pipe the experiment: pipe diameter and pressure sensor (estimated based on ΔP estimation). Always check to open the valve for cooling water supply and to open the valves in all pipe diameter. Install the pressure sensor on the selected pipe diameter.
2. Fill the balance tank with the sample (approximately 100-120 L).
3. Turn on the computer (password: Nytt081017), then open the **NiLabVIEW 2018** (from Win 7 desktop).
4. Open **LTHrigg2020** and choose **New DHM Coldspot.vi** to open the display menu of the front panel.
5. Ensure all the channels have been set up (PT02, PT03, TT01, FT01 – including the selection of pressure sensor range 0-2.5 bar or 0-16 bar).
6. Start running the cooling system while start pumping the product by opening the cold-water supply (check the valve for cooling water).
7. Check the temperature of the product at the display front panel of **New DHM Coldspot** by pressing the “**run**” icon.
8. Put the hose outlet into the balance tank (not hanging position), then filling the product into each pipe during ± 5 min at 300 L/h to ensure all pipe diameters are filled with the product.
9. Open all valves, then recirculate the product at 300 L/h for 10 min to pre-shear the product.
10. **Measurement.** Close the valves from two other (unmeasured) pipe diameters. Set the target velocity (flow rate) by changing the frequencies of the pump while reading the flowrate display (in L/h) until it reaches the target flowrate, then lets it is stabilized for 1 min. Design of measurements:

Diameter 0.020 m	0.25 m/s, 0.50 m/s, 1.00 m/s, 2.00 m/s
Diameter 0.0380 m	0.25 m/s, 0.50 m/s, 1.00 m/s, 1.50 m/s
Diameter 0.020 m	0.25 m/s, 0.50 m/s, 1.00 m/s, 2.00 m/s

Each velocity requires 5 min measurement time (stabilization time included).

11. **Data logging.** To start recording the data, press the “**start logger**” icon on the **New DHM Coldspot** front panel display (indicated by the “*green*” light). The data recording can be started from the lowest flowrate. Name the data by writing the comment or label in the *Put Comment* box. The response of the measurement will be pressure drop (P2 and P3 in bar), product temperature (T1 in °C), and flowrate (v in L/h). After measurement at four different shear rates is done, stop the data logging by pressing again the “**start logger**” icon. Turn off the pump and closed the cooling water supply. All the data will be collected on a daily base. The data location can be seen from the display of LabView and obtained in the form of *lvm*. extension.
12. **Changing the diameter.** Drain the product from the rig system by opening the pipe junction, then put it together again. Place the pressure sensor into the selected pipe diameter that will be used for measurement. After that, open valves in all pipe diameters and redo step (8) and (9) to recirculate the product at low velocity (300 L/s) for 10 min. Then conduct the measurement and data logging by following step (10) and (11).
13. **Changing the pressure sensors.** In this case, the data logging system needs to be set (click *Window* option, select *Block Diagram*, double click the *DAQ assistant button*, then change

the selected pressure sensor range). After that, conduct the measurement and data logging by following step (10) and (11).

7.5. Pressure drop rig cleaning procedure

1. **PRODUCT DRAINING.** Drain the product through pumping into the waste tank until it reaches the level around 10 L in the balance tank, then turn off the pump.
2. **HOT WATER RINSING.** Open the valve of hot water (45 C), flow the hot water to the balance tank and fill it until it reaches level 120 L. Afterward, pumping the hot water through the rig to rinse out and flush the remaining product into the drainage until the water clear. Then, turn off the pump.
3. **HOT WATER CIRCULATION.** Move the hose outlet from the drainage into the balance tank. Fill in the balance tank with hot water up to 120 L. Afterward, turn on the pump and circulate the hot water for 5 minutes. Then, turn off the pump.
4. **DETERGENT SOLUTION CIRCULATION.** Add the detergent (20-30 ml per 120 L hot water) into the balance tank. Turn on the pump. Then, circulate the diluted detergent for 10 min including circulation in each pipe diameter (circulation in each pipe diameter by closing the valves of the other two diameters to increase the flow rate in each pipe). In the end, turn off the pump.
5. **HOT WATER RINSING.** Remove the hose outlet from the balance tank to the drainage, then drain the detergent solution by turning on the pump. Afterward, open the valve for the hot water supply. Turn on the pump to rinse out the detergent with the hot water until the water coming from the outlet is clear. In the end, turn off the pump.
6. **COLDWATER FINAL RINSING.** Change the hot water supply into a cold-water supply (do not forget to put the gasket). Open the valve of the cold-water supply. Flush the remaining hot water with cold water supply by turning on the pump, until the water coming from the outlet is cold. After that, drain manually the cold water from the balance tank by opening manually the outlet of the tank. Let the rig self-drained overnight.

7.6. Bucket method for flowmeter calibration

1. Fill the balance tank with the sample (approximately 100-120 L).
2. Set the pump and run at three different frequencies in duplicate: 10, 20, and 40 Hz.
3. Collect the sample from outlet hose into a volumetric bucket for each frequency setting for 30 s.
4. Measure how much sample is collected in the volumetric bucket (L).
5. Experimental flowrate value is calculated by using this following formula:

$$flowrate_{experiment} = \frac{volume (L)}{time (h)}$$

Correction constant is calculated by calculating the ratio between the experimental value and the average of measured flowrate values from the flowmeter reading.

7.7. Filling rig test procedure

1. **Sample preparation for five-systematic blends.** Prepare the amount of sample based on the weight proportion of *Långfill* and *Naturell Lätt yoghurt*. The products were homogenized by tilting up and down: 10 times for *Naturell* and 40 times for *Långfil* yoghurt. Then, pour both products from the top of the package into the volumetric bucket and mix gently by stirring 40 times in the clockwise direction. Store the sample in the chiller (6 °C) and thaw the sample overnight at room temperature (20-22 °C) before the experiment.
2. **Sample preparation for ambient drinking yoghurt (ADY).** Prepare the sample by titling the product (in 200 mL package) up and down 10 times, then pour the product into a volumetric bucket. For ADY without particles, the particulates were removed by straining the ADY by using kitchen utensils (strainer). Store the sample in the chiller (6 °C) and keep at room temperature (20-22 °C) overnight before the experiment.
3. **Sequence execution.** The filling test was executed by the following steps below.
 - a. Secure that everyone knows their task (responsibility) during the test/experiment.
 - b. Stir the prepared sample (20 times) and fill it to the rig with one of the below options:
 - (1) Fill product tank up to 55% indication of the level probe
 - (2) Mount smaller tank on the rig, fill, and disable level probe.
 - c. Take the sample from the feeder tank or volumetric bucket, to check the density and product rheology of the sample at Tetra Pak and LTH laboratory, respectively. Sample rheology was measured by using Kinexus rotational rheometer as followed Muhammad method (sweep up & down $1 - 1000 \text{ s}^{-1}$) and stabilization time 50 s for all samples.
 - d. Mount the transparent package.
 - e. Ensure that the Beckhoff logger is up and running.
 - f. Run the filling sequence.
 - g. Confirm with the Beckhoff and Sympathy for data that the curves are as intended.
 - h. Take out a package, check the filling weight. If needed, adjust, and confirm with another filling sequence.
 - i. Clean and dry the transparent package.
 - j. Mount the transparent package.
 - k. Ensure that the Beckhoff logger is up and running.
 - l. Start the filming device.
 - m. Run the filling sequence.
 - n. Take out the transparent package.
 - o. Check and note the filling weight in the embedded file "*TestResults*".
 - p. Check splash on filling pipe and splash plate. Estimate the size of drops and document in the embedded file "*TestResults*".
 - q. Save the film sequence.
 - r. Repeat point (d) to (q) the times decided.
 - s. Save the Beckhoff data file.
 - t. Check splash inside packages by counting and estimated size of drops. Document it in the embedded file "*TestResults*".

- u. Clean filling pipe and splash transparent plate every 5 fill cycles.
 - v. Empty the transparent packages, clean, and dry.
4. **Data analysis (post-work with the movie).** Collect the impact splash distance, dripping, and filamentation data by playing the movie in slow motion. Then input the data and make a statistic evaluation on it.

7.8. Cup-bob geometry selection for tomato puree at different dilution % (w/w)

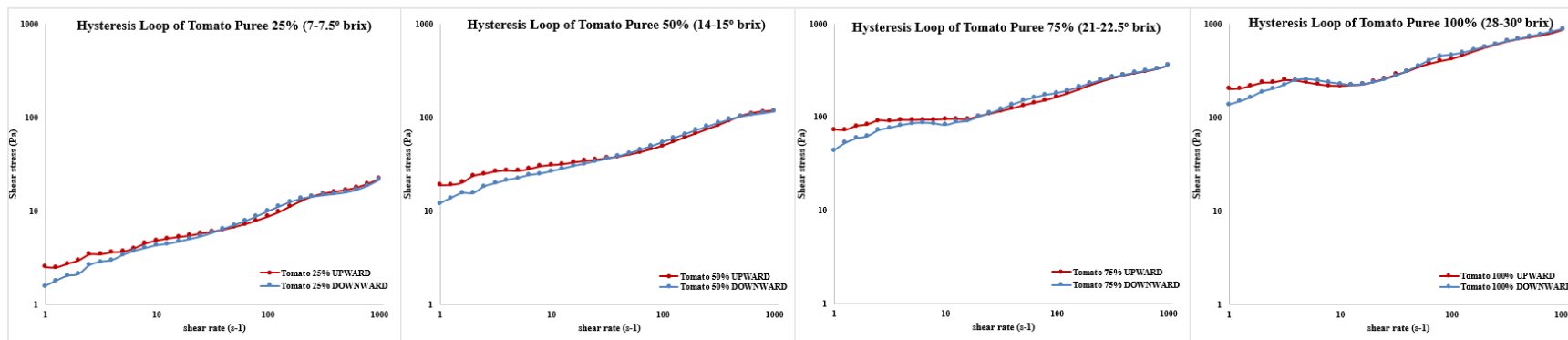


Figure 40. Hysteresis loop of tomato puree at different dilution % (w/w) by using smooth cup-bob geometry. Measurement was done in one replication.

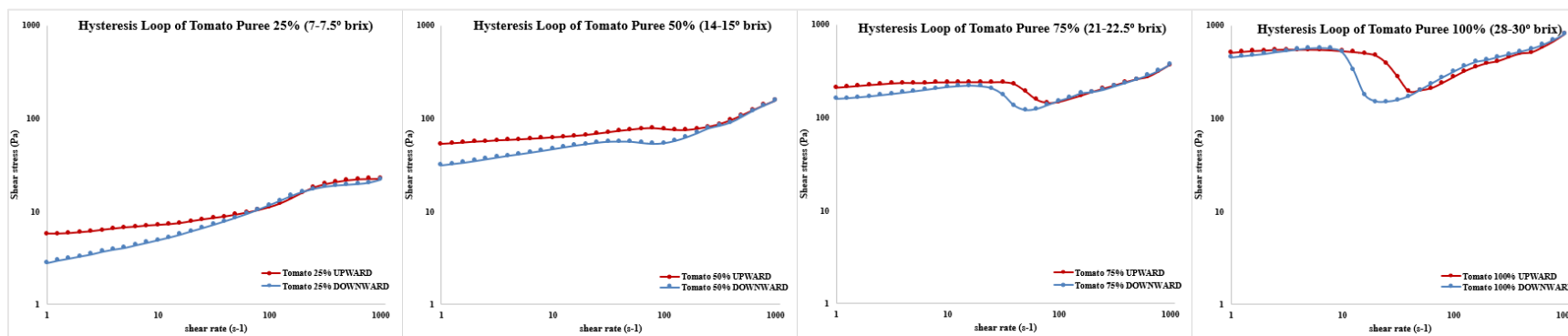


Figure 41. Hysteresis loop of tomato puree at different dilution % (w/w) by using serrated cup-bob geometry. Measurement was done in one replication

7.9. Build-up test with pre-shearing at 100 s^{-1}

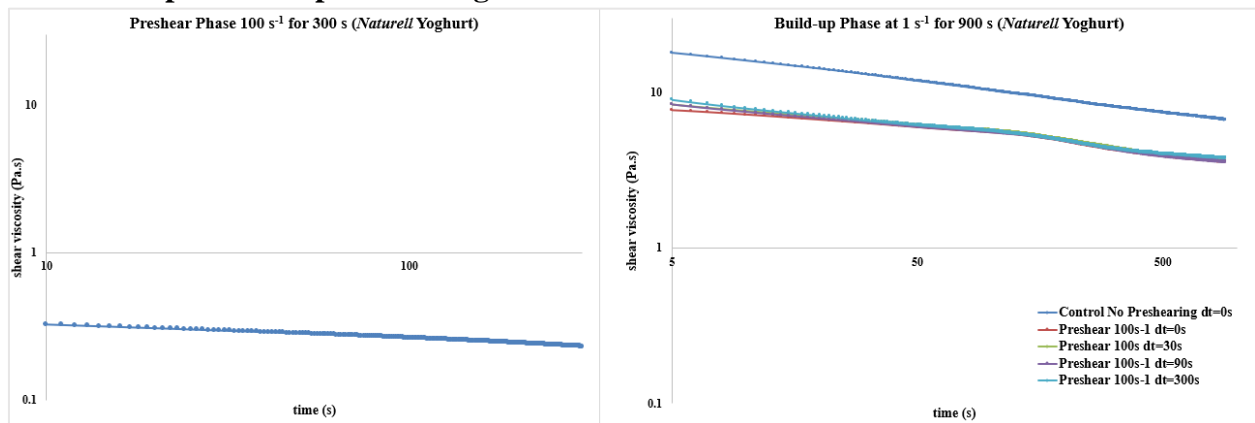


Figure 42. Build-up test of *Naturell lätt* yoghurt with pre-shearing at 100 s^{-1} (serrated geometry, triplicate). The first 10 points and the first 4 points of shear viscosity at pre-shearing and build-up phase were negligible due to shear rate adjustment. Data was obtained from *Muhammad (2020)*.

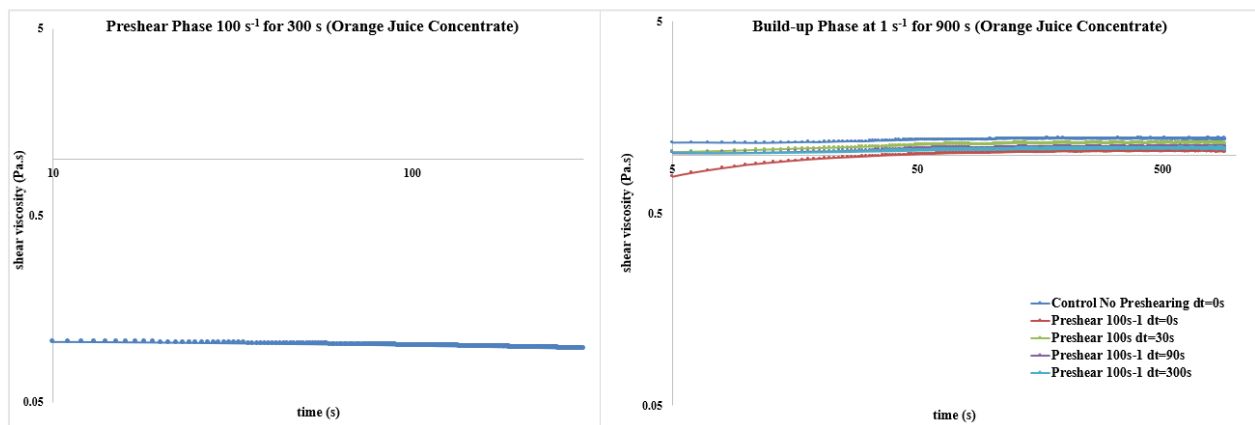


Figure 43. Build-up test of orange juice concentrate with pre-shearing at 100 s^{-1} (serrated geometry, one replication). The first 10 points and the first 4 points of shear viscosity at pre-shearing and build-up phase were negligible due to shear rate adjustment.

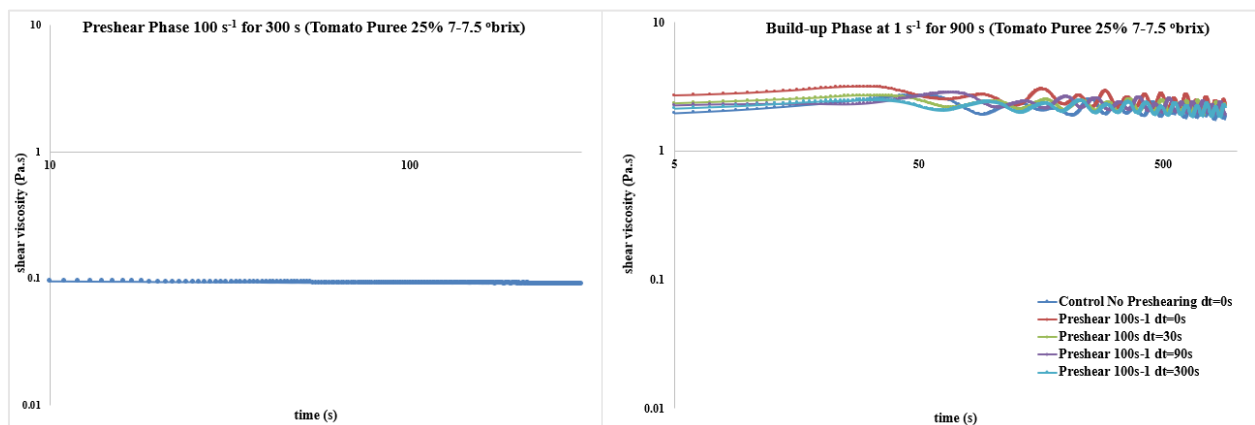


Figure 44. Build-up test of tomato puree 25% ($7-7.5\text{ }^{\circ}\text{brix}$) with pre-shearing at 100 s^{-1} (smooth geometry, one replication). The first 10 points and the first 4 points of shear viscosity at pre-shearing and build-up phase were negligible due to shear rate adjustment.

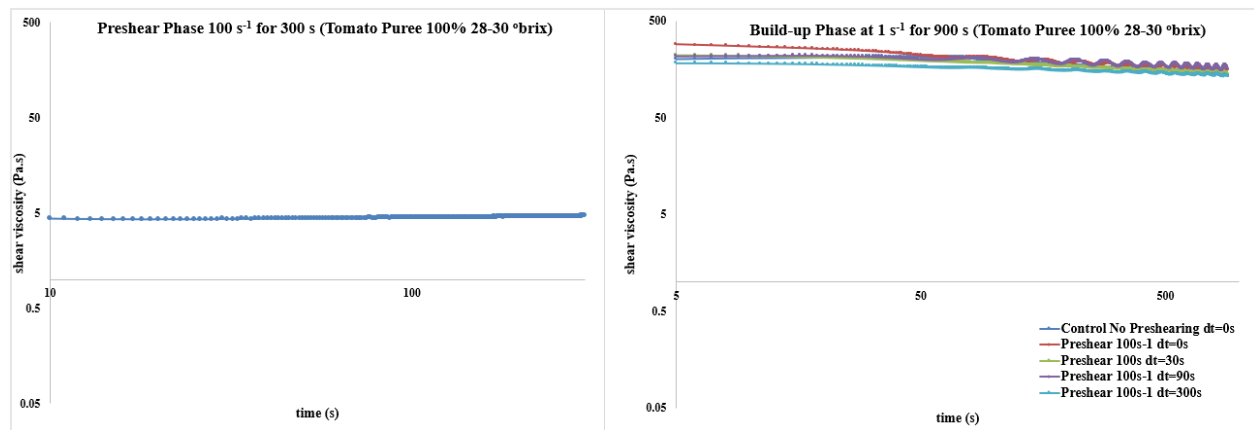


Figure 45. Build-up-test of tomato puree 100% (28-30 °brix) with pre-shearing at 100 s^{-1} (smooth geometry, one replicate). The first 10 points and the first 4 points of shear viscosity at pre-shearing and build-up phase were negligible due to shear rate adjustment.

7.10. Pressure drop data of orange juice concentrate

Table 17. Pressure drop (dP) prediction for orange juice concentrate by using Power Law model.

D ₀	Wall shear rate γ_w (s ⁻¹)	1 st sample		1 st sample		2 nd sample		2 nd sample		dP experiment (bar)
		UPWARD		DOWNWARD		UPWARD		DOWNWARD		
		dP cal (bar)		dP cal (bar)		dP cal (bar)		dP cal (bar)		
		1-79.44 s ⁻¹	100-1000s ⁻¹	1-79.44 s ⁻¹	100-1000s ⁻¹	1-79.44 s ⁻¹	100-1000s ⁻¹	1-79.44 s ⁻¹	100-1000s ⁻¹	
D20	139-157	0.16	0.16	0.14	0.14	0.16	0.16	0.13	0.11	0.16
	277-313	0.25	0.26	0.22	0.25	0.24	0.26	0.20	0.20	0.25
	555-627	0.37	0.44	0.33	0.44	0.36	0.43	0.31	0.37	0.40
	1109-1254	0.55	0.74	0.49	0.76	0.53	0.72	0.48	0.67	0.65
D38	65-74	0.05	0.04	0.05	0.04	0.05	0.05	0.04	0.03	0.05
	131-148	0.08	0.07	0.07	0.07	0.08	0.08	0.06	0.05	0.07
	262-296	0.12	0.13	0.11	0.12	0.12	0.12	0.09	0.10	0.11
	392-443	0.15	0.17	0.13	0.16	0.15	0.17	0.12	0.14	0.14
D20	139-157	0.16	0.16	0.14	0.14	0.16	0.16	0.13	0.11	0.15
	277-313	0.25	0.26	0.22	0.25	0.24	0.26	0.20	0.20	0.24
	555-627	0.37	0.44	0.33	0.44	0.36	0.43	0.31	0.37	0.39
	1109-1255	0.55	0.74	0.49	0.76	0.53	0.72	0.48	0.67	0.63
Rheology parameter		1.12	0.48	0.94	0.33	1.09	0.53	0.65	0.22	K-value
		0.58	0.75	0.59	0.81	0.58	0.73	0.64	0.85	n-value
		0.76	16.15	0.93	16.05	0.95	5.97	0.54	16.08	SSR

Note: experiment was conducted in one replicate. The wall shear rate (γ_w) was calculated from the *Rabinowitsch-Mooney* equations. Experiment dP was based on the average value.

Table 18. Pressure drop (dP) prediction for orange juice concentrate by using Herschel-Bulkley model.

D ₀	Wall shear rate γ_w (s ⁻¹)	1 st sample		1 st sample		2 nd sample		2 nd sample		dP experiment (bar)
		UPWARD		DOWNWARD		UPWARD		DOWNWARD		
		dP cal (bar)		dP cal (bar)		dP cal (bar)		dP cal (bar)		
		1-79.44 s ⁻¹	100-1000s ⁻¹	1-79.44 s ⁻¹	100-1000s ⁻¹	1-79.44 s ⁻¹	100-1000s ⁻¹	1-79.44 s ⁻¹	100-1000s ⁻¹	
D20	132-147	0.17	0.18	0.15	0.16	0.17	0.17	0.13	0.14	0.16
	262-295	0.27	0.27	0.25	0.25	0.27	0.27	0.21	0.22	0.25
	525-596	0.43	0.45	0.40	0.42	0.43	0.44	0.36	0.37	0.40
	1055-1189	0.69	0.77	0.66	0.76	0.68	0.74	0.60	0.70	0.65
D38	62-70	0.05	0.07	0.05	0.06	0.05	0.06	0.04	0.05	0.05
	125-140	0.08	0.09	0.07	0.08	0.08	0.08	0.06	0.07	0.07
	250-282	0.13	0.13	0.12	0.12	0.13	0.13	0.10	0.10	0.11
	372-420	0.17	0.17	0.16	0.16	0.17	0.17	0.14	0.14	0.14
D20	132-147	0.17	0.18	0.15	0.16	0.16	0.17	0.13	0.14	0.15
	266-295	0.27	0.27	0.25	0.25	0.27	0.27	0.21	0.22	0.24
	529-598	0.43	0.45	0.41	0.42	0.43	0.44	0.36	0.38	0.39
	1056-1189	0.69	0.77	0.66	0.76	0.69	0.73	0.59	0.70	0.63
Rheology parameter		0.71	0.14	0.54	0.10	0.64	0.24	0.39	0.06	K-value
		0.68	0.92	0.71	0.97	0.69	0.84	0.75	1.03	n-value
		0.77	7.79	0.81	7.00	0.85	5.30	0.56	6.31	Y _s
		0.01	2.37	0.00	2.19	0.02	0.81	0.00	2.48	SSR

Note: experiment was conducted in one replicate. The wall shear rate (γ_w) was calculated from the *Rabinowitsch-Mooney* equations. Experiment dP was based on the average value.

7.11. Pressure drop data of *Naturell lätt yoghurt*

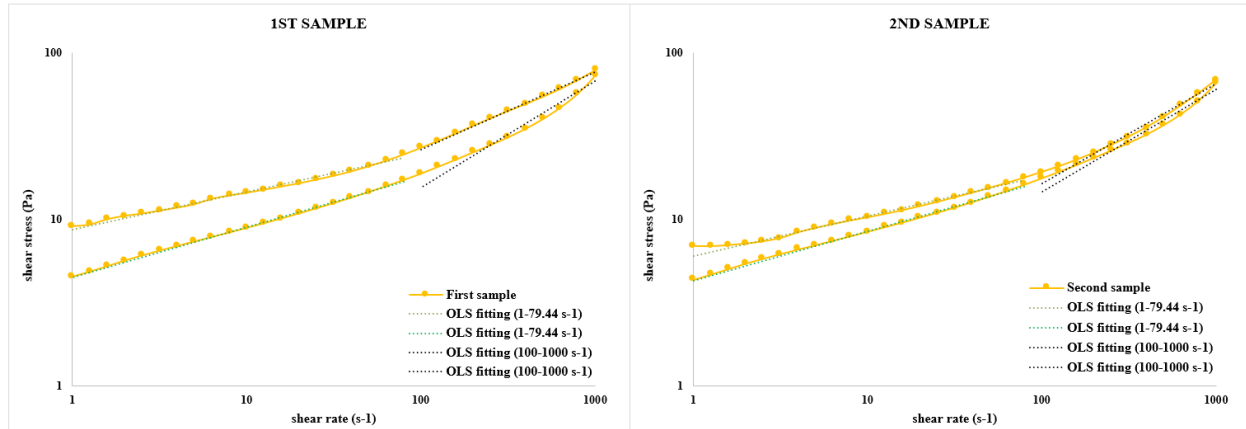


Figure 46. Logarithmic plot of hysteresis loop curve and OLS fitting curve of *Naturell lätt yoghurt* (left: 1st sample, right: 2nd sample) for Herschel-Bulkley model. The measurement was done in one replicate.

Table 19. Pressure drop (dP) prediction for *Naturell lätt yoghurt* by using Power Law model.

D ₀	Wall shear rate $\dot{\gamma}_w$ (s ⁻¹)	1 st sample		1 st sample		2 nd sample		2 nd sample		dP experiment (bar)
		UPWARD		DOWNWARD		UPWARD		DOWNWARD		
		dP cal (bar)		dP cal (bar)		dP cal (bar)		dP cal (bar)		
		1-79.44 s ⁻¹	100-1000s ⁻¹	1-79.44 s ⁻¹	100-1000s ⁻¹	1-79.44 s ⁻¹	100-1000s ⁻¹	1-79.44 s ⁻¹	100-1000s ⁻¹	
D20	143-231	0.24	0.25	0.17	0.16	0.17	0.16	0.16	0.14	0.34
	278-448	0.28	0.34	0.21	0.24	0.20	0.24	0.20	0.21	0.46
	549-884	0.32	0.47	0.26	0.37	0.24	0.36	0.25	0.32	0.68
	1091-1757	0.38	0.64	0.32	0.57	0.28	0.54	0.30	0.49	0.94
D38	68-109	0.10	0.09	0.07	0.05	0.07	0.05	0.07	0.04	0.09
	135-217	0.12	0.12	0.08	0.07	0.09	0.08	0.08	0.07	0.11
	269-433	0.14	0.17	0.10	0.12	0.10	0.12	0.10	0.10	0.13
	404-650	0.15	0.20	0.12	0.15	0.11	0.15	0.11	0.13	0.14
D20	143-231	0.24	0.25	0.17	0.16	0.17	0.16	0.16	0.14	0.19
	278-448	0.28	0.34	0.21	0.24	0.20	0.24	0.20	0.21	0.26
	548-882	0.32	0.47	0.26	0.37	0.24	0.36	0.25	0.32	0.39
	1087-1750	0.38	0.64	0.31	0.57	0.28	0.54	0.30	0.49	0.63
Rheology parameter		8.67	3.10	4.48	0.83	6.04	1.03	4.29	0.87	<i>K-value</i>
		0.23	0.46	0.30	0.64	0.24	0.60	0.30	0.61	<i>n-value</i>
		3.83	5.88	0.49	86.22	2.18	33.00	0.50	65.29	<i>SSR</i>

Note: experiment was conducted in one replicate. The wall shear rate ($\dot{\gamma}_w$) was calculated from the *Rabinowitsch-Mooney* equations. Experiment dP was based on the average value.

Table 20. Pressure drop (dP) prediction for *Naturell lätt* yoghurt by using Herschel-Bulkley model.

D ₀	Wall shear rate γ_w (s ⁻¹)	1 st sample		1 st sample		2 nd sample		2 nd sample		dP experiment (bar)
		UPWARD		DOWNWARD		UPWARD		DOWNWARD		
		dP cal (bar)		dP cal (bar)		dP cal (bar)		dP cal (bar)		
		1-79.44 s ⁻¹	100-1000s ⁻¹	1-79.44 s ⁻¹	100-1000s ⁻¹	1-79.44 s ⁻¹	100-1000s ⁻¹	1-79.44 s ⁻¹	100-1000s ⁻¹	
D20	120-181	0.25	0.26	0.18	0.21	0.19	0.20	0.17	0.19	0.34
	231-345	0.30	0.35	0.22	0.25	0.23	0.25	0.21	0.22	0.46
	456-688	0.37	0.47	0.28	0.34	0.29	0.36	0.26	0.29	0.68
	912-1364	0.46	0.65	0.36	0.55	0.37	0.57	0.33	0.45	0.94
D38	56-85	0.10	0.10	0.07	0.09	0.07	0.08	0.07	0.08	0.09
	112-169	0.12	0.13	0.09	0.10	0.09	0.10	0.08	0.09	0.11
	224-336	0.15	0.17	0.11	0.12	0.11	0.13	0.10	0.11	0.13
	337-505	0.17	0.20	0.13	0.15	0.13	0.15	0.12	0.13	0.14
D20	120-181	0.25	0.26	0.18	0.21	0.19	0.20	0.17	0.19	0.19
	231-345	0.30	0.35	0.22	0.25	0.23	0.25	0.21	0.22	0.26
	456-688	0.37	0.47	0.28	0.34	0.29	0.36	0.26	0.29	0.39
	907-1364	0.46	0.65	0.36	0.55	0.37	0.57	0.33	0.45	0.63
Rheology parameter		3.61	1.20	3.23	0.01	2.38	0.06	2.99	0.01	<i>A-value</i>
		0.37	0.58	0.36	1.24	0.40	0.99	0.36	1.20	<i>b-value</i>
		5.73	9.69	1.48	17.02	4.22	13.81	1.53	15.64	<i>Ys</i>
		1.54	2.21	0.21	9.59	0.41	0.21	0.22	7.24	<i>SSR</i>

Note: experiment was conducted in one replicate. The wall shear rate (γ_w) was calculated from the *Rabinowitsch-Mooney* equations. Experiment dP was based on the average value.

Table 21. Percentage (%) of relative deviation for pressure drop (dP) prediction of *Naturell lätt* yoghurt by using Power Law model.

D ₀	Wall shear rate γ_w (s ⁻¹)	1 st sample		1 st sample		2 nd sample		2 nd sample	
		UPWARD		DOWNWARD		UPWARD		DOWNWARD	
		1-79.44 s ⁻¹	100-1000s ⁻¹	1-79.44 s ⁻¹	100-1000s ⁻¹	1-79.44	100-1000	1-79.44 s ⁻¹	100-1000s ⁻¹
D20	143-231	30%	25%	49%	54%	49%	52%	51%	58%
	278-448	40%	26%	55%	48%	56%	48%	57%	54%
	549-884	52%	31%	62%	46%	65%	47%	64%	52%
	1091-1757	60%	32%	67%	39%	70%	42%	68%	48%
D38	68-109	-13%	-1%	22%	45%	18%	42%	26%	49%
	135-217	-7%	-12%	23%	31%	22%	29%	26%	37%
	269-433	-3%	-26%	22%	13%	24%	12%	26%	22%
	404-650	-6%	-43%	18%	-7%	22%	-5%	21%	6%
D20	143-231	-23%	-31%	11%	19%	10%	16%	15%	26%
	278-448	-7%	-32%	19%	8%	22%	8%	23%	18%
	548-882	17%	-20%	34%	6%	39%	8%	37%	17%
	1087-1750	40%	-2%	50%	9%	55%	14%	52%	22%
Rheology parameter	<i>K-value</i>	8.67	3.10	4.48	0.83	6.04	1.03	4.29	0.87
	<i>n-value</i>	0.23	0.46	0.30	0.64	0.24	0.60	0.30	0.61
	<i>SSR</i>	3.83	5.88	0.49	86.22	2.18	33.00	0.50	65.29

Note: negative (-) % relative deviation = overestimation or dP experiment < dP calculation, and positive (+) % relative deviation = underestimation or dP experiment > dP calculation. The wall shear rate (γ_w) was calculated from the *Rabinowitsch-Mooney* equations.

7.12. Pressure drop data of tomato puree 100%

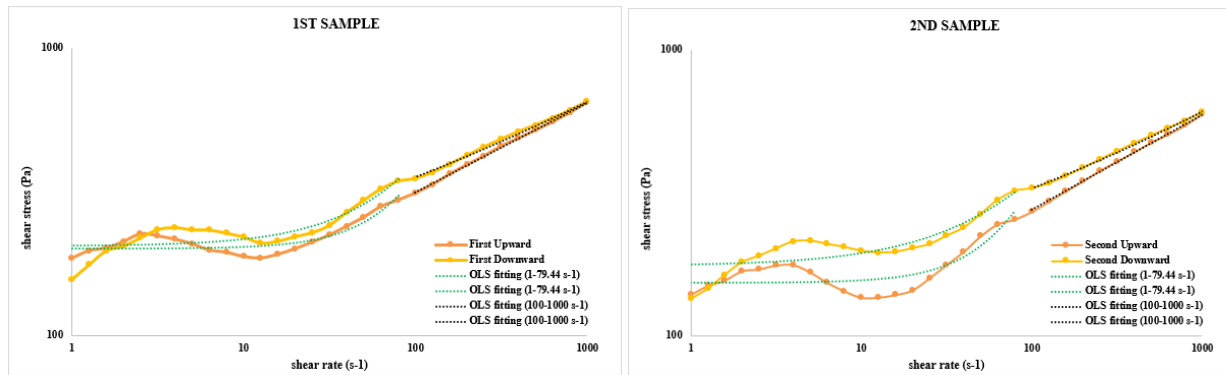


Figure 47. Logarithmic plot of hysteresis loop curve and OLS fitting curve of tomato puree 100% (28-30 °brix) (*left*: 1st sample, *right*: 2nd sample) for Herschel-Bulkley model. The measurement was done in one replicate.

Table 22. Pressure drop (dP) prediction for tomato puree 100% (28-30 °brix) by using Power Law model.

D _o	Wall shear rate γ_w (s ⁻¹)	1 st sample		1 st sample		2 nd sample		2 nd sample		dP experiment (bar)
		UPWARD		DOWNWARD		UPWARD		DOWNWARD		
		dP cal (bar)		dP cal (bar)		dP cal (bar)		dP cal (bar)		
		1-79.44 s ⁻¹	100-1000s ⁻¹	1-79.44 s ⁻¹	100-1000s ⁻¹	1-79.44 s ⁻¹	100-1000s ⁻¹	1-79.44 s ⁻¹	100-1000s ⁻¹	
D20	189-542	2.25	3.02	2.73	3.41	1.94	2.61	2.68	3.08	2.78
	368-1055	2.36	3.71	2.94	4.09	2.07	3.25	2.94	3.69	3.21
	716-2053	2.47	4.56	3.16	4.89	2.22	4.05	3.23	4.41	3.52
	1384-3968	2.58	5.59	3.40	5.84	2.37	5.03	3.54	5.27	4.05
D38	86-247	1.06	1.18	1.25	1.38	0.90	1.01	1.20	1.25	1.08
	169-485	1.12	1.46	1.35	1.66	0.96	1.26	1.32	1.49	1.30
	328-941	1.17	1.79	1.45	1.98	1.02	1.56	1.45	1.79	1.46
	475-1362	1.20	2.01	1.51	2.19	1.06	1.77	1.52	1.98	1.55
D20	176-504	2.24	2.95	2.71	3.35	1.93	2.55	2.65	3.02	2.54
	343-983	2.34	3.63	2.91	4.01	2.06	3.17	2.91	3.62	2.92
	680-1949	2.46	4.49	3.14	4.82	2.20	3.98	3.20	4.35	3.14
	1382-3962	2.58	5.59	3.40	5.84	2.37	5.03	3.54	5.27	3.98
Rheology parameter		185.07	75.28	181.70	103.02	136.05	59.14	152.84	92.99	K-value
		0.07	0.31	0.11	0.27	0.10	0.33	0.14	0.27	n-value
		10366.24	107.16	11082.46	93.38	14088.22	93.90	9246.12	127.06	SSR

Note: experiment was conducted in one replicate. The wall shear rate (γ_w) was calculated from the *Rabinowitsch-Mooney* equations. Experiment dP was based on the average value.

Table 23. Pressure drop (dP) prediction for tomato puree 100% (28-30 °brix) by using Herschel-Bulkley model.

D _o	Wall shear rate γ_w (s ⁻¹)	1 st sample		1 st sample		2 nd sample		2 nd sample		dP experiment (bar)
		UPWARD		DOWNWARD		UPWARD		DOWNWARD		
		dP cal (bar)		dP cal (bar)		dP cal (bar)		dP cal (bar)		
		1-79.44 s ⁻¹	100-1000s ⁻¹	1-79.44 s ⁻¹	100-1000s ⁻¹	1-79.44 s ⁻¹	100-1000s ⁻¹	1-79.44 s ⁻¹	100-1000s ⁻¹	
D20	111-195	3.81	3.02	4.11	3.41	3.41	2.60	3.58	3.13	2.78
	218-383	6.96	3.72	6.46	4.03	6.95	3.25	5.17	3.71	3.21
	426-743	16.96	4.57	11.64	4.81	18.24	4.05	8.13	4.43	3.52
	822-1432	48.32	5.60	23.22	5.79	54.21	5.03	13.70	5.37	4.05
D38	51-89	1.32	1.18	1.45	1.43	1.09	1.01	1.31	1.31	1.08
	100-175	1.79	1.46	1.93	1.66	1.57	1.26	1.69	1.53	1.30
	195-339	3.08	1.79	2.95	1.96	2.99	1.56	2.40	1.80	1.46
	283-492	4.76	2.01	3.98	2.16	4.89	1.77	3.03	1.98	1.55
D20	103-184	3.63	2.96	3.95	3.35	3.19	2.54	3.47	3.08	2.54
	202-353	6.40	3.63	6.11	3.96	6.34	3.17	4.95	3.64	2.92
	401-699	15.51	4.48	11.05	4.74	16.77	3.97	7.81	4.37	3.14
	822-1432	48.32	5.60	23.22	5.79	54.21	5.03	13.70	5.37	3.98
Rheology parameter		0.05	75.28	0.69	44.43	0.05	59.14	2.01	32.27	<i>A-value</i>
		1.74	0.31	1.22	0.36	1.76	0.33	0.97	0.39	<i>b-value</i>
		201.12	0.00	205.11	125.17	153.34	0.00	175.71	134.56	<i>Y_s</i>
		3088.16	107.16	6975.82	233.08	4726.61	93.90	6723.87	136.30	<i>SSR</i>

Note: experiment was conducted in one replicate. The wall shear rate (γ_w) was calculated from the *Rabinowitsch-Mooney* equations. Experiment dP was based on the average value.

Table 24. Percentage (%) of relative deviation for pressure drop (dP) prediction of tomato puree 100% (28-30 °brix) by using Herschel-Bulkley model.

D _o	Wall shear rate γ_w (s ⁻¹)	1 st sample		1 st sample		2 nd sample		2 nd sample	
		UPWARD		DOWNWARD		UPWARD		DOWNWARD	
		1-79.44 s ⁻¹	100-1000s ⁻¹	1-79.44 s ⁻¹	100-1000s ⁻¹	1-79.44 s ⁻¹	100-1000s ⁻¹	1-79.44 s ⁻¹	100-1000s ⁻¹
D20	111-195	-37%	-9%	-48%	-23%	-23%	6%	-29%	-13%
	218-383	-117%	-16%	-101%	-26%	-117%	-1%	-61%	-16%
	426-743	-382%	-30%	-231%	-37%	-418%	-15%	-131%	-26%
	822-1432	-1094%	-38%	-474%	-43%	-1239%	-24%	-239%	-33%
D38	51-89	-22%	-9%	-34%	-32%	0%	7%	-21%	-21%
	100-175	-37%	-12%	-48%	-27%	-20%	4%	-30%	-17%
	195-339	-111%	-23%	-102%	-34%	-104%	-7%	-64%	-23%
	283-492	-207%	-29%	-156%	-39%	-215%	-14%	-95%	-28%
D20	103-184	-43%	-17%	-55%	-32%	-26%	0%	-37%	-21%
	202-353	-119%	-24%	-109%	-35%	-117%	-9%	-70%	-25%
	401-699	-393%	-43%	-252%	-51%	-434%	-26%	-148%	-39%
	822-1432	-1114%	-41%	-483%	-45%	-1262%	-26%	-244%	-35%
Rheology parameter	<i>A-value</i>	0.05	75.28	0.69	44.43	0.05	59.14	2.01	32.27
	<i>b-value</i>	1.74	0.31	1.22	0.36	1.76	0.33	0.97	0.39
	<i>Y_s</i>	201.12	0.00	205.11	125.17	153.34	0.00	175.71	134.56
	<i>SSR</i>	3088.16	107.16	6975.82	233.08	4726.61	93.90	6723.87	136.30

Note: negative (-) % relative deviation = overestimation or dP experiment < dP calculation, and positive (+) % relative deviation = underestimation or dP experiment > dP calculation. The wall shear rate (γ_w) was calculated from the *Rabinowitsch-Mooney* equations.

7.13. Pressure drop rig system calibration

Table 25. Pressure drop rig system calibration by using rapeseed oil.

Pipe diameter (mm) and Pressure sensor (bar)	Frequency (Hz)	Calculated dP (bar)	Experiment dP (bar)	Ratio (dP Exp/Cal)	Relative deviation (%)
D ₂₀ (D _{in} =0.0175 m) Pressure sensor: 0-16 bar	10	0.20	0.22	1.10	9%
	20	0.39	0.42	1.07	7%
	40	0.77	0.84	1.09	8%
D ₂₀ (D _{in} =0.0175 m) Pressure sensor: 0-2.5 bar	10	0.20	0.23	1.18	16%
	20	0.39	0.44	1.13	11%
	40	0.77	0.87	1.12	11%

7.14. Systematic blends hysteresis loop and curve fitting

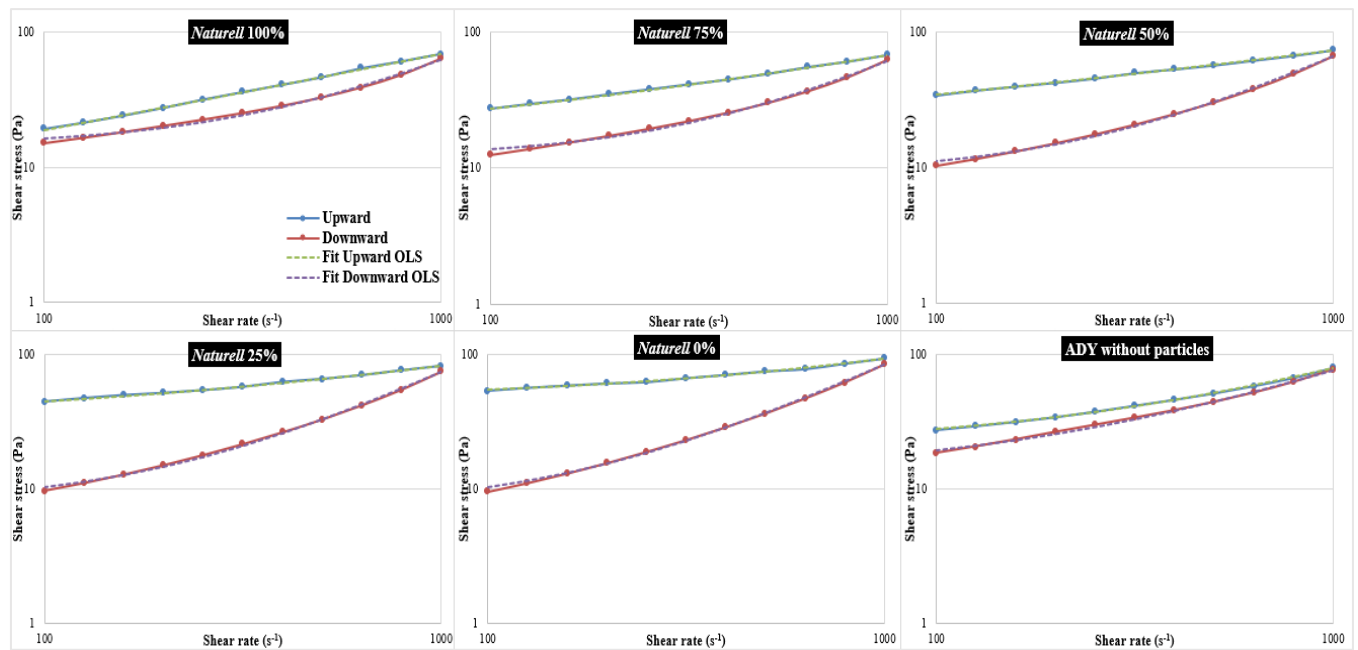


Figure 48. Logarithmic plot of hysteresis loop curves and Herschel-Bulkley curve fitting of five blends *Naturell lätt* yoghurt and *Långfil* and ADY without particles. Measurements were conducted one replicate for each sample.

7.15. Visualization of *Kaye* effect in theory

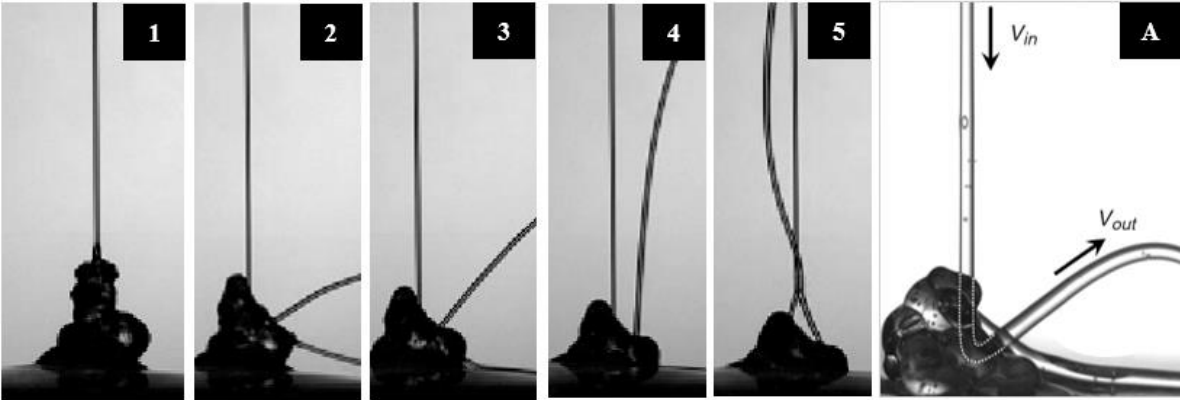


Figure 49. Visualization of *Kaye* effects for shear thinning fluid (shampoo). [1] formation of a viscous heap through piling, buckling, and coiling, [2] ejection of a thin streamer of fluid initiating *Kaye* effect, [3] [4] rising of the jet, [5] the outgoing jet disrupt the incoming jet as the end of *Kaye* effect, [A] schematic view of the flow cross section, v indicating the jet velocity (Versluis, Blom, D, Weele, & Lohse, 2006).

7.16. Filling responses in the one-shot filling rig

Table 26. Filling behavior responses (per shot) of systematic blends and ambient drinking yogurt (ADY) from one-shot filling rig machine.

Sample	Density (g/mL)	Splash outside		Splash inside Occurrence		Impact splash distance (cm)		Filament Occurrence		Dripping Occurrence	
		Mean	95% CI of mean	Mean	95% CI of mean	Mean	95% CI of mean	Mean	95% CI of mean	Mean	95% CI of mean
Naturell 100%	1.0343	4.80	1.53	17.53	4.95	-2.00	0.82	0.00	0.00	1.00	0.00
Naturell 75%	1.0337	4.20	1.61	18.70	2.57	-0.56	1.11	0.03	0.06	1.00	0.00
Naturell 50%	1.0313	1.33	1.32	14.90	3.04	7.00	0.98	0.90	0.11	0.97	0.07
Naturell 25%	1.0290	1.03	0.61	11.37	2.16	8.57	0.63	1.00	0.00	1.00	0.00
Naturell 0%	1.0275	1.00	1.05	7.27	1.90	11.00	0.95	1.00	0.00	1.00	0.00
ADY no particle	1.0676	0.93	1.06	8.47	2.30	9.65	2.09	1.00	0.00	1.00	0.00
ADY with particle	1.0676	0.43	0.45	11.70	1.74	9.24	0.67	1.00	0.00	1.00	0.00

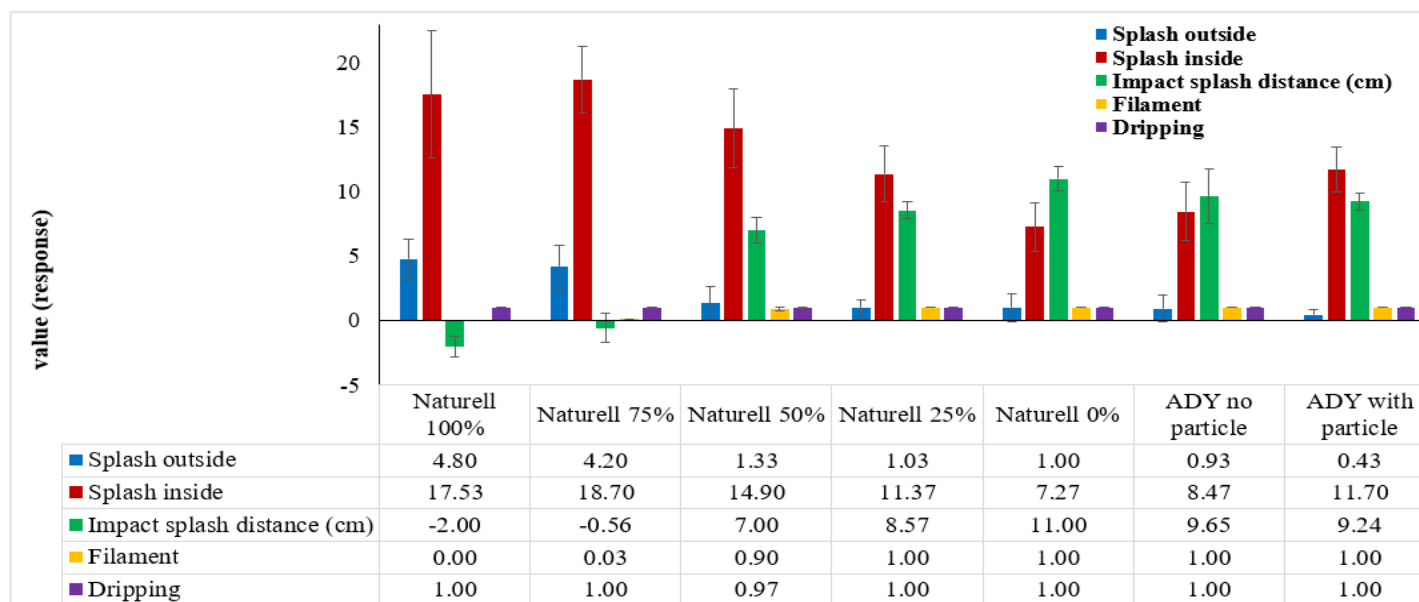


Figure 50. Bar chart of filling behavior responses from one-shot filling rig machine. Data is presented as an average value per shot from 6 data points (outside splash) and 30 data points (inside splash, impact splash distance in cm, and filament). The line bar indicating 95% Confidence Interval (CI) for mean.

7.17. Statistical analysis of outside splash and impact splash distance by using SPSS 25

Table 27. Homogeneity of variance test for the systematic blends.

		Levene Statistic	df1	df2	Sig.
Outside_splash	Based on Mean	1.112	4	25	.373
	Based on Median	.526	4	25	.718
	Based on Median and with adjusted df	.526	4	15.235	.718
	Based on trimmed mean	1.050	4	25	.402
Impact_splash	Based on Mean	3.278	4	145	.013
	Based on Median	2.636	4	145	.036
	Based on Median and with adjusted df	2.636	4	131.729	.037
	Based on trimmed mean	3.219	4	145	.014

Table 28. ONE-WAY ANOVA test for the systematic blends.

		Sum of Squares	df	Mean Square	F	Sig.
Outside_splash	Between Groups	83.632	4	20.908	14.109	.000
	Within Groups	37.047	25	1.482		
	Total	120.679	29			
Impact_splash	Between Groups	3971.877	4	992.969	165.250	.000
	Within Groups	871.291	145	6.009		
	Total	4843.168	149			

Table 29. Post hoc test (Duncan) of outside splash response for systematic blends.

		Subset for alpha = 0.05		
Sample	N	1	2	
Duncan ^a	0%_Naturell	6	1.00	
	25%_Naturell	6	1.03	
	50%_Naturell	6	1.33	
	75%_Naturell	6		4.20
	100%_Naturell	6		4.80
	Sig.		.659	.401

Means for groups in homogeneous subsets are displayed.
a. Uses Harmonic Mean Sample Size = 6.000.

Table 30. Post hoc test (Dunnett T3) of impact splash distance response for systematic blends.

(I) Sample	(J) Sample	Mean Difference (I-J)	Std. Error	Sig.	95% Confidence Interval	
					Lower Bound	Upper Bound
100%_Naturell	75%_Naturell	-1.44667	.67787	.306	-3.4212	.5279
	50%_Naturell	-8.99333*	.62424	.000	-10.8078	-7.1789
	25%_Naturell	-10.58000*	.51227	.000	-12.0706	-9.0894
	0%_Naturell	-12.99667*	.61426	.000	-14.7816	-11.2118
75%_Naturell	100%_Naturell	1.44667	.67787	.306	-.5279	3.4212
	50%_Naturell	-7.54667*	.72403	.000	-9.6504	-5.4429
	25%_Naturell	-9.13333*	.63005	.000	-10.9794	-7.2872
	0%_Naturell	-11.55000*	.71545	.000	-13.6294	-9.4706
50%_Naturell	100%_Naturell	8.99333*	.62424	.000	7.1789	10.8078
	75%_Naturell	7.54667*	.72403	.000	5.4429	9.6504
	25%_Naturell	-1.58667	.57196	.073	-3.2567	.0834
	0%_Naturell	-4.00333*	.66486	.000	-5.9339	-2.0727
25%_Naturell	100%_Naturell	10.58000*	.51227	.000	9.0894	12.0706
	75%_Naturell	9.13333*	.63005	.000	7.2872	10.9794
	50%_Naturell	1.58667	.57196	.073	-.0834	3.2567
	0%_Naturell	-2.41667*	.56105	.001	-4.0538	-.7796
0%_Naturell	100%_Naturell	12.99667*	.61426	.000	11.2118	14.7816
	75%_Naturell	11.55000*	.71545	.000	9.4706	13.6294
	50%_Naturell	4.00333*	.66486	.000	2.0727	5.9339
	25%_Naturell	2.41667*	.56105	.001	.7796	4.0538

*. The mean difference is significant at the 0.05 level.

Table 31. Independent sample t-test for ambient drinking yoghurt (ADY) with/out particles.

		Independent Samples Test									
		Levene's Test for Equality of Variances		t-test for Equality of Means						95% Confidence Interval of the Difference	
		F	Sig.	t	df	Sig. (2-tailed)	Mean Difference	Std. Error Difference	Lower	Upper	
Outside_splash	Equal variances assumed	3.637	.086	1.117	10	.290	.500	.447	-.497	1.497	
	Equal variances not assumed			1.117	6.737	.302	.500	.447	-.566	1.566	
Impact_splash	Equal variances assumed	44.234	.000	.375	58	.709	.40000	1.06533	-1.73248	2.53248	
	Equal variances not assumed			.375	34.931	.710	.40000	1.06533	-1.76288	2.56288	

7.18. One-shot filling machine testing

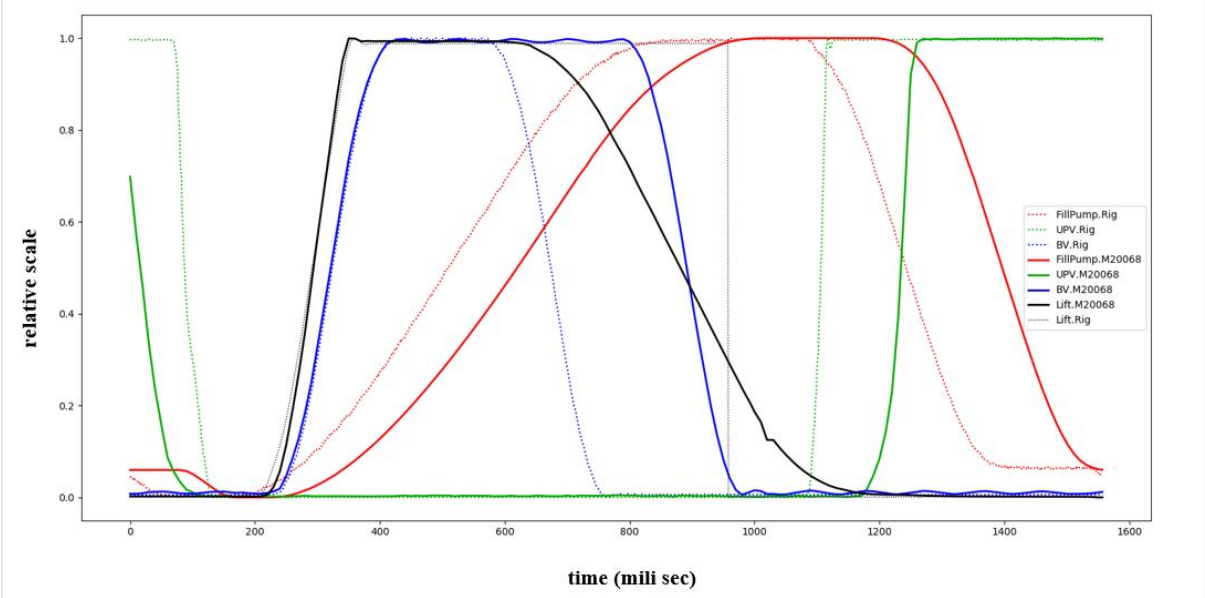


Figure 51. Filling sequence (machine setting) of one-shot filling rig. Dashed line = setting 1; solid line = setting 2.